

STRUCTURAL STUDIES ON ANTIFOLATE DRUGS

Joan Colby Hill  
Master of Philosophy  
The University of Aston in Birmingham  
July 1987

STRUCTURAL STUDIES ON ANTIFOLATE DRUGS

The structures of four compounds are reported, having been determined by single crystal X-ray crystallography. The four compounds fall into two categories :-

Protonated antifolates with anions  
Substituted antifolates.

The first category has been complemented with molecular orbital calculations on protonated and unprotonated :-

2-amino-4-oxo-pyrimidines (2-aminopyrimidin-4-ones)  
2,4 diaminopyrimidines  
triazines.

Further calculations are reported on one of the structures to determine whether the atoms appear to be in a minimum energy position.

Joan Colby Hill

Master of Philosophy

THE UNIVERSITY OF ASTON IN BIRMINGHAM

July 1987

## ACKNOWLEDGEMENTS

All the work described in this thesis was conducted at the Pharmacy Department, The Univeristy of Aston in Birmingham under a research grant from the Science and Engineering Research Council (no. 82314925). Unless otherwise stated it is my own work and has not been previously submitted in whole or in part to this or any other university or polytechnic.

I would like to extend thanks to Dr.C.H.Schwalbe for his supervision and encouragement and to Dr.R.J.Griffin for the preparation of crystals.

## LIST OF CONTENTS

	Page
CHAPTER ONE	
1	Introduction 1
1.1	Selection of a Crystal 3
1.2	Limitations and scope of X-ray Crystallography 5
	Direct Methods 7
	Refinement and Weighting 8
	The 'R' Value 9
1.2.1	Scattering factors and Thermal Motion 11
1.2.2	Electron and Neutron Diffraction as a complement to X-ray methods 14
1.2.3	Solid state versus Natural state structure 15
1.3	Molecular Geometry calculations 18
1.3.1	Charge distribution and Mulliken Population analysis 20
1.3.2	Quantitative Structure-Activity Relationships (QSAR) 22
CHAPTER TWO	
2.1	The importance of Folic Acid 23
2.2.1	The Metabolism of Folic Acid (simplified description) 25
2.2.2	The Metabolism of Folic Acid 26
2.3	Dihydrofolate Reductase (DHFR)

	Page
An Introduction	31
2.3.1 Bacterial and Animal DHFR's -	
Physical and Chemical Differences	34
CHAPTER THREE	
3.1 General Considerations of the Enzyme-Substrate-Inhibitor Relationship	35
3.2 Enzyme Inhibition	37
3.3 Considerations of binding between the enzyme protein and substrate or inhibitor	39
3.4 Specificity	41
CHAPTER FOUR	
4 Inhibitors of Dihydrofolate Reductase	42
4.1 Known Inhibitors of DHFR	44
4.2 Structural Studies of Antifolate Drugs	46
4.2.1 Dihydrofolate Reductase Binding	52
4.3 Membrane Transport of Antifolates	55
4.4 Antimalarials	56
4.4.1 Cycloguanil - common features with other antifolates	58
4.5 Sulphonamides	60
CHAPTER FIVE	
5 Structures of Antifolate Carboxylates	
5.1 PYRIMETHAMINE ACETATE HYDRATE	

	Page	
5.1.1	Abstract	62
5.1.2	Experimental	64
5.1.3	Structure Analysis	66
5.2	PYRIMETHAMINE SALICYLATE ISOPROPRANOL SOLVATE	
5.2.1	Abstract	84
5.2.2	Experimental	86
5.2.3	Structure Analysis	88
5.3	PYRIMETHAMINE SALICYLATE	
5.3.1	Abstract	108
5.3.2	Experimental	110
5.3.3	Structure Analysis	112
CHAPTER SIX		
6	Structure of Substituted Antifolate AZIDOPYRIMETHAMINE ETHANESULPHONATE	
6.1	Abstract	132
6.2	Experimental	134
6.3	Structure Analysis	137
CHAPTER SEVEN		
7	Conformational Analysis	
7.1	The Theoretical Calculations of possible drug conformations and electron distribution	165
7.1.1	The Schroedinger Equation	166
7.2	Atomic Orbitals and Orbital	

	Page
Approximation	168
7.3 Molecular Orbitals	170
7.4 The Gaussian 70 Package	172
CHAPTER EIGHT	
8 Conformational Analysis and Quantitative Structure Analysis Relationships of Folates and Folate Analogues	
8.1 Conformational Analysis	174
8.2 QSAR of DHFR Inhibitors	176
CHAPTER NINE	
9 Molecular Orbital Calculations	177
Results	178
Discussion of Results	181
CHAPTER TEN	
10 Discussion and Conclusion of the Determined Crystal Structures	182
REFERENCES	194

LIST OF FIGURES

	Page
1. Structure of Folic Acid	24
2. Structure of Tetrahydrofolic Acid	27
3. The Reduction of Folic Acid	28
4. Biosynthetic Functions of Folic Acid	
Coenzymes	29
5. Comparison of the orientation of the binding of methotrexate with the pteridine ring of DHFR as compared to that of the substrate, dihydrofolate	50
6. Chloroquine and amodiaquin	57
7. Cycloguanil	59
8. Sulphonamide and p-aminobenzoic acid	61
PYRIMETHAMINE ACETATE HYDRATE	
9. Structure	63
10. Molecular Diagram	68
11. Space Filling Diagram	69
12. Packing Diagram	70
PYRIMETHAMINE SALICYLATE ISOPROPANOL SOLVATE	
13. Structure	85
14. Molecular Diagram	90
15. Space Filling Diagram	91
16. Packing Diagram	92
PYRIMETHAMINE SALICYLATE	
17. Structure	109

	Page
18. Molecular Diagram	114
19. Space Filling Diagram	115
20. Packing Diagram	116
AZIDOPYRIMETHAMINE ETHANESULPHONATE	
21 Structure	133
22. Molecular Diagram	139
23. Space Filling Diagram	140
24. Packing Diagram	141
25. Model of the Ionic and Hydrogen Bonding Link between the Antifolate Drug and a side chain carboxylate ion of DHFR	190

## LIST OF TABLES

	Page
1. Inhibitors of Dihydrofolate Reductase	45
PYRIMETHAMINE ACETATE HYDRATE	
5.1 Positional Parameters	71
5.2 Anisotropic and Isotropic Temperature Factors	73
5.3 Bond Distances	75
5.4 Interatomic Angles	77
5.5 Torsion Angles	79
5.6 Calculation of $\theta$ angle between planes	83
PYRIMETHAMINE SALICYLATE ISOPROPRANOL SOLVATE	
5.7 Positional Parameters	93
5.8 Anisotropic and Isotropic Temperature Factors	96
5.9 Bond Distances	99
5.10 Interatomic Angles	101
5.11 Torsion Angles	103
5.12 Calculation of $\theta$ angles between planes	107
PYRIMETHAMINE SALICYLATE	
5.13 Positional Parameters	117
5.14 Anisotropic and Isotropic Temperature Factors	121
5.15 Bond Distances	125
5.16 Interatomic Angles	126
5.17 Torsion Angles	128

	Page
AZIDOPYRIMETHAMINE ETHANESULPHONATE	
6.1	Positional Parameters 142
6.2	Anisotropic and Isotropic Temperature Factors 146
6.3	Bond Distances 150
6.4	Interatomic Angles 152
6.5	Torsion Angles 155
6.6	Calculation of $\theta$ angles between planes 162
9	Results of Molecular Orbital Calculations 179
10.1	Pyrimidine Ring Geometry 183
10.2	Other Geometry Features of the Pyrimidine Ring 186
10.3	Distances between Atoms connected by Hydrogen Bonds in the Determined Antifolate Carboxylate Structures 191

## Chapter One

### 1. Introduction

Crystallography today is one of the most widely used disciplines across the whole spectrum of natural and applied science. It is not only confined to its historical origin of geology but it is an accepted part of chemistry, physics, metallurgy, materials science, molecular biology and electronic engineering.

Single crystal X-ray crystallography was pioneered by W.H.Bragg and W.L.Bragg, whose technique enabled basic information of the crystals to be obtained from X-ray analysis. The distances between the various crystal planes and the angles at which the planes intersect are determined, from which the arrangement of the particles and the distances between them can be ascertained. From the X-ray diffraction patterns the electron density in different parts of a crystal can be deduced. As X-ray scattering is caused not by atomic or ionic nuclei but by the electrons round the nuclei, the scattering is greater where the electron density is larger, i.e. in the immediate neighbourhood of the nuclei.

From electron density maps of this kind, shapes of molecules and ions can be found, as well as their structural formulae and the bond lengths between the nuclei. Bond lengths in turn give information about the nature of the bond, for example the amount of ionic character present and whether the bonds are

single or multiple.

X-ray crystallography is not a means to an end by itself, it must be used in parallel with the more standard and routine chemical techniques such as infra-red and nuclear magnetic resonance spectra, as well as using subjective judgement and experience to interpret its results.

## 1.1 Selection of a Crystal

Crystals are built up from simple structural units composed of a few atoms, ions or molecules. The crystal is merely a repetition of the basic unit, just as the pattern woven into a piece of cloth consists of the same design repeated over and over again. For a crystal to be satisfactory for collection of X-ray diffraction data, two main requirements must be met :-

1. It must possess uniform internal structure
- and 2. it must be of proper size and shape.

To fulfil the first requirement, the crystal must be pure at the molecular, ionic or atomic level. It must be a single crystal in the usual sense, i.e. not twinned, which is the existence of two different orientations of a lattice in what is apparently one crystal, nor composed of microscopic subcrystals. The crystal need not have particularly well-formed or uniform external faces but should not be physically distorted.

All single crystals are in a sense, imperfect as they are composed of slightly misaligned, not more than  $0.2^\circ$  to  $0.5^\circ$  for most crystals, minute crystal blocks. These crystals with a mosaic structure are desirable as the diffracted intensities are much greater than from perfect crystals.

Crystals are easily screened by examination between crossed polaroid sheets, by rotation about an axis normal to the polarizing material, in which the crystals should appear bright and extinguish once every  $90^\circ$ .

The preferred crystal size is of 0.1 to 0.3mm because of the difficulties in aligning the crystal precisely with a plateau of uniform intensity in the primary X-ray beam. The size of crystal is also determined by the absorption of X-rays by the crystal (1).

## 1.2 Limitations and scope of X-ray Crystallography

Apart from the obvious difficulty of growing a suitable crystal which will diffract X-rays to the desired extent, the collection of X-ray diffraction data has been facilitated in recent years by the development of computer software and hardware. Analysis of the data has also been made easier by computer integration.

For simple crystals, knowledge of the symmetry and unit cell dimensions enables the exact structure to be determined. Each measured observed intensity of X-rays must be related to the distribution of atoms within a known set of planes (hkl). Theory shows that the measured intensity  $I_{hkl}$  after suitable correction is equal to the square of the structure factor  $F_{hkl}$ . The significance of  $F_{hkl}$  is that it can also be calculated once the positions and scattering power of the atoms within the unit cell are known. An obvious approach, therefore, would be to guess the position of all the atoms and then calculate the  $F_{hkl}$  values. Good agreement between calculation and experimental data would confirm the correct structure. Unfortunately this trial and error method is not practical because there are many possible positions for each atom in the unit cell, even though some intelligent guesses can be made.

In practice, the reverse procedure is adopted in which the atomic positions are determined from the measured intensities, by the use of a mathematical technique, Fourier synthesis, which

maps out the electron density distribution within a unit cell. The positions of atoms can be determined by noting where the electron density rises to peak values.

A major obstacle in the use of Fourier synthesis is the phase problem, in that in order to construct the electron density map both the phases and magnitudes of  $F_{hkl}$  must be known. Experimentally, only the magnitudes of  $F_{hkl}$  are measured as intensity  $I$  is proportional to  $F_{hkl}^2$ .

In 1955 it was thought that the limit of complexity in structural determination by X-rays had been reached when Hodgkin determined the structure of vitamin B<sub>12</sub> which consists of 181 atoms. However Perutz in 1953 realised that the isomorphous replacement technique was equally applicable to protein molecules which contain thousands or even tens of thousands of atoms. To determine the structure of such an enormously complex system, some 500,000 intensities must be accurately measured and perhaps one million calculations performed. Largely as a result of the recent rapid development in high speed digital computers and the improvement in instrumentation for recording and measuring intensities, the task is not as hopeless as it may seem at first.

Computers have then allowed data to be collected for hours on end by complete automation, correcting for any absorption of X-rays by the crystal and for any degeneration of the crystal while it is subjected to the X-rays or unfavourable atmospheric conditions.

To overcome this phase problem either direct or indirect

methods may be used. Direct methods are the more objective in that they depend upon mathematical relationships to determine the phases of the structure factors. Indirect methods are more subjective in that they depend upon the interpretation of the data by the investigator.

#### DIRECT METHODS

Direct method computer programs require that the structure factors be placed on an absolute basis. The magnitude of a structure factor depends not only on the degree to which atoms scatter co-operatively but also on the scattering angles, since atoms scatter less strongly at high angles. From a theoretical point of view there is an advantage in producing a structure factor which is corrected for fall off in scattering angle such that the numerical value of the structure factor is independent of its position in reciprocal space.

The computer programs which have been used in the structure determinations are :-

- ( i)       MULTAN 78 - which is used to calculate normalised structure factors and carries out direct methods for the largely automatic solution of crystal structures with up to about 150 atoms in the asymmetric unit; it is applicable to both centrosymmetric and non-centrosymmetric structures (2).
- (ii)       EES (SHELX) - an alternative centrosymmetric direct methods approach. This approach is to start with a very large number of permutations of signs

(of the order of  $2^{10}$  to  $2^{20}$ ) and to eliminate early on during sign expansion those sets which are giving poor agreement. If, at any stage, the agreement fails to reach a prescribed level then the expansion is discontinued and the set rejected. For the surviving sets electron density maps are computed and figures of merit are calculated (3).

The choice of which direct methods package to use can be largely determined by whether the structure was centrosymmetric or not. For centrosymmetric structures SHELX was favoured, whilst for the non-centrosymmetric structures MULTAN became the standard choice.

#### REFINEMENT AND WEIGHTING

A refinement program based on the least squares procedure calculates structure factors and accumulates least squares totals which are then solved for the parameter changes. The parameters which are then refined are :-

- ( i ) either the individual atomic isotropic vibration parameters or the six components of the individual atomic anisotropic vibration tensors.
- ( ii ) the  $|F_{\text{calc}}|$  scale factor.
- (iii) the atomic co-ordinates.

The parameters are treated as functions of  $|F_{\text{calc}}|$  and the least squares procedure minimises the function :

$$w ( |F_{\text{obs}}| - |F_{\text{calc}}| )^2$$

where ' w ' is a weight allocated to each structure factor.

Small variations are made to these parameters to produce

the test agreement between observed and calculated structure factors. A cyclic process is carried out and after each cycle an improved value for each parameter is obtained. The procedure is repeated until no further improvement takes place, as shown by the discrepancy index, R.

The actual weighting system used reflects the reliability of the particular measurement and the weight parameter is determined by the reciprocal of the square of the standard deviation of the measurement.

In the initial stages of refinement a weight of unity may be used for all reflections, but in later stages a weighting scheme is introduced which is dependent on  $F_{obs}$ .

THE ' R ' VALUE - DISCREPANCY INDEX OR RESIDUAL

This is defined as :-

$$R = \frac{\sum |F_{obs} - F_{calc}|}{\sum |F_{obs}|}$$

The  $F_{calc}$  's must include temperature factors for the structure factors to be comparable.

The lower the value of R the greater the confidence that can be placed in the calculated structure. At present R values in the range 0.03 to 0.08 i.e. 3% to 8% are being quoted for the most reliable determined structures.

The R value is by no means a perfect guide to the correctness of fit of the structure and much subjective judgment

and experience must be used in analysing the results to date  
and the further steps needed in the refinement.

### 1.2.1 Scattering factors and Thermal motion

A further limitation of X-ray diffraction is that as the scattering factors increase steadily with increasing atomic number  $Z$ , it becomes more difficult to distinguish between atoms of close atomic number and also that the scatter from the lighter elements is low by comparison. This is particularly the case for hydrogen and causes difficulty in locating these atoms in a structure.

The scattering factor falls off with increasing angle of scatter since the wavelength of the radiation is of comparable size with the scattering centre.

The normal scattering factor curves are calculated on the basis of the electron distribution in a stationary atom, but in fact, the atoms in crystals are always vibrating about their rest points. The magnitude of the vibration depends on the temperature, the mass of the atom and the firmness with which it is held in place by covalent bonds or other forces. In general though, the higher the temperature the greater the vibration.

The effect of such thermal motion is to spread the electron cloud over a larger volume and thus to cause the scattering power of the real atom to fall off more rapidly than that of the ideal stationary model. An approximation of the corrected structure factor for thermal motion can be made mathematically by the use of the Wilson plot (4).

The correction for thermal motion may be applied to structure factor calculations at several levels of approximation. The simplest of these is that of over-all isotropic vibrations which assumes that all the atoms are vibrating with the same amplitude and that their motions, like their shapes, are spherically symmetric. This approximation makes for faster computation as the thermal factor need only be evaluated once per reflection and the result used to multiply the calculated structure factor.

This approximation of equal amplitudes is not a very good one because, for example an atom at the end of a long aliphatic chain can reasonably be expected to be less firmly braced by its neighbours than say a quaternary carbon in a rigid ring structure. The individual isotropic assumption permits the assignment of temperature factors to each atom but retains the idea of spherical symmetry and can improve the fit between the observed and calculated data markedly as the individual temperature factors have physical significance. This assumption can then be utilized in the early stages of a structural analysis to identify significant incorrectly placed atoms by their abnormally high temperature factors.

This added computation must then be evaluated for each atom contributing to each reflection and must be used to modify the scattering factor for that atom.

A different approximation can be made, the individual anisotropic, in which the assumption of spherical symmetry is

abandoned and the single atomic thermal parameter is replaced by six parameters which describe the size and orientation of the vibration ellipsoid. Each atom must then be treated individually, again increasing computation time significantly.

### 1.2.2 Electron and Neutron Diffraction as a complement to X-ray methods

---

Initially it was thought that X-rays were the only radiation which would give the desired diffraction effect. However, it was found that if electrons and neutrons were given the required velocity then from the de Broglie theory, diffraction effects would result at the molecular level, i.e. wavelengths in the region of 0.1 to 2.0 Å.

Using X-ray radiation it is difficult to detect the hydrogen atom as it has a relatively low scattering factor, whereas both electron and neutron diffraction methods are suitable for positioning the hydrogens in a structure and this could be done after the heavier atoms have been positioned using X-ray methods. Practical difficulties involved with both electron and neutron diffraction however make it very unlikely that either of them will replace X-ray diffraction as the most convenient and useful method of structure determination.

### 1.2.3 Solid state versus Natural state structure

X-ray crystallography looks at the structure of compounds, particularly with reference to enzyme substrates and inhibitors, out of their biological environment. There is then the question of how similar the structure so determined is to that in biological systems. Are the atoms in the active site of the crystalline enzyme in the same position as they are in the biological system? This question is of great importance pharmaceutically as the development of drugs may rely on X-ray determined structures of the enzyme which the drug is intended to inhibit.

The folding, structural stability and dynamics of globular proteins are thought extensively controlled by solvent interactions, stress being generally placed on the poorly understood so-called "hydrophobic" or "apolar" interactions. Similar driving forces are invoked to explain the energetics of enzyme-substrate binding, the binding of a hormone to its receptor and protein-protein interactions in general.

Crystalline proteins contain upward of about 25% solvent, a typical value being 45%, and at the molecular level solvent-protein interactions would be expected. Thus, provided the structure of the crystal can be solved by X-ray diffraction techniques to a sufficiently high resolution, it is possible to extract significant information concerning the results of solvent interactions especially at the protein-solvent interface.

This information can then be used to test the predictions of any protein-solvent interaction model (5).

The reduced number of solvent interactions that may occur in the X-ray structure must then be borne in mind in analysing the structure. The development of such techniques as interactive computer graphics has greatly aided the study of drug design. Such apparatus as the Evans and Sutherland Picture System is capable of rapid transformation of three dimensional data with combinations of rotation, translation, scaling and perspective. This system is extremely efficient for the display and manipulation of complex biological molecular structures. The electron density based on the method of isomorphous replacement or calculated on the basis of the refined atomic positions is displayed in the form of a "chicken wire" and the model is manipulated into the density.

The existence of highly refined models of enzymes together with the ability of manipulation of these molecular structures offers the attractive possibility of a rational approach to drug design. This method has already been used on the detailed structure of an enzyme and a complex with a substrate analogue to aid investigation concerning the design of a good inhibitor. Dihydrofolate reductase inhibitors ( which form the theme of this thesis) have already been investigated by this technique.

The enzyme active sites can be displayed in various ways : van der Waals surfaces or accessible surfaces, highlighting hydrophobic or charged groups or specific residues. Complementary

surfaces can be generated; models of putative inhibitors placed in the active site while the energy, change of surface accessibility and other parameters are continuously monitored (6).

### 1.3 Molecular Geometry Calculations

Conformation is the molecular property which is of most interest to researchers interested in small biologically active molecules. As the majority of "interesting" molecules are conformationally flexible, molecular models can be used to answer questions about the molecular geometry of a molecule which may have a whole range of possible conformations because of free rotation about single bonds. Computer programs are available which calculate the ab initio molecular wave function and then optimize the geometry using a gradient of the energy with respect to the nuclear coordinates. The computer program used in this thesis was a version of the Gaussian 70 package and is further detailed in a later chapter.

Some twenty years ago molecular wave functions were calculated by using semi-empirical methods which were only approximations to the true value and the advent of computers aided such calculations.

Since modern quantum theory began nearly 60 years ago the basic idea of quantum theory has been applied to all kinds of chemical problems. However the major difficulty is that of obtaining reasonably good wave functions for any but the smallest molecules. Crystal data in molecular orbital calculations must be used with caution as molecules may not have precisely similar shapes in a crystal and in solution or in an active environment. Crystal structures of ions may vary

depending on the nature of the counter-ions.

Similarly the active conformation of a drug may not be that stable in the solid or in solution and indeed may not be stable at all except in the receptor environment. It has also been proposed that several local minima may exist on the energy hypersurface besides the one corresponding to the experimental configuration (7).

In principle the Schrodinger equation does contain all the answers and in time it will no doubt be possible to run calculations for huge systems which will include solvent, receptor, counter-ions and all the particles involved in biological recognition and activity.

### 1.3.1 Charge Distribution and Mulliken Population Analysis

Apart from nuclear conformation, of interest are details of the electronic charge distributions which can be revealed by calculation. Such calculations are of particular pharmaceutical interest; where a pharmacological receptor experiences the influences of a drug or transmitter molecule, it must do so by the interaction of electron densities on the two partners. Charge distribution is unobtainable from experiment and hence the application of quantum mechanics to pharmacology is of central importance.

A conveniently programmed method of gaining an idea of charge distribution in molecules comes from the so called Mulliken Population Analysis. This produces the number of electrons associated with a particular atom, even though they may not spend much time very close to the particular nucleus. In this way all the electrons in the molecule are assigned to nuclei. The limitation of this approach is that all the charge is associated with nuclei i.e. the charge between two nuclei is divided equally between the two, even if the atoms have very different electronegativities. The use of the information on the distribution of electrons derives from the fact that the chemistry, the affinity, the efficacy and the reactivity of a molecule are properties of electrons. When molecules encounter each other it is the electrons which interact and such calculations of charge distribution on similar molecules indicate

trends rather than absolute values which are more meaningful.

### 1.3.2 Quantitative Structure-Analysis Relationships (QSAR)

---

This mathematical technique uses computerized statistical studies of the relationship between chemical structure and biological activity. The QSAR model assumes that in varying substituents on a parent structure one changes its hydrophobic, steric and electronic characteristics and these perturbations which are reflected in the biological response of a standard system can be more or less accounted for in the physicochemical properties of the substituents.

The research using QSAR on dihydrofolate reductase inhibitors which is the subject of this thesis is reviewed in a later chapter.

## Chapter Two

### 2.1 The importance of Folic Acid (Folacin or Pteroyl-Glutamic Acid)

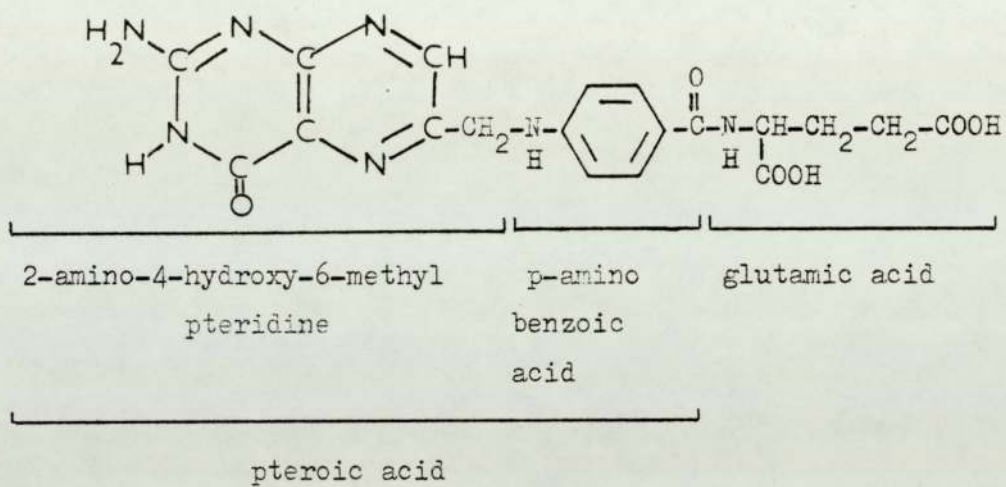
Folic acid is broadly distributed in plants and its deficiency in mammals results in failure to grow and in various forms of anaemia. It contains three characteristic building blocks: (1) a substituted pteridine, (2) p-aminobenzoic acid and (3) glutamic acid (see Fig. 1).

Pteridine is the bicyclic nitrogenous parent compound of the pterins which are derivatives of 2-amino-4-hydroxypteridine. The pterin present in folic acid is 6-methyl pterin. In some species folic acid is attached by the  $\gamma$ -carboxyl group of the glutamic acid to one or more additional glutamic acid residues joined in peptide linkages involving the  $\gamma$ -carboxyl groups of the glutamic residues. Some organisms require only the p-aminobenzoic acid portion of folic acid; they can synthesize folic acid if p-aminobenzoic acid is available (8).

The most conspicuous biochemical symptom of folic acid deficiency is impaired biosynthesis of purines and the pyrimidine, thymine. Recent studies have shown a relationship in mammals between folate deficiency, heme content and microsomal drug metabolism (9).

FIGURE 1.

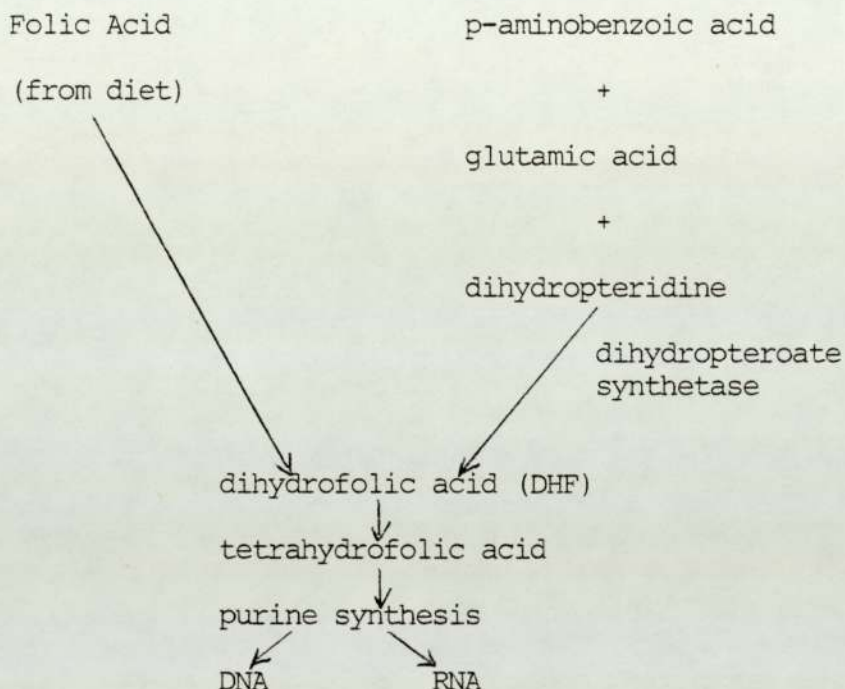
STRUCTURE OF FOLIC ACID



2.2.1 The Metabolism of Folic Acid, simplified  
biological mechanism

For mammals :

For some micro-organisms :



Animal cells are incapable of synthesizing folate and it must then be obtained from exogenous sources.

The folic acid is transferred into the cells by an active transport mechanism.

Unicellular organisms are wholly dependent on the synthesis of DHF de novo.

For both animal and micro-organism, although folic acid is the vitamin, its reduction products are the actual coenzyme forms.

### 2.2.2 The metabolism of Folic Acid

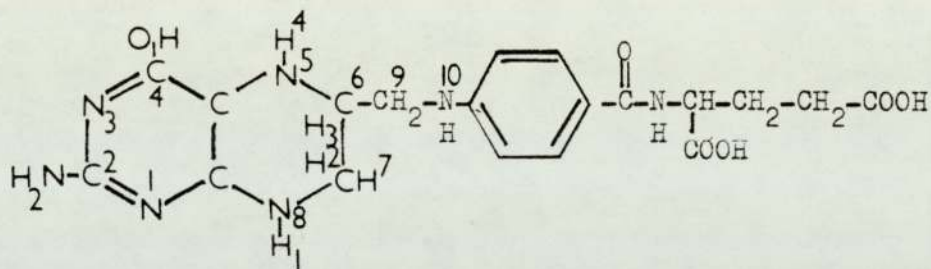
The B vitamin, folic acid I is reduced enzymatically in the cell to tetrahydrofolic acid (  $\text{FAH}_4$  or 5,6,7,8 tetrahydrofolate) III (see Fig.2) via 7,8 dihydrofolic acid (  $\text{FAH}_2$ ) II. Any one of five enzymes can then be used by a cell to catalyze the attachment of a one carbon fragment at the formaldehyde or formic acid oxidation level by  $\text{FAH}_4$  on either  $\text{N}^5$  or  $\text{N}^{10}$  or both (see Fig. 3).

The one carbon fragment may be either hydroxymethyl ( $\text{CH}_2\text{OH}$ ), formyl ( $\text{CHO}$ ), or methyl ( $\text{CH}_3$ ) groups in a large number of enzymatic reactions in which such groups are transferred from one metabolite to another or are interconverted (see Fig.4 ). These complex one-carbon transfer reactions are involved in the intermediary metabolism of amino acids, purines and pyrimidines. The former are used in the formation of proteins and the latter in DNA synthesis.

The function of folic acid is then to insert a single carbon unit wherever required in the biosynthesis. For example, a sequence of enzymatic reactions in which the hydroxymethyl group of the amino acid, serine is enzymatically removed to form the  $\text{N}^5, \text{N}^{10}$  methylene derivative of tetrahydrofolate ( $\text{FAH}_4$  ), which is reduced to the  $\text{N}^5$  methyl derivative. The latter then donates its methyl group to homocysteine to yield methionine. Tetrahydrofolate thus serves as a shuttle to which the one carbon group is covalently but transiently attached :-

FIGURE 2.

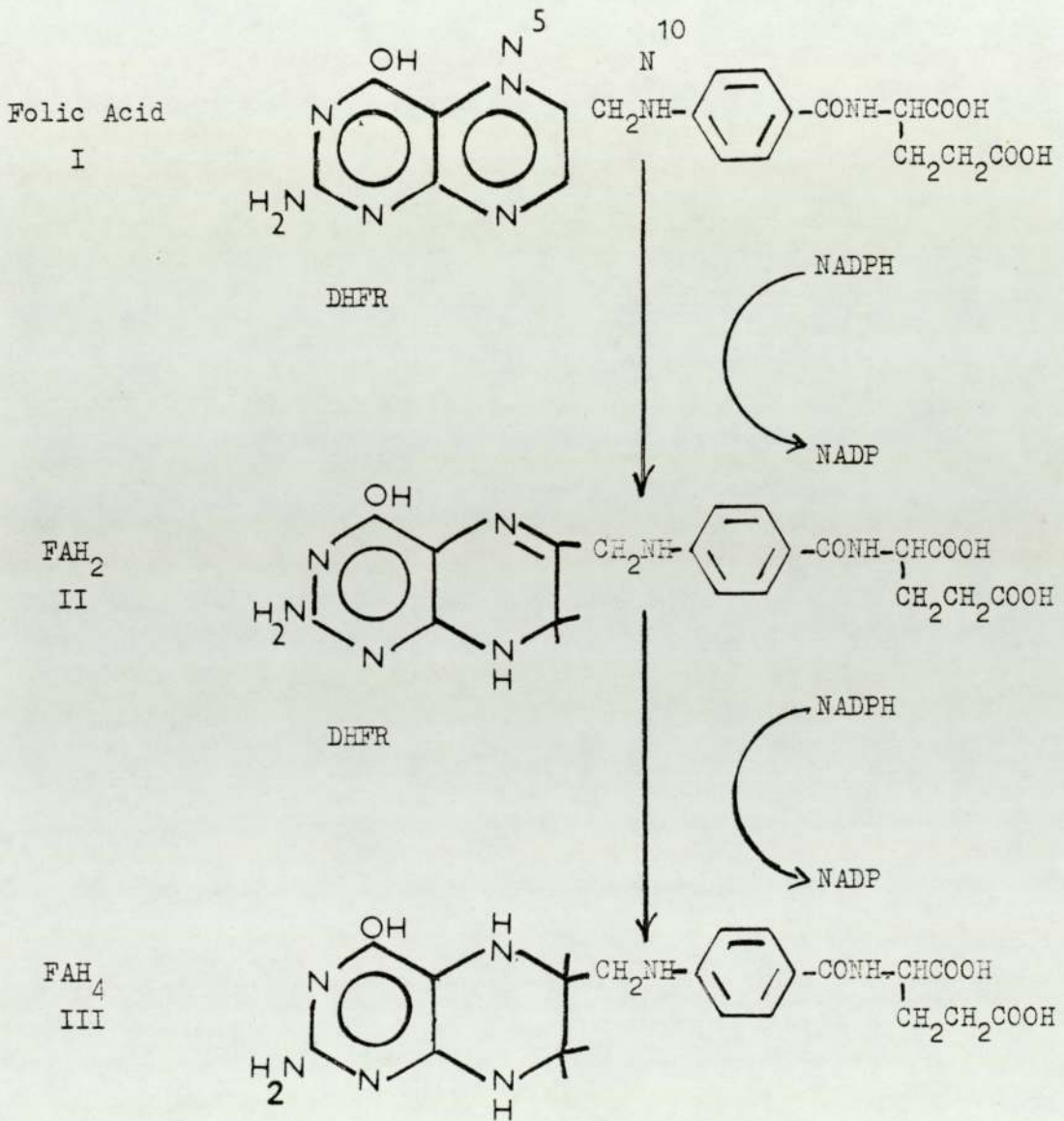
STRUCTURE OF TETRAHYDROFOLIC ACID



The hydrogens H<sub>1</sub> to H<sub>4</sub> (inclusive) are those added to folic acid to give tetrahydrofolic acid. The N<sub>5</sub> and N<sub>10</sub> nitrogen atoms participate in the transfer of one-carbon groups.

FIGURE 3

THE REDUCTION OF FOLIC ACID

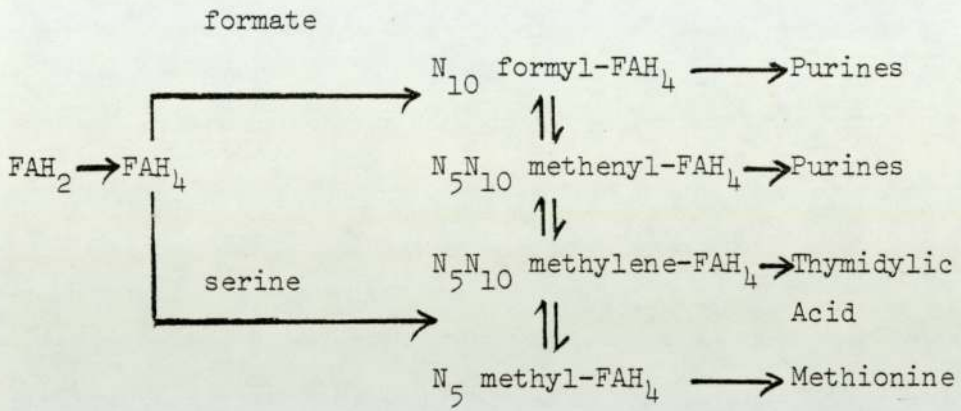


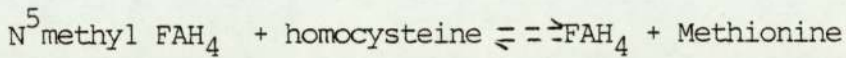
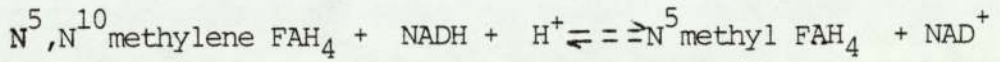
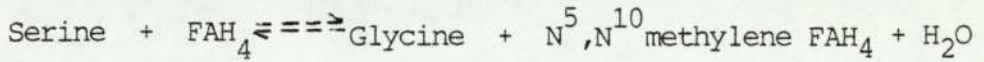
NADP : nicotinamide adenine dinucleotide phosphate

DHFR : dihydrofolate reductase

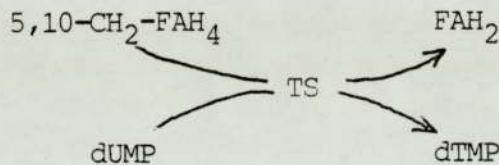
Figure 4. Biosynthetic Functions of Folic Acid Coenzymes  
( 10 ).

---





Another enzyme vital to the folic acid reduction is thymidylate synthetase which is uniquely involved in the internal oxidation reduction of an intermediate which takes place when deoxyuridylate (dUMP-2'-deoxyuridylate) is converted to thymidylate (dTMP).



TS = Thymidylate synthetase

As a result a blockade of dihydrofolic reductase prevents the coupled thymidylate synthetase from operating, leading to a cellular deficiency of dTMP. Therefore blockade of either dihydrofolic reductase or thymidylate synthetase in a cell will lead to 'thymine-less death', if the cell is unable to use the alternate pathway via thymidine with thymidine kinase (11).

### 2.3 Dihydrofolate Reductase (DHFR) - An Introduction

DHFR is classified into structural class No. 4, i.e.  $\alpha$ -helix and  $\beta$ -sheet tend to alternate along the amino acid chain. The whole of the protein is defined as the structural domain in relation to the globular protein with 160 - 180 residues (depending on species) in the domain, with one domain per globular protein. There are two structurally known enzymes with NADP as cofactor, one of which is dihydrofolate reductase. In DHFR, NADP is bound to the domain containing a  $\beta$ -sheet and  $\alpha$ -helices (12). The polypeptide backbone is folded into an eight-stranded  $\beta$ -sheet consisting of seven parallel strands and ending with a single anti-parallel strand at the carboxyl end, with approximately 35% of the backbone being in the  $\beta$ -sheet (13).

The other enzyme, glutathione reductase, binds the NADP in a domain with a central pleated sheet. This sheet contains a Rossmann fold which binds the adenosine moiety of NADP in a position corresponding to the equivalent site in dehydrogenases.

DHFR and TS appear to be ubiquitous having been found in bacteria, plants, certain phages as well as in animal tissues and cell lines. It has been found that high levels of these enzymes are present in cells that are actively dividing. Since rapid cell proliferation and therefore DNA synthesis is one characteristic of most malignant tissue, inhibition of the thymidylate cycle at the level of either DHFR or TS should cause

the cessation of malignant tissue growth.

To date only a few amino acid sequences of DHFR from both prokaryotes and eukaryotes have been determined and there are no crystallographic studies to date on folate or dihydrofolate bound to DHFR. However structural studies have been carried out, to 1.7 Å resolution, on the binary complex (inhibitor only bound to the enzyme) of Methotrexate (MTX)-resistant E.Coli DHFR with MTX (13), the ternary complex (inhibitor and coenzyme bound to the enzyme) of MTX-resistant *Lactobacillus casei* DHFR with MTX and NADPH (13) and to 2.9 Å resolution on the avian DHFR ternary complex with phenyltriazine and NADPH(14). These structures are considered in further detail in Chapter Four.

These studies have defined the overall shape of the enzyme molecule, identified regions of secondary structure and binding areas for inhibitor and cofactor. As there are indications of differences between the protein conformational structures in the enzyme-MTX and enzyme-substrate complexes, direct analogy from the X-ray results to a description of enzyme-substrate binding is not easy.

It appears that although there are considerable changes in the primary structure of the enzyme (i.e. amino acid sequence) between species the tertiary structure and hence function of the enzyme remains comparatively unchanged. For example, the backbone of *Lactobacillus casei* DHFR is structurally similar to that of E.Coli although there is only an amino acid sequence homology of approximately 27% (14). There is also considerable

species-to-species variability in sensitivity towards different inhibitors in this group of enzymes.

### 2.3.1 Bacterial and Animal DHFR - Physical and Chemical Differences

---

All mammalian and avian, but only a few bacterial DHFR's can utilize folic acid as a substrate, as previously stated; however the  $pH_{\text{maximum}}$  with folic acid is between 4 - 5.5 and reduction is near zero at pH 7. The enzymes utilizing folate as a substrate with dihydrofolate usually show a double maximum, one at pH 4- 5.5 and the other near pH 7.4; at pH 7.4 folate is a good inhibitor of DHFR, being complexed to the enzyme better than the dihydrofolate. Those bacterial enzymes which cannot utilize folic acid as a substrate have only one  $pH_{\text{maximum}}$  near pH 7.4.

An inhibitor profile for each enzyme from inhibitor binding analysis could be prepared. It was found that intergroup differences could be very large. For example 50% inhibition of mammalian enzymes required concentrations of one inhibitor, trimethoprim, of the order of  $10^{-4}$  M while for bacterial enzymes less than  $10^{-8}$  M was required. In contrast a dihydrotriazine inhibited mammalian enzymes at  $10^{-7}$  M. Intragroup differences were found more so among bacterial than among mammalian enzymes (15).

The majority of the enzymes had molecular weights of the order of 20,000. Bacterial enzymes have molecular weights nearer 18,000 whilst mammalian enzymes are about 21,000.

## Chapter Three

### 3.1 General Considerations of the Enzyme - Substrate - Inhibitor Relationship

---

Enzymes are a billion times more efficient than man-made catalysts although they operate within the limits of biological conditions. A fascinating property of enzymes is their catalytic power. Enzyme - catalyzed reactions proceed at rates that are from  $10^8$  to  $10^{20}$  times faster than the corresponding uncatalyzed reaction. Traditionally, enzymes are compared with man - made catalysts which as a rule are  $10^8$  to  $10^9$  times less effective in accelerating a given reaction than the corresponding enzyme.

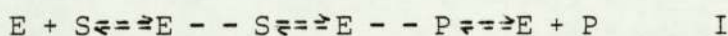
Another attribute of an enzyme, which a chemical catalyst possesses only in rare cases, is specificity of action. Only one or a few compounds, the substrate(s), are acted upon and only a single type of reaction takes place. Side - reactions or by - products do not occur, a reflection of the fact that uncontrolled pollution cannot be tolerated in a living cell (12).

The characteristic of enzyme catalysis is then that the enzyme specifically binds its substrates and the reactions take place in the confines of the enzyme-substrate complex. To understand then how an enzyme works, not only must the structure of the native enzyme be known but also that of the complexes of enzyme with substrate intermediates and products. Once these are determined, how the substrate is bound, what catalytic

groups are close to the substrate and what structural changes occur in the substrate and enzyme on binding will be known. In these determinations there is one major difficulty: enzyme-substrate complexes react to give products in fractions of a second whilst the acquisition of X-ray data usually takes several hours. It is therefore necessary to determine the structures of the complexes of enzymes with the reaction products, inhibitors or substrate analogues (16).

### 3.2 Enzyme Inhibition

In simple terms an enzyme E complexes with a substrate S and converts S to the product P :-

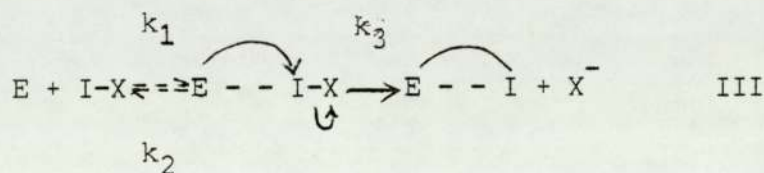


An inhibitor of the enzyme I must have an affinity for the enzyme :-



Since the inhibitor can complex reversibly in this case with the enzyme to form an E - I complex, less free enzyme E is then available for conversion of S to P; hence the resultant conversion is inhibited to an extent depending upon the relative concentrations of S and I and their relative equilibrium constants with E, namely  $K_S$  and  $K_I$  respectively.

The study of the inhibition of dihydrofolate reductases involved both reversible and irreversible mechanism, including for the irreversible type: an inhibitor I bearing a properly positioned leaving group X which can form a reversible complex with the enzyme E - I-X and then react further irreversibly:-



The kinetics of such reactions are described in reference (16).

In contrast to the reversible E - I complex in II which can dissociate to free inhibitor and active enzyme E, the irreversibly inhibited enzyme E - I in III can vary from

inoperative to poorly operative. The rate of formation of such a covalently linked enzyme-inhibitor complex is dependent upon the concentrations of the E - - I-X complex, the nucleophilicity of the enzymic group being alkylated, the relative reactivity of the leaving group X and the ease of formation of the transition state E - - I-X is in turn dependent upon the concentration of the inhibitor I-X and upon the reversible dissociation constant of the enzyme-inhibitor complex.

Irreversible inhibitors then have an extra dimension of specificity dependent on the equilibrium constant  $k_3$  in III that does not exist with reversible inhibitors. Also, the affinity of the enzyme for the inhibitor is most usually due to the complexing ability of the enzymic active-site for a substrate and its mimic, the inhibitor. Such a neighbouring group reaction within an enzyme-inhibitor complex to give an irreversibly inhibited enzyme is called active-site directed irreversible inhibition (17).

### 3.3 Considerations of binding between the enzyme protein and substrate or inhibitor

As an intermediate complex is formed in an irreversible inhibition reaction, much research has been done on the binding forces that cause an affinity of the enzyme for the inhibitor. On the enzyme itself, the binding groups can only arise from the nature of the twenty different amino acids which may occur in the enzyme plus any metal ions associated with the enzyme and cofactor; on the inhibitors much greater variation may be incorporated into the types of groups.

There are only four major types of interaction between enzyme and inhibitor and the strength of the complex is dependent upon the nature and strength of each bonding :-

1. anionic-cationic(electrostatic) interactions
2. hydrogen bonds
3. charge-transfer complexes
4. hydrophobic bonding and the accompanying van der Waals forces (17).

It is possible therefore for a multi-atom functional group, such as an amide or a phosphate, to have several modes of binding simultaneously, for example, with the -CONH group, the hydrogen can be an acceptor and the oxygen a donor - the type of bonding responsible for the helical portions of proteins.

For the design of active-site-directed irreversible inhibitors it is then necessary to know which groups on the substrate or inhibitor complex with the enzyme. Although the type of bonding present may not be able to be differentiated, for example, between hydrogen bonding and charge transfer, X-ray crystallographic studies of inhibitors complexed with the enzyme will give an indication of which amino acid on the protein is adjacent to an inhibitor functional group.

3.4 Specificity :- How much difference in protein structure must there be for an active-site inhibitor to inhibit the tumorigenic cell and not the original normal cell?

---

When a tumorigenic virus invades a normal cell the viral coding information becomes an integral part of the original cell. This produces a cancer cell which contains the genetic information of both the virus and the original cell. In order for the cell to reproduce more rapidly, DNA must be synthesized more rapidly which requires more dihydrofolate reductase and more thymidylate synthetase. As the new enzymes are coded by the nucleic acid present originally in the virus, they could presumably be subtly different from the original two enzymes.

Active-site directed irreversible inhibitors use the similarity in the active site, used by reversible inhibitors but also use the specificity of less functional parts of the enzyme for irreversible covalent bond formation. The area of the enzyme outside the active-site is one in which structural differences of the substrate-identical enzyme in different tissues are likely to occur, as little structural change can be tolerated in the active-site before the enzyme ceases to be functional.

## Chapter Four

### 4. Inhibitors of Dihydrofolate Reductase

Folate and dihydrofolate have quite complex structures compared to most monomeric substrates in that they have eleven different polar groups and two  $\pi$ -electron systems that can complex with dihydrofolate reductase: it has been estimated that in the order of three to six of these groups would be sufficient for binding to give the observed binding constants (18).

The mode of binding of inhibitors to dihydrofolate reductase is still not completely understood even after much research. Complications arise when the binding of individual groups on inhibitors are assigned, as strongly hydrophobic bonding occurs with the dihydrofolate reductases. As a result of this extreme hydrophobic bonding, it is likely that an inhibitor can complex to DHFR in one of several possible rotameric conformations, depending upon the one giving maximum hydrophobic bonding. Hence conclusions on a single type of inhibitor are not general but relate to the binding of specific groups on an inhibitor.

Inhibitors of DHFR have commonly been termed "antifolates". The earliest reported small molecule antifolates were the 2,4 diaminopteridines, by Daniel et al (19,20), which were synthesized to simulate the pteridine portion of the folate molecule and the authors concluded that the 2,4 diamino

derivatives were much more potent inhibitors of lactic acid bacteria than the chemically more nearly related 2-amino-4-hydroxypteridines. It was also noted that there were differences in responses between *Lactobacillus casei* and *Streptococcus faecalis* and it was concluded that these micro-organisms had multiple systems dealing with folates which existed in different proportions in the two.

In 1945, Hitchings et al (21) studied 2,4 diamino-5-methyl pyrimidine and then used the elaboration of the 5-methyl group to develop a family of inhibitors. By 1948, (22) evidence was gathered that all derivatives of 2,4 diamino pyrimidines were antagonists of folic acid and in 1951 (23) a variety of substances were developed primarily toward antimalarials. This latter study queried the association between antifolate and antimalarial activity.

Antimalarial activity had been postulated for the antifolates on the basis of a formal resemblance between 2,4 diamino-5-p-chlorophenoxy pyrimidine and the antimalarial chlorguanide (24), but chlorguanide was the more potent antimalarial and relatively weak as an antifolate. However this discrepancy was resolved when the biologically active chlorguanide metabolite was found (25) to be a dihydrotriazine derivative with an appropriate degree of antimalarial activity.

In Table 1. are listed some inhibitors of DHFR that are close analogs of folic acid except pyrimethamine. Folic acid is an excellent inhibitor of the vertebrate DHFR, being complexed two to ten times better than the substrate, dihydrofolate. Replacement of the 4-hydroxy group of folates by a 4-amino group as in aminopterin gives a tremendous enhancement in binding.

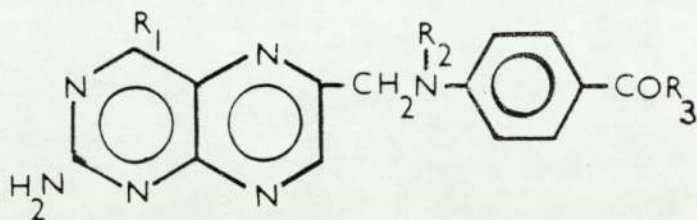
Pyrimethamine has a considerably abbreviated structure compared to the others. Methotrexate and aminopterin bind 10,000 to 50,000 times more tightly to DHFR's than does folate.

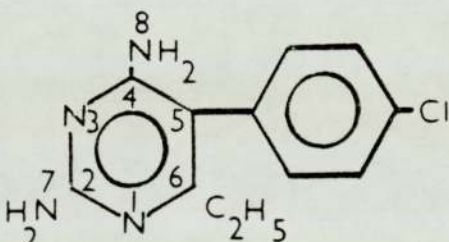
The binding of trimethoprim TMP has been found to be sufficiently different to chicken and E.Coli dihydrofolate reductases perhaps to explain TMP's much weaker binding to the chicken enzyme. This has been reported to be due to the residues on opposite sides of the active site cleft being 1.5 - 2.0 Å further apart in the chicken dihydrofolate reductase than the structurally equivalent residues in the E.Coli enzyme and other factors notably :

1. differences in exact positioning of the 2,4 diaminopyrimidine ring,
2. differences in the benzyl group binding sites as well as other stereochemical factors (26).

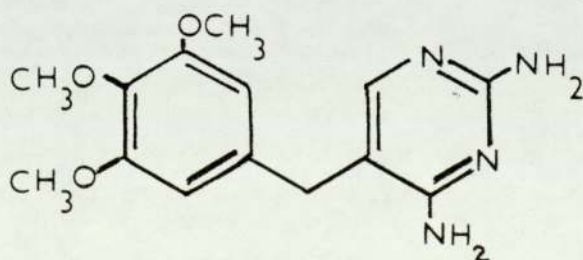
Table 1.

INHIBITORS OF DIHYDROFOLATE REDUCTASE



Name	R <sub>1</sub>	R <sub>2</sub>	R <sub>3</sub>
Folic Acid	OH	H	-NHCHCOOH   CH <sub>2</sub> CH <sub>2</sub> COOH
10-Formyl Folic Acid	OH	$\begin{array}{c} \text{O} \\    \\ -\text{CH} \end{array}$	-NHCHCOOH   CH <sub>2</sub> CH <sub>2</sub> COOH
Aminopterin	NH <sub>2</sub>	H	-NHCHCOOH   CH <sub>2</sub> CH <sub>2</sub> COOH
Pyrimethamine			
Amethopterin (Methotrexate - MTX)	NH <sub>2</sub>	CH <sub>3</sub>	-NHCHCOOH   CH <sub>2</sub> CH <sub>2</sub> COOH
Aspartate analog of Amethopterin	NH <sub>2</sub>	CH <sub>3</sub>	-NHCHCOOH   CH <sub>2</sub> COOH

Trimethoprim

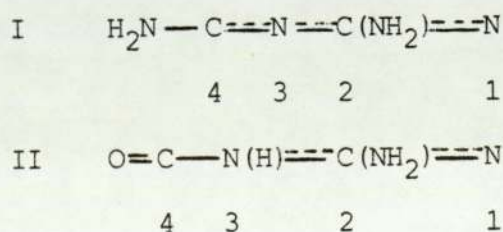


#### 4.2 Structural Studies of Antifolate Drugs

The natural substrates for DHFR contain a 2-amino-4-oxo pteridine moiety whereas the most effective inhibitors are 2,4 diamino derivatives of pyrimidine, triazine, pteridine or quinazoline. The enhanced affinity of these antifolates can be explained by the modified pattern of hydrogen bond donors and acceptors or on an increased basicity of the heterocycle (27,28). By analysing the hydrogen bonding and molecular packing of these compounds in the crystal lattice, molecular details can be obtained of the hydrogen bond strength and directionality of drug binding to the enzyme active site.

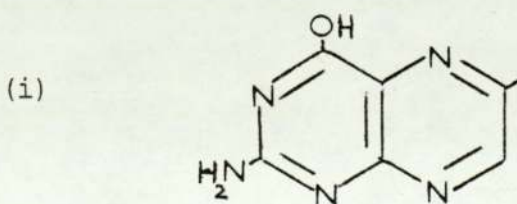
The antifolate diamino groups can act as hydrogen bond donors, while N1 and N3 can act as hydrogen bond acceptors or be protonated. This is in contrast to those of the natural substrates in which only the 2-amino group can be a proton donor, when N3 has a proton and where the enzymatic protonation site is N5, although N1 or N8 can be protonated.

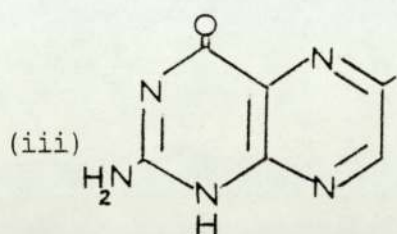
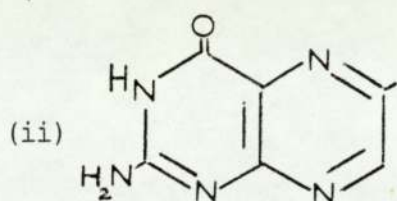
Although antifolate drugs differ in their chemical nature they contain a common structural unit (I) replacing a portion (II) of the pteridine ring of folates :-



One factor which would be expected to be inimical to an inhibitor binding is that of the increased size of C(4)NH<sub>2</sub> in the inhibitors relative to C(4)O; however it is thought that there is a great stereochemical adaptability of the NH<sub>2</sub> group which helps structure (I) to fit the enzyme well (29). The amino group of the inhibitor may act as both a proton donor and acceptor, to enable it to form two hydrogen bonds to the E.Coli enzyme, compared with just one for the carbonyl oxygen atom of the substrate. Also, the enzyme itself may be "floppy".

The formally single exocyclic C-NH<sub>2</sub> bonds in the 2,4 diaminopyrimidine unit are similar in length to the formally multiple endocyclic C - N, suggesting electron donation by the amino groups. An almost universal phenomenon in the antifolates is that of base-paired dimerization about a centre or pseudo-centre of symmetry involving NH<sub>2</sub> as a proton donor and ring N as acceptor. The hydrogen bonding system involves 2- and 4- amino groups and pyrimidine nitrogen atoms 1 and 3. The protonation of N1 of the pteridines can be drawn as three reasonable tautomers, of which (ii) is generally accepted. However (iii)- like tautomers occur in pyrimidines, and maybe pteridines too.





Spectroscopic studies have shown that only one-third of the difference in binding energy between folate and methotrexate could be attributed to protonation (30) indicating that as well as the protonation difference the two substrates are bound somewhat differently. It has been shown that the pteridine ring of the substrates is bound upside down compared with the inhibitor, methotrexate (31).

The mode of binding to the enzyme active-site is still not completely understood. It had been previously found that when the pteridine ring was bound in the hydrophobic pocket on the enzyme the carboxylate side-chain of the aspartate residue (Asp-27) of DHFR from the MTX-resistant strain of *E. Coli* (32) was in close proximity to N1 of methotrexate. However it is now known that Asp-27 is only conserved in some enzymes, to date bacterial only, being replaced by asparagine or glutamic acid depending on the method of aligning

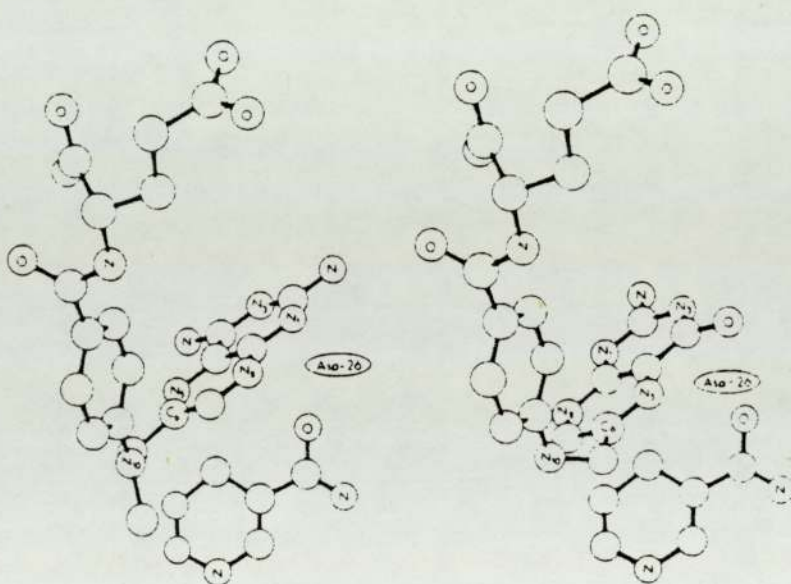
the sequences in mammals (33), but both of these still have polar groups in the area.

Further evidence of a protonated N1 atom in methotrexate when bound to DHFR and that a charge interaction exists between aspartate (bacterial) or a glutamate (vertebrate) in the enzyme and the protonated N1 has been obtained from X-ray diffraction and  $^{13}\text{C}$  nuclear magnetic resonance studies (32,34). Details of the MTX and DHFR interaction (35) revealed that since methotrexate binds with pteridine ring in a flipped orientation as compared with the substrate, dihydrofolate, an additional hydrogen bond forms at the 4-amino which cannot form for dihydrofolate, see Fig.5. This indicates that the charge-interaction is probably not responsible for the entire  $10^4$  to  $10^5$  higher affinity DHFR as for methotrexate versus dihydrofolate (36).

Directed mutagenesis of dihydrofolate reductase has been done which involved residue 27, aspartate replaced by an asparagine and at residue 95, glycine replaced with alanine in the mutant E.Coli DHFR (37). It was found that for the asparagine 27 mutant the enzyme does not protonate methotrexate in the binary complex although the binding constant is lowered by only one hundred fold. Surprisingly, the asparagine 27 enzyme retains one thousandth of the enzymatic activity but the pH optimum has apparently shifted to pH 3.5 verses pH 7.0 for the wild type DHFR. However, it was found that gly 95 to ala mutation shows no detectable enzymatic activity. The

Fig. 5

Conformation of MTX (left) and DHF (right) as it would be after rotation of the  $C_6-C_9$  bond through  $180^\circ$  with appropriate adjustments of adjacent bonds (15)



alanine substitution for glycine at this position appears to have distorted the conserved backbone cis-dipeptide conformation and presumably has eliminated the enzyme's ability to activate NADPH by shifting a carbonyl oxygen (Ile 94) away from the nicotinamide C4 in the active-site. The enzyme is not grossly unfolded since it still binds to NADPH and to methotrexate (38).

Much research in this area of mutagenesis is still to be undertaken, as well as research into the expression and amplification of engineered dihydrofolate reductase minigenes (39).

#### 4.2.1 Dihydrofolate Reductase Binding

The known crystal binary and ternary structures of DHFR from *Escherichia Coli* (13,32) and the other from *Lactobacillus Casei* complexed with NADPH (13,40) both show considerable hydrogen bonding between enzyme and inhibitor. The enzymes supply a carboxylate anion near the protonated N1, a proton acceptor for the 2-amino group and another proton acceptor near the 4-substituent. The protonated N1 atom indicates the importance of protonation at that atom and basicity.

Hydrogen bonding studies of pyrimidine and related compounds, show that base-paired dimerization about a centre or pseudo centre of symmetry in the crystal lattice involving  $\text{NH}_2$  as a proton donor and a ring nitrogen as an acceptor, is an almost universal phenomenon. Unsolvated neutral molecules of trimethoprim for example (41) form two such base pairs, each utilizing only one of the amine hydrogens. However when oxygen functions are available from solvents,  $\text{N-H} \dots \text{O}$  hydrogen bonds are formed, usually at the expense of a base pair (42). In most cases, the  $\text{N(4)-H} \dots \text{H(3)}$  hydrogen bond links the base pair dimers, with the other protons hydrogen bonded to the counter ion or solvent oxygens. In those structures which have other  $\text{NH}_2$  functions present on the antifolate, additional hydrogen bonds of the type  $\text{X-H} \dots \text{NH}_2$  are formed.

From the earlier studies (32,40) the E.Coli but not the L.Casei DHFR appeared to furnish a proton donor in the vicinity of the 4-substituent. If the 4-amino group is capable of rehybridisation it would be possible for it to act as both proton donor and acceptor and form two hydrogen bonds to the E.Coli enzyme as compared with just one for the carbonyl oxygen of the substrate (29). If it acted purely as a proton donor it could form one hydrogen bond to the L.Casei DHFR as compared with none for the carbonyl oxygen of the substrate. This reasoning would still hold for the flipped orientation in bound methotrexate. In the latest studies it is now evident that two hydrogen bonds are formed by the 4-amino group of methotrexate.

In the other known ternary complex of avian DHFR containing phenyltriazine and NADPH (14) the triazine ring of the phenyltriazine inhibitor is in a position analogous to that occupied by the pyrimidine portion of methotrexate when the latter binds to bacterial dihydrofolate reductase. A hydrogen-bonded charge-charge interaction occurs between the carboxylate side chain Glu-30 and the inhibitor's N1 and 2-amino group. This interaction closely resembles a similar one between Asp-27, E.Coli and pteridine ring of methotrexate. The inhibitor's phenyl ring occupies a space analogous to that utilized for binding the pyrazine and C9-N10 portion of methotrexate. NADPH lies in a long shallow groove winding across one face of the enzyme molecule. As in L.Casei DHFR

the cofactor is held in an extended conformation by numerous hydrophobic, hydrogen-bonded, and ionic interactions.

The overall backbone chain folding in the avian DHFR is very similar to that observed in E.Coli and L.Casei with about 70% of the additional residues present in the avian enzyme which occur in three loops far removed from the substrate and cofactor binding sites.

The conformation of the inhibitor methotrexate and its interactions with the enzyme are very similar in the E.Coli binary and L.Casei ternary complex (32,40). Also amino acid comparisons among the known dihydrofolate reductases (14) show that most of the residues involved in methotrexate binding are highly conserved.

Certain generalizations have been proposed as a result of studies of the binding of inhibitors to bacterial and vertebrate DHFR (26). These proposals include that for each species of DHFR there are two potential binding sites, the upper and lower clefts for inhibitor side chains. Effective inhibitors in both classes of DHFR for example MTX, overlap both sites.

#### 4.3 Membrane Transport of Antifolates

The glutamate side chain in folate and in MTX is thought to be involved in the active transport processes for these analogs. Mammals have two separate transport systems with varying specificities towards folate compounds. Some folate antagonists have extracellular and intracellular target enzymes, which suggest that possible folate-binding proteins could be used. (Ref. 43 - A general explanation of the binding interactions of substrates and inhibitors, as well as catalytic mechanism is given in this reference.)

Much evidence for a critical role of membrane transport in the cytotoxic action of folate analogs has been provided by studies with a variety of mammalian cell types. The question of selectivity of anti-tumour action of this general category of agents has been studied using tumour models and erythrocytes (44,45).

#### 4.4 Antimalarials

Malaria is caused by an infection with protozoan parasites which are carried by the anopheles mosquito (the insect vector). Antimalarial drugs act at various points in the life cycle of the parasite. The centuries old treatment with quinine in the form of chinchona bark has been superseded by less toxic aminoquinoline derivatives, Fig. 6.

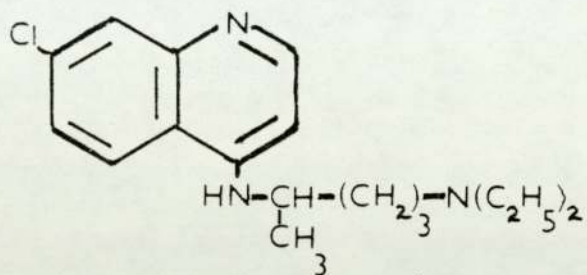
The problem with all these drugs is that they have many side effects which are sometimes fatally toxic. But the biggest drawback is that there are very few places left in the world where the malaria parasites have not developed resistance to them.

Quinine, chloroquine and pyrimethamine kill parasites by blocking their ability to synthesize nucleic acids and primaquine disrupts the energy metabolism of parasite cells.

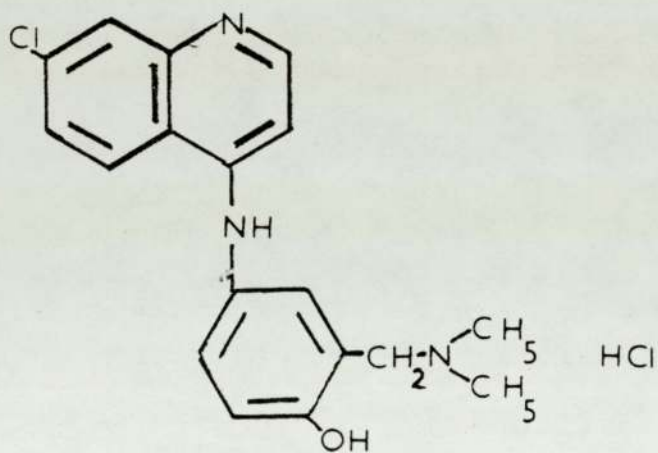
A new strategy for developing novel antimalarials is one which mimics the simplest mechanism the body has for combating infection, the so-called non-specific immunity (46).

Fig. 6

Chloroquine



Amodiaquin



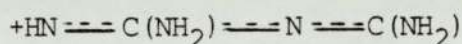
4.4.1 Cycloguanil - common features with other  
antifolates

The antimalarial drug 4,6 diamino-1-p-chlorphenyl-1,2 dihydro 2,2 dimethyl s triazine, (cycloguanil) is shown in Fig. 7. It is an active metabolite of proguanil B.P. (47). It is believed to act by blocking the interconversion of dihydrofolate and tetrahydrofolate.

The drug, cycloguanil has been shown to share the following features with other antifolate agents studied crystallographically :-

1. protonation at N3
2. a phenyl ring nearly perpendicular to the heterocycle.

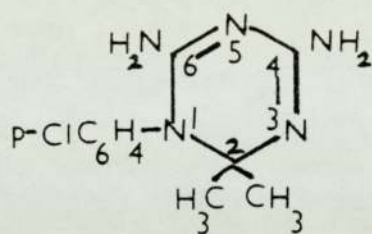
A comparison of cycloguanil and the complex DHFR-MTX (32) was made (48) and it was concluded that the same :-



unit is present as in the protonated drugs MTX (32), pyrimethamine (49) and others. The acidic hydrogen of protonated cycloguanil participates in N - H---Cl<sup>-</sup> hydrogen bonding. The C - N bonds to the amino groups appear to match acceptor groups in DHFR. Bond distances indicate extensive delocalization within the heterocyclic ring which could be advantageous for  $\pi$ - $\pi$  interaction with DHFR (32,49).

Figure 7.

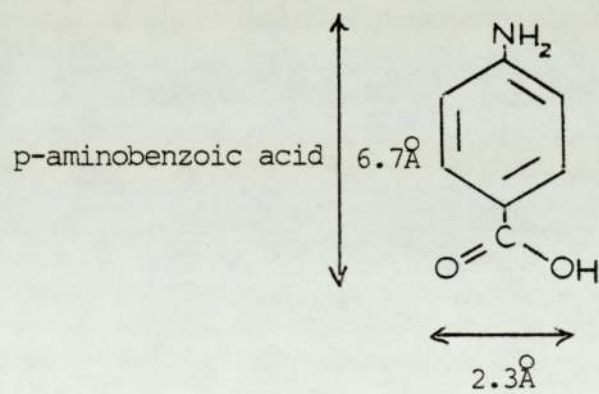
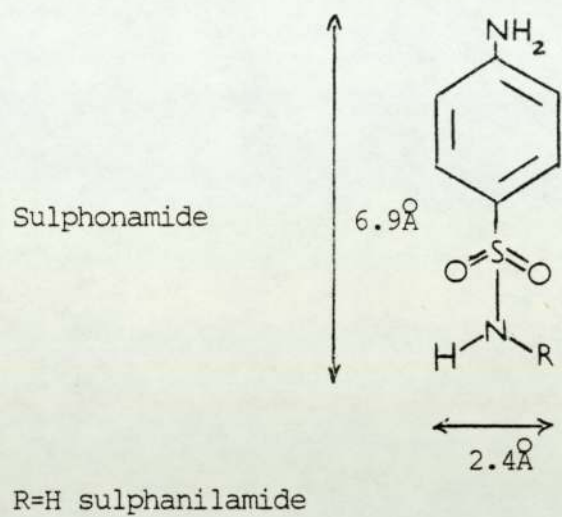
CYCLOGUANIL



#### 4.5 Sulphonamides

There is a close structural relationship between sulphonamides and p-aminobenzoic acid, the latter being a necessary metabolic factor for dihydrofolic acid synthesis, which explains the antimetabolic character of sulphonamides. As shown in Fig. 8 the sulphonamide and carboxyl groups have similar dimensions and are isosteric. Also both molecules are relatively planar, where the exception is that the R group of the sulphonamides is out of the plane. The sulphonamides in clinical use differ only in the nature of this R group, which modifies some of the physicochemical properties but not the fundamental antibacterial effect. The sulphonamide could then compete as an analog of p-aminobenzoic acid. It is known that the addition then of p-aminobenzoic acid, gives a reversal of the sulphonamide action (50).

Figure 8.



## Chapter Five

### Structures of Antifolate Carboxylates

#### 5.1 PYRIMETHAMINE ACETATE HYDRATE

##### 5.1.1 Abstract

2,4-diamino-5-(4-chlorophenyl)-6-ethyl pyrimidine  
acetate hydrate

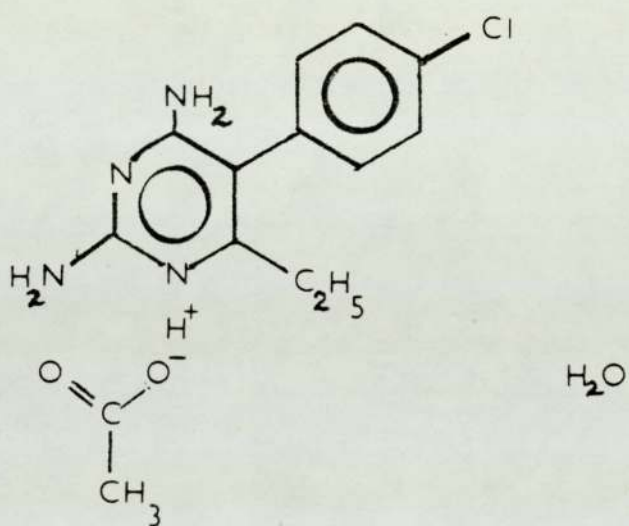
Pyrimethamine acetate hydrate ( $C_{12}H_{13}ClN_4 \cdot CH_3COOH \cdot H_2O$ )  
crystallises in the monoclinic space group C 2/c with unit  
cell dimensions of  $a = 26.246(5) \text{ \AA}$ ;  $b = 10.254(5) \text{ \AA}$  ;  
 $c = 14.562(5) \text{ \AA}$  ;  $\alpha = 90.066(4)^\circ$  ;  $\beta = 120.694(2)^\circ$  ;  
 $\gamma = 89.992(3)^\circ$ .

The unit cell has a volume of  $3370(2) \text{ \AA}^3$  and there  
are eight molecules per unit cell. The relative molar mass  
is  $326.78(4) \text{ gmol}^{-1}$  giving a calculated density  $D_x$  of  
 $1.288(6) \text{ gcm}^{-3}$ .

Using  $M_o\text{-K}\alpha$  radiation of wavelength  $0.71069 \text{ \AA}$ , the  
linear absorption coefficient  $\mu$  is  $2.01 \text{ cm}^{-1}$ , a F(000) of  
1376.0 and the final value of R was 0.059 using 2294 unique  
reflections.

Figure 9

STRUCTURE OF PYRIMETHAMINE ACETATE HYDRATE



### 5.1.2 Experimental

#### Crystal Preparation

The crystals were prepared by Dr. R.Griffin by the addition of 1.0g of pyrimethamine (Wellcome A.5) to 10ml of acetic acid glacial. The suspension was then gently boiled until all the solid had dissolved. The solution was allowed to stand overnight and crystals collected. The crystals were recrystallised from ethyl acetate to give the crystallographic sample.

#### Data Collection

The data were collected from a spear shaped crystal of size 0.06mm x 0.18mm x 0.15mm by 0.11mm thick mounted along its long axis on an Enraf-Nonius CAD4 diffractometer using an  $\omega$ - $2\theta$  scan with graphite monochromated  $M_{O-K\alpha}$  radiation ( $\lambda = 0.71069 \text{ \AA}$ ). The scan range in terms of  $\theta$  was  $(0.96 + 0.35 \tan \theta^\circ)$  at a scan rate of  $3 \frac{1}{3} \text{ min}^{-1}$  to  $0.95 \text{ min}^{-1}$  depending upon the individual intensities. Intensity monitor reflections were measured every two hours and subsequently fitted to a linear function of intensity against time that was used to rescale the data.

The monitor reflections used were 8,4,-8 and -8,2,-2 being h,k and l respectively and the intensity of these reflections declined by 18.6% and 26.9% during the data collection. Orientation controls were used every 160

reflections on these monitor reflections.

Initially the unit cell dimensions were determined by least squares analysis from the setting angles of 25 reflections which were :-

1 3 -7 ; 3 3 -7 ; 8 4 -8 ; 7 3 -7; 0 2 -6 ; -5 1 -4 ;  
-9 1 -2 ; 5 3 -6 ; -8 2 -2 ; 8 4 -4; 2 4 -6 ; -3 1 -5 ;  
4 2 -7 ; -1 1 -5 ; -3 1 -4 ; 4 2 -6; 0 2 -5 ; -7 1 -2 ;  
-9 1 -1 ; -4 2 3 ; 3 3 -5 ; 5 3 -5; 6 6 -6 ; 1 3 -4 ;  
-3 3 -3

The data were collected using  $\theta$  limits of  $2^\circ$  and  $24^\circ$  for  $\pm h, k, l$  with  $h_{\max} = 30$  ;  $k_{\max} = 11$  and  $l_{\max} = 16$  and 2762 reflections collected of which 2294 were unique and 1268 unobserved with an F value of greater than  $3\sigma(F)$  as the criterion for recognizing unobserved reflections. The value of  $R_{\text{int}}$  was 0.0626. The maximum value of  $(\sin \theta) / \lambda$  reached in intensity measurements was 0.5947.

### 5.1.3 Structure Analysis

The structure was solved by direct methods, SHELX (3), and F magnitudes were used in the least squares refinement. The hydrogen atoms identified in the difference Fourier were refined and by using an option in the program the bonds from hydrogen atoms to the atoms N2, N4, C3P and C5P were set at lengths of 1.01 Å with maximum deviation of 0.05 Å. The parameters which were refined were scale, co-ordinates, anisotropic temperature factors for non-hydrogen atoms and isotropic temperature factors for hydrogen atoms.

The final value of R from the last refinement was 0.0559 and  $wR = 0.0591$ . The parameter, w was calculated by :-

$$1.000 / (\text{Sigma}^{**2}(\text{F}) + \text{weight} * \text{F} * \text{F})$$

where the weight was initially set to 0.01.

The ratio of maximum least squares shift to error in the final refinement cycle,  $(\Delta / \sigma)_{\text{max}}$  was 0.699 for hydrogen atoms (HW1) and 0.346 for non-hydrogen atoms (O3). The maximum positive and negative electron density in the final difference Fourier synthesis were  $(\Delta \rho)_{\text{max}} 0.3381$  and  $(\Delta \rho)_{\text{min}} -0.2396$  respectively.

The results of the final refinement cycle are to be found in Tables 5.1 and 5.2 and also results of the co-ordinate data being processed by GEOM and the computer graphics program PLUTO (51) to calculate torsion angles and least squares planes are given in Tables 5.3 to 5.6 (inclusive) and which also used

to produce the following crystal structure diagrams :

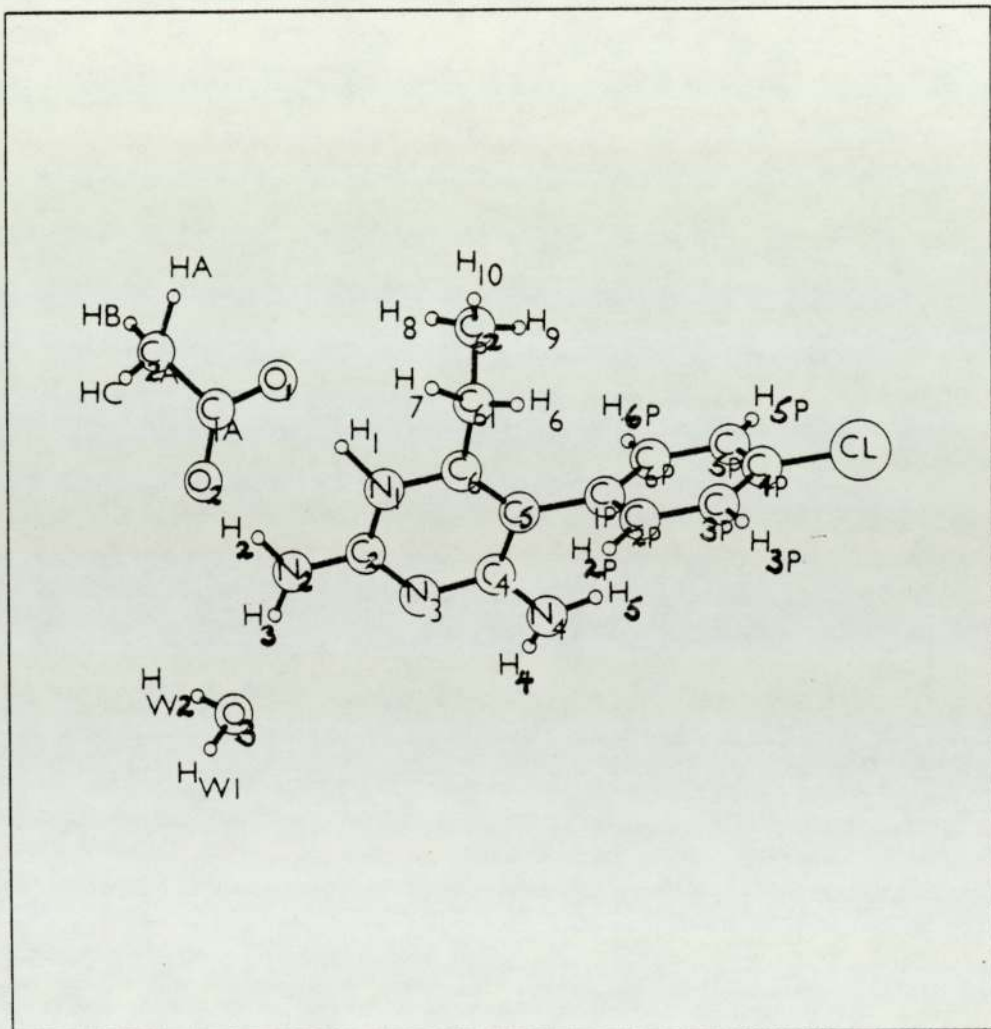
Figs. 10 - 12.

The angle calculated by GEOM between the two rings in pyrimethamine acetate hydrate was found to be  $75^{\circ} 42'$ .



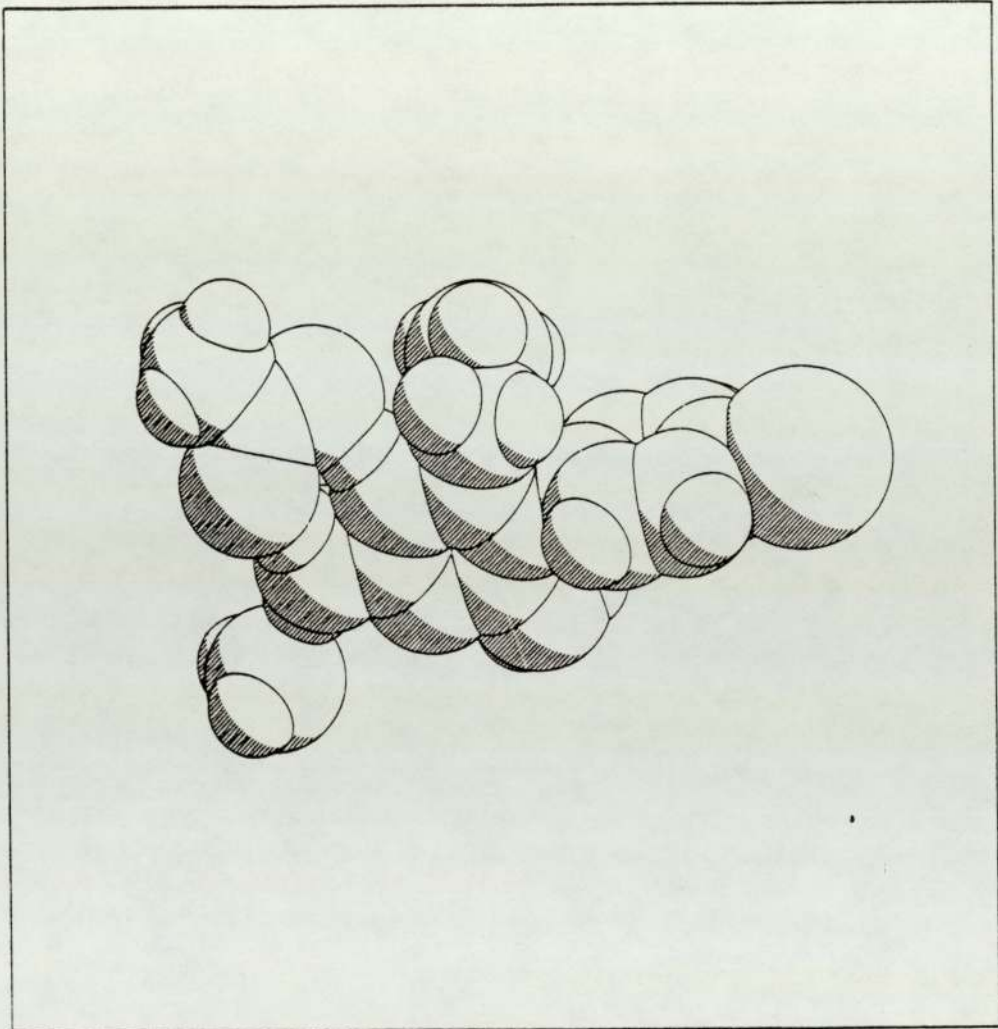
PYRIMETHAMINE ACETATE HYDRATE

Fig. 10 Molecular Diagram



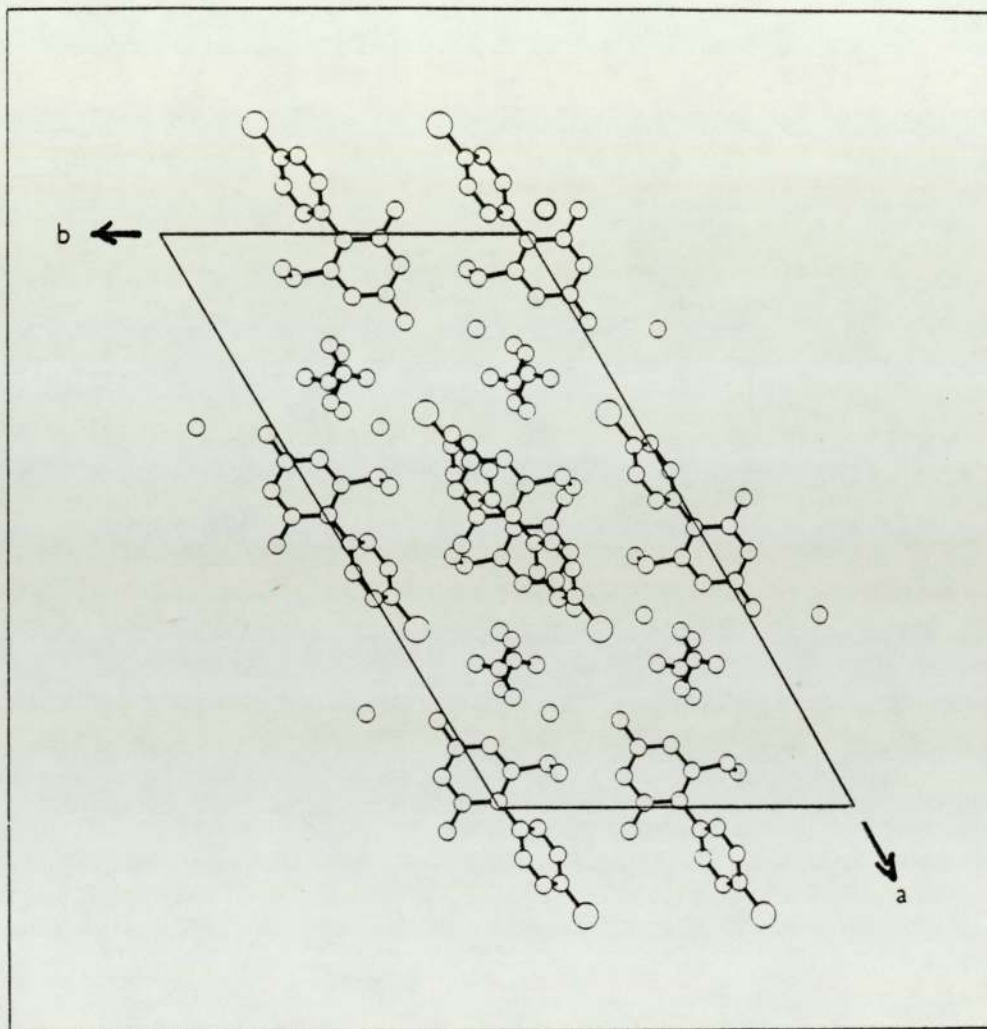
PYRIMETHAMINE ACETATE HYDRATE

Fig. 11 Space Filling Diagram



PYRIMETHAMINE ACETATE HYDRATE

Fig. 12 Packing Diagram



Pyrimethamine Acetate Hydrate

Table 5.1

Positional parameters (fractional co-ordinates  
 $\times 10^4$  )

With estimated standard deviations in parentheses

Atom	X/a	Y/b	Z/c
N1	1085(2)	1610(4)	749(3)
C2	1043(2)	1837(5)	-205(3)
N3	541(1)	2265(4)	-1054(3)
C4	79(2)	2516(4)	-921(4)
C5	115(2)	2414(4)	88(4)
C6	634(2)	1966(5)	918(4)
N2	1519(2)	1593(5)	-268(4)
N4	-414(2)	2891(4)	-1788(3)
C61	764(3)	1777(7)	2038(5)
C62	605(4)	452(8)	2196(6)
C1P	-385(2)	2842(5)	223(4)
C2P	-360(3)	3989(6)	722(5)
C3P	-826(4)	4374(7)	849(6)
C4P	-1313(3)	3602(8)	469(5)
C5P	-1351(2)	2485(8)	-26(5)
C6P	-888(2)	2088(6)	-161(4)
CL	-1886(1)	4145(2)	640(2)
C1A	-2576(2)	4822(6)	-2766(4)
C2A	-2077(3)	5661(8)	-1972(5)

Table 5.1 (contd.)

Atom	X/a	Y/b	Z/c
O1	-3074 (1)	4991 (4)	-2852 (3)
O2	-2493 (1)	4034 (4)	-3317 (3)
O3	-1645 (1)	2229 (4)	-2913 (3)
H1	1456 (23)	1081 (47)	1405 (42)
H2	1915 (25)	1411 (57)	527 (50)
H3	1543 (17)	1764 (43)	-852 (29)
H4	-439 (15)	2779 (37)	-2402 (27)
H5	-737 (17)	2901 (47)	-1751 (38)
H6	594 (27)	2338 (60)	2289 (52)
H7	1226 (17)	1867 (38)	2779 (31)
H8	750 (35)	-249 (76)	1939 (65)
H9	173 (28)	315 (67)	1691 (54)
H10	858 (37)	770 (83)	3129 (80)
H2F	0000 (22)	4596 (49)	1015 (39)
H3F	-794 (23)	5191 (42)	1206 (41)
H5F	-1649 (20)	1896 (48)	-317 (42)
H6F	-911 (18)	1286 (46)	-472 (36)
HW1	1752 (23)	1410 (57)	-2308 (45)
HW2	-1949 (20)	2886 (47)	-3091 (37)
HA	-2107 (32)	5980 (76)	-1303 (65)
HB	-2076 (36)	3343 (94)	2762 (70)
HC	-1780 (24)	5327 (55)	-1892 (44)

Pyrimethamine Acetate Hydrate

Table 5.2

Anisotropic temperature factors ( non-hydrogen atoms)

Isotropic temperature factors (hydrogen atoms)

With standard deviations in parentheses

Atom	U11	U22	U33	U23	U13	U12
N1	.0459(20)	.0673(30)	.0482(23)	.0085(21)	.0268(19)	.0021(20)
C2	.0456(25)	.0555(32)	.0424(26)	-.0018(25)	.0245(22)	-.0091(23)
N3	.0401(19)	.0619(28)	.0423(21)	-.0004(19)	.0247(18)	-.0031(18)
C4	.0457(25)	.0446(30)	.0437(26)	-.0082(22)	.0250(22)	-.0082(21)
C5	.0504(26)	.0469(31)	.0449(25)	-.0040(22)	.0302(23)	-.0058(22)
C6	.0588(28)	.0629(35)	.0458(27)	-.0015(25)	.0324(24)	-.0055(25)
N2	.0477(21)	.0947(35)	.0564(26)	.0010(25)	.0355(20)	.0000(22)
N4	.0396(21)	.0785(34)	.0404(23)	.0013(22)	.0229(19)	-.0004(21)
C61	.0882(40)	.0886(50)	.0645(35)	.0073(35)	.0499(32)	.0061(36)
C62	.1145(48)	.0889(55)	.1086(53)	-.0025(43)	.0678(43)	-.0107(44)
C1P	.0564(26)	.0562(35)	.0503(26)	-.0037(25)	.0359(23)	.0011(25)
C2P	.0952(38)	.0599(39)	.0857(38)	-.0107(33)	.0663(33)	-.0098(31)
C3P	.1414(54)	.0653(45)	.1089(46)	.0042(37)	.0979(43)	.0202(42)
C4P	.0935(41)	.0924(50)	.0999(45)	.0193(39)	.0771(37)	.0300(38)
C5P	.0675(34)	.1095(55)	.0892(42)	-.0109(40)	.0559(33)	-.0059(35)
C6P	.0691(32)	.0720(42)	.0811(37)	-.0220(33)	.0517(29)	-.0100(31)
CL	.1576(17)	.1758(22)	.1883(20)	.0458(17)	.1489(17)	.0714(15)
C1A	.0472(27)	.0674(37)	.0543(32)	-.0007(28)	.0259(24)	.0027(26)

Table 5.2 (contd.)

Atom	U11	U22	U33	U23	U13	U12
C2A	.0562(30)	.1119(56)	.0874(43)	.0316(41)	.0314(30)	.0148(35)
O1	.0477(17)	.0957(29)	.0830(25)	.0271(22)	.0360(17)	.0069(19)
O2	.0491(18)	.0846(28)	.0769(23)	.0171(21)	.0322(17)	-.0024(18)
O3	.0467(17)	.0845(29)	.0731(23)	-.0122(22)	.0387(17)	-.0109(19)

## Uiso

H1	.0901(118)
H2	.1221(133)
H3	.0616(107)
H4	.0325(89)
H5	.0823(118)
H6	.1195(144)
H7	.0494(92)
H8	.1935(155)
H9	.1431(145)
H10	.2422(157)
H2P	.0888(117)
H3P	.1074(131)
H5P	.0984(133)
H6P	.0606(112)
HW1	.1075(131)
HC	.0931(134)

Pyrimethamine Acetate Hydrate

Table 5.3

Bond distances in Angstroms with estimated standard deviation in parentheses

Bond	Interatomic Distance	Bond	Interatomic Distance
N1-C2	1.356(5)	N1-C6	1.375(5)
N1-H1	1.098(53)	C2-N3	1.339(5)
C2-N2	1.322(5)	N3-C4	1.346(5)
C4-C5	1.427(6)	C4-N4	1.322(5)
C5-C6	1.359(6)	C5-C1P	1.489(6)
C6-C61	1.498(7)	N2-H2	1.107(60)
N2-H3	0.901(34)	N4-H4	0.870(31)
N4-H5	0.876(35)	C61-C62	1.473(9)
C61-H6	0.911(62)	C61-H7	1.143(38)
C62-H8	0.973(78)	C62-H9	0.997(61)
C62-H10	1.213(97)	C1P-C2P	1.366(7)
C1P-C6P	1.378(7)	C2P-C3P	1.384(8)
C2P-H2P	1.025(50)	C3P-C4P	1.358(9)
C3P-H3P	0.966(37)	C4P-C5P	1.329(8)
C5P-C6P	1.387(7)	C5P-H5P	0.904(36)
C6P-H6P	0.925(46)	C1A-C2A	1.498(8)
C1A-O1	1.259(5)	C1A-O2	1.234(5)

Table 5.3 (contd.)

Bond	Interatomic Distance	Bond	Interatomic Distance
O3-HW1	0.990 (60)	O3-HW2	0.973 (48)
H3-HW1	2.473	H3-HW2	2.550
HW1-HW2	1.609	CL-C4P	1.737 (5)

Pyrimethamine Acetate Hydrate

Table 5.4

Interatomic angles ( $^{\circ}$ ) with estimated standard deviations in parentheses (for non-hydrogen atoms and those hydrogens attached to primary amine groups)

Atoms	Bond Angle ( $^{\circ}$ )	Atoms	Bond Angle ( $^{\circ}$ )
C2-N1-C6	120.7(.4)	C2-N1-H1	123.2(2.6)
C6-N1-H1	115.9(2.6)	N1-C2-N3	121.9(.4)
N1-C2-N2	116.9(.4)	N3-C2-N2	121.1(.4)
C2-N3-C4	117.6(.4)	N3-C4-C5	122.9(.4)
N3-C4-N4	115.6(.4)	C5-C4-N4	121.5(.4)
C4-C5-C6	116.7(.4)	C4-C5-C1F	121.0(.4)
C6-C5-C1F	122.2(.4)	N1-C6-C5	119.6(.4)
N1-C6-C61	114.9(.4)	C5-C6-C61	125.4(.4)
C2-N2-H2	112.0(3.1)	C2-N2-H3	123.5(2.7)
H2-N2-H3	122.6(4.1)	C4-N4-H4	117.8(2.3)
C4-N4-H5	116.8(3.1)	H4-N4-H5	119.8(4.0)
C6-C61-C62	111.3(.6)	C6-C61-H6	118.0(4.3)
C6-C61-H7	124.0(2.0)	C62-C61-H6	106.5(4.3)
C62-C61-H7	100.1(2.1)	H6-C61-H7	94.1(4.5)
C61-C62-H8	115.1(5.0)	C61-C62-H9	108.7(4.2)
C61-C62-H10	83.7(4.2)	H8-C62-H9	97.6(6.0)
H8-C62-H10	122.1(6.1)	H9-C62-H10	129.0(5.6)

Table 5.4 (contd.)

Atoms	Bond Angle (°)	Atoms	Bond Angle (°)
C5-C1P-C2P	121.2(.4)	C5-C1P-C6P	120.5(.5)
C2P-C1P-C6P	118.3(.5)	C1P-C2P-C3P	120.7(.6)
C1P-C2P-H2P	121.9(2.7)	C3P-C2P-H2P	117.4(2.7)
C2P-C3P-C4P	119.4(.6)	C2P-C3P-H3P	118.6(3.5)
C4P-C3P-H3P	122.0(3.4)	C3P-C4P-C5P	121.2(.5)
C4P-C5P-C6P	120.1(.6)	C4P-C5P-H5P	129.6(3.7)
C6P-C5P-H5P	110.4(3.7)	C1P-C6P-C5P	120.3(.6)
C1P-C6P-H6P	120.4(2.7)	C5P-C6P-H6P	119.1(2.7)
C2A-C1A-O1	116.8(.5)	C2A-C1A-O2	120.2(.5)
O1-C1A-O2	123.0(.4)	HW1-O3-HW2	110.1(4.2)
N2-H3-HW1	158.9	N2-H3-HW2	155.4
HW1-H3-HW2	37.3	O3-HW1-H3	51.2
O3-HW1-HW2	34.6	H3-HW1-HW2	73.9
O3-HW2-H3	46.4	O3-HW2-HW1	35.3
H3-HW2-HW1	68.7	CL-C4P-C3P	117.2(.6)
CL-C4P-C5P	121.5(.6)		

Pyrimethamine Acetate Hydrate

Table 5.5

Torsion Angles(°)

Atoms	Angle(°)
C6-N1-C2-N3	-8.2
C6-N1-C2-N2	173.1
H1-N1-C2-N3	167.4
H1-N1-C2-N2	-11.4
C2-N1-C6-C5	7.4
C2-N1-C6-C61	-174.3
H1-N1-C6-C5	-168.4
H1-N1-C6-C61	9.8
N1-C2-N3-C4	2.6
N2-C2-N3-C4	-178.7
N1-C2-N2-H2	-10.9
N1-C2-N2-H3	-175.7
N3-C2-N2-H2	170.3
N3-C2-N2-H3	5.5
C2-N3-C4-C5	3.6
C2-N3-C4-N4	-177.7
N3-C4-C5-C6	-4.0
N3-C4-C5-C1F	173.1
N4-C4-C5-C6	177.2
N4-C4-C5-C1F	-5.6
N3-C4-N4-H4	14.1
N3-C4-N4-H5	167.6

Table 5.5 (contd.)

Atoms	Angle (°)
C5-C4-N4-H4	-167.1
C5-C4-N4-H5	-13.6
C4-C5-C6-N1	-1.5
C4-C5-C6-C61	-179.6
C1F-C5-C6-N1	-178.6
C1F-C5-C6-C61	3.3
C4-C5-C1F-C2F	-104.0
C4-C5-C1F-C6F	75.6
C6-C5-C1F-C2F	72.9
C6-C5-C1F-C6F	-107.4
N1-C6-C61-C62	-87.8
N1-C6-C61-H6	148.6
N1-C6-C61-H7	31.6
C5-C6-C61-C62	90.3
C5-C6-C61-H6	-33.2
C5-C6-C61-H7	-150.3
C2-N2-H3-HW1	-132.6
C2-N2-H3-HW2	116.6
H2-N2-H3-HW1	64.2
H2-N2-H3-HW2	-46.6
C6-C61-C62-H8	48.4
C6-C61-C62-H9	-59.9
C6-C61-C62-H10	170.9
H6-C61-C62-H8	178.2
H6-C61-C62-H9	69.9

Table 5.5 (contd.)

Atoms	Angle (°)
H6-C61-C62-H10	-59.2
H7-C61-C62-H8	-84.4
H7-C61-C62-H9	167.3
H7-C61-C62-H10	38.1
C5-C1F-C2F-C3F	-179.6
C5-C1F-C2F-H2F	.4
C6F-C1F-C2F-C3F	.6
C6F-C1F-C2F-H2F	-179.2
C5-C1F-C6F-C5F	179.5
C5-C1F-C6F-H6F	3.5
C2F-C1F-C6F-C5F	-.9
C2F-C1F-C6F-H6F	-176.9
C1F-C2F-C3F-C4F	-.2
C1F-C2F-C3F-H3F	180.0
H2F-C2F-C3F-C4F	179.7
H2F-C2F-C3F-H3F	-.1
C2F-C3F-C4F-C5F	-.2
H3F-C3F-C4F-C5F	179.6
C3F-C4F-C5F-C6F	.1
C3F-C4F-C5F-H5F	-179.3
C4F-C5F-C6F-C1F	.5
C4F-C5F-C6F-H6F	176.5
H5F-C5F-C6F-C1F	-180.0
H5F-C5F-C6F-H6F	-4.0
HW2-O3-HW1-H3	122.8

Table 5.5 (contd.)

Atoms	Angle(°)
HW2-O3-HW1-HW2	0.0
HW1-O3-HW2-H3	-118.7
HW1-O3-HW2-HW1	0.0
N2-H3-HW1-O3	-169.8
N2-H3-HW1-HW2	-140.1
HW2-H3-HW1-O3	-29.8
HW2-H3-HW1-HW2	0.0
N2-H3-HW2-O3	179.3
N2-H3-HW2-HW1	146.4
HW1-H3-HW2-O3	32.9
HW1-H3-HW2-HW1	0.0
O3-HW1-HW2-O3	0.0
O3-HW1-HW2-H3	42.9
H3-HW1-HW2-O3	-42.9
H3-HW1-HW2-H3	0.0

Pyrimethamine Acetate Hydrate

Table 5.6

Calculation of  $\theta$  Angle between planes

Plane 1:            L = .3381  
                      M = .9374  
                      N = .0833  
                      D = 2.3910

Deviations:        -0.0458  
                          0.0294  
                          0.0109  
                      -0.0327  
                          0.0150  
                          0.0231

Plane 2:            L = .4131  
                      M = -.4813  
                      N = .7731  
                      D = -1.1165

Deviations:        0.0046  
                          -0.0023  
                          -0.0012  
                          0.0023  
                          0.0002  
                          -0.0036

If  $\theta$  = Angle between planes  $P_1$  and  $P_2$

Then  $\cos \theta = L_1 L_2 + M_1 M_2 + N_1 N_2$

Provided that  $L_1^2 + M_1^2 + N_1^2 = 1$

and  $L_2^2 + M_2^2 + N_2^2 = 1$

5.2 PYRIMETHAMINE SALICYLATE ISOPROPANOL SOLVATE

5.2.1 Abstract

2,4-diamino-5-(4-chlorophenyl)-6-ethyl pyrimidine  
salicylate isopropanol solvate

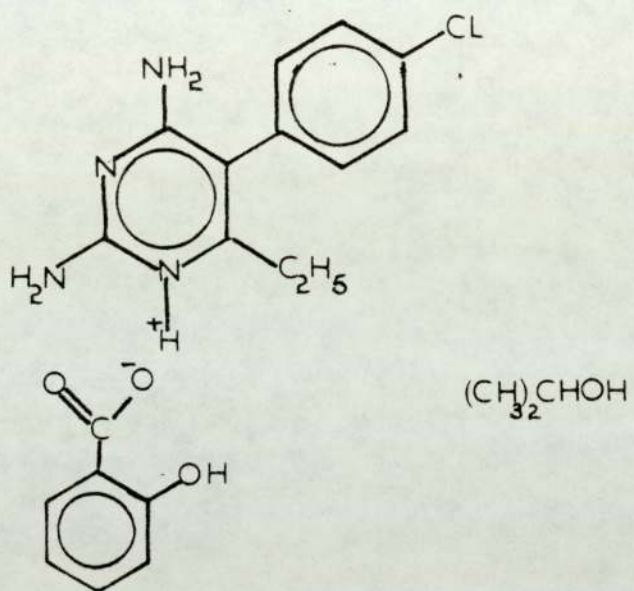
Pyrimethamine salicylate isopropanol solvate ( $C_{12}H_{13}ClN_4 \cdot C_7H_6O_3 \cdot (CH_3)_2CHOH$ ) crystallises in the triclinic space group  $P\bar{1}$  with unit cell dimensions of  $a = 9.101(2) \text{ \AA}$ ;  $b = 9.538(8) \text{ \AA}$ ;  $c = 14.979(2) \text{ \AA}$ ;  $\alpha = 84.05(7)^\circ$ ;  $\beta = 74.81(5)^\circ$ ;  $\gamma = 74.45(4)^\circ$ .

The unit cell has a volume of  $1208.2(9) \text{ \AA}^3$  and there are two molecules per unit cell. The relative molar mass is  $446.93(5) \text{ g mol}^{-1}$  giving a calculated density  $D_x$  of  $1.229 \text{ g cm}^{-3}$ .

Using  $M_o-K_\alpha$  radiation of wavelength  $0.71069 \text{ \AA}$ , the linear absorption coefficient  $\mu$  is  $1.52 \text{ cm}^{-1}$ ,  $F(000)$  of 472.00 and the final value of R was 0.0931 using 1546 unique reflections.

Figure 13

STRUCTURE OF PYRIMETHAMINE SALICYLATE ISOPROPANOL SOLVATE



## 5.2.2 Experimental

### Crystal Preparation

The crystals were prepared by Dr. R.Griffin by the following method. A mixture of pyrimethamine (Wellcome A.5) (2.0g) and salicylic acid (1.2g) was suspended in propan-2-ol (10ml-isopropanol) and gently boiled. Water was added dropwise until all the solids had just dissolved whereupon the solution was cooled rapidly to afford a microcrystalline crop. Recrystallisation was from propan-2-ol/water in equal proportions twice to give the requisite crystals.

### Data Collection

The data were collected from a spear shaped crystal of size 0.11mm x 0.05mm x 0.31mm mounted along its long axis on an Enraf-Nonius CAD4 Diffractometer using an  $\omega$ - $2\theta$  scan with graphite monochromated  $M_o-K_{\alpha}$  radiation ( $\lambda = 0.71069 \text{ \AA}$ ). the scan range in terms of  $\theta$  was  $(1.00 + 0.35 \tan \theta^{\circ})$  at a scan rate of  $2.5^{\circ} \text{ min}^{-1}$  to  $0.69^{\circ} \text{ min}^{-1}$  depending upon the individual intensities. Intensity monitor reflections were measured every two hours and subsequently fitted to a linear function of intensity against time that was used to rescale the data.

The monitor reflections were 4,0,2 and 3,5,0 being h,k, and l respectively and the intensity of these reflections declined by 24.3% and 26.6% during the data collection.

Orientation controls were used every 160 reflections on these monitor reflections.

Initially the unit cell dimensions were determined by least squares analysis from the setting angles of 24 reflections which were :-

5 1 -4 ; 6 2 -3 ; 5 1 -3 ; 7 1 -1 ; 5 1 2 ; 7 1 1 ;  
6 1 -1 ; 4 0 -5 ; 4 0 2 ; 3 0 -6 ; 5 1 1 ; 4 0 -4 ;  
4 2 -4 ; 4 0 -1 ; 5 2 -2 ; 3-3 1 ; 3 2 -4 ; 4 4 0 ;  
6 2 0 ; 3 1 -4 ; 6 2 1 ; 3 5 0 ; 5 2 -4 ; 4 -3 3

The data were collected using  $\theta$  limits of  $2^\circ$  and  $22.5^\circ$  for  $h, \pm k, \pm l$  with  $h_{\max} = 10$ ;  $k_{\max} = 34$ ; and  $l_{\max} = 16$  and 1776 reflections collected of which 1546 were unique and 591 unobserved with an  $F$  value of greater than  $3\sigma(F)$  as the criterion for recognizing unobserved reflections. The value of  $R_{\text{int}}$  from merging equivalent reflections was 0.0281. the maximum value of  $(\sin \theta) / \lambda$  reached in intensity measurements was 0.5385.

### 5.2.3 Structure Analysis

The structure was solved by direct methods, SHELX (3), and F magnitudes were used in the least squares refinement. The hydrogen atoms were identified in the difference Fourier and refined. The parameters which were refined were scale, co-ordinates, anisotropic temperature factors for the chlorine atoms only and isotropic temperature factors for all other atoms.

The final value of R from the last refinement was 0.0931 and wR = 0.1073. The parameter, w was calculated by :-

$$1.000/(\text{Sigma}^{**2}(\text{F}) + \text{weight}*\text{F}*\text{F})$$

where the weight was initially set to 0.001.

The ratio of maximum least squares shift to error in the final refinement cycle,  $(\Delta/\sigma)_{\text{max}}$  was 3.883 for hydrogen atoms (H5S) and 0.068 for non-hydrogen atoms (ClI). All other values of  $(\Delta/\sigma)_{\text{max}}$  were less than one for hydrogen atoms except the atom H10 which had a value of 1.038. These values indicate the uncertainty of the atoms' positions. The maximum positive and negative electron density in the final difference Fourier synthesis was  $(\Delta\rho)_{\text{max}}$  0.2913 and  $(\Delta\rho)_{\text{min}}$  -0.2404 respectively.

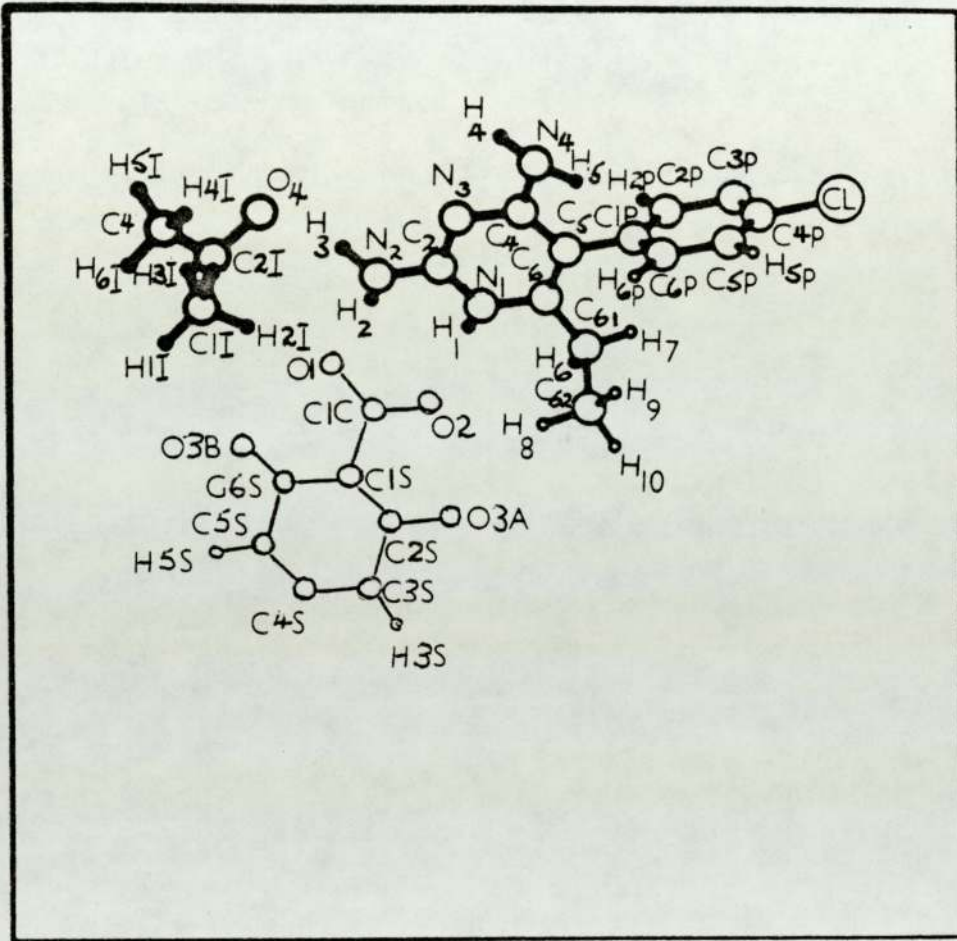
The results of the final refinement cycle are to be found in Tables 5.7 and 5.8 and also results of the co-ordinate data being processed by GEOM and the computer graphics program PLUTO (51) to calculate torsion angles and least squares

planes are given in Tables 5.9 to 5.12 (inclusive). The program PLUTO was also used to give the crystal structure diagrams Figs. 14 - 16.

The angle calculated by GEOM between the pyrimidine and chlorophenyl rings in pyrimethamine salicylate isopropanol solvate was found to be  $80^{\circ} 10'$ .

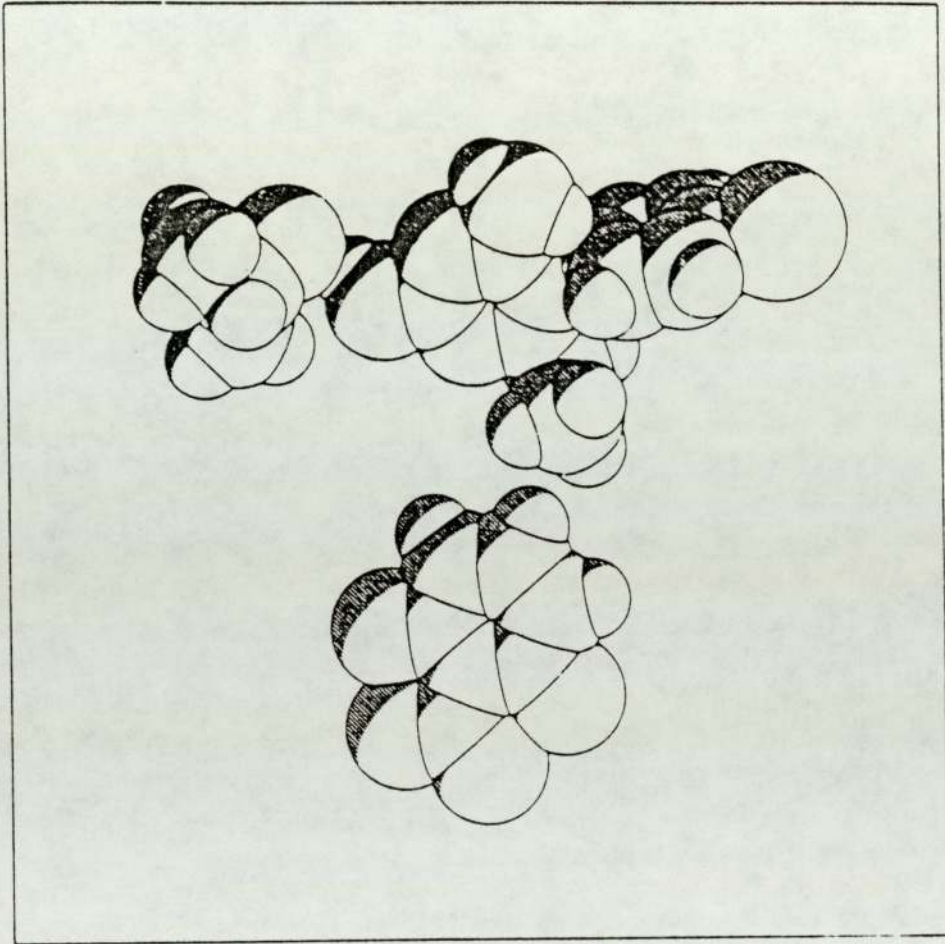
PYRIMETHAMINE SALICYLATE ISOPROPANOL SOLVATE

Fig. 14 Molecular Diagram



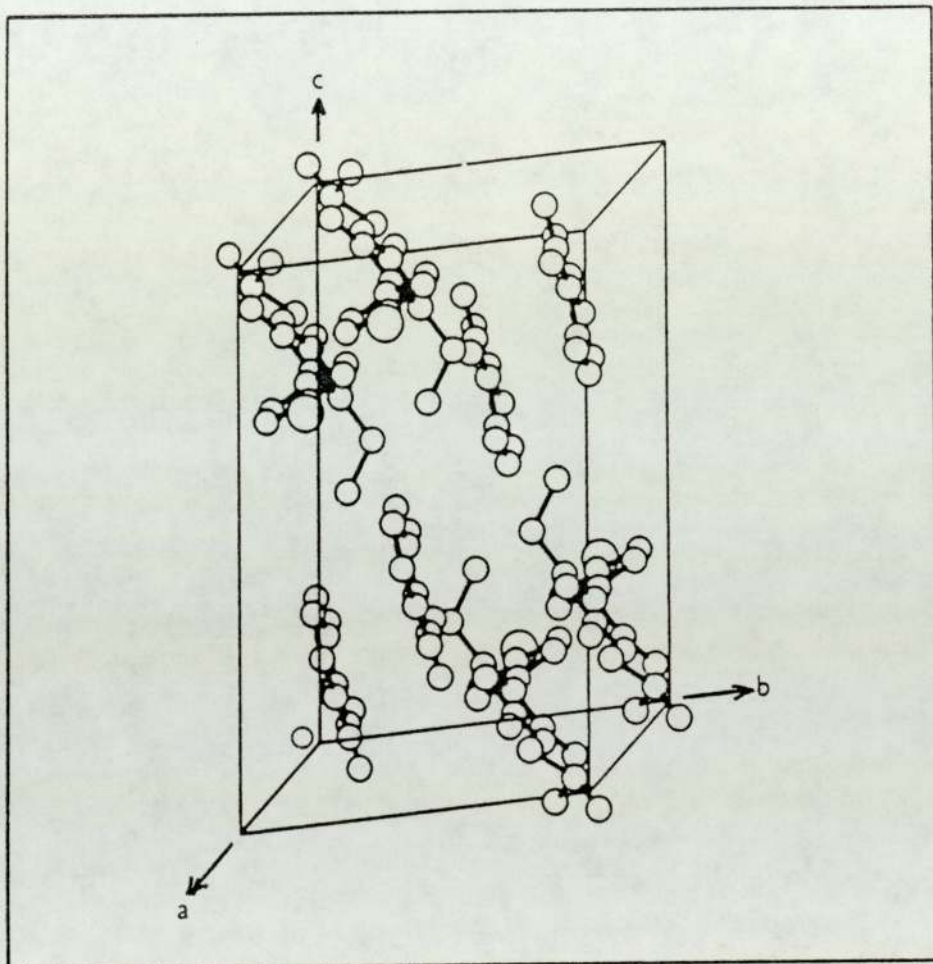
PYRIMETHAMINE SALICYLATE ISOPROPANOL SOLVATE

Fig. 15 Space Filling Diagram



PYRIMETHAMINE SALICYLATE ISOPROPANOL SOLVATE

Fig. 16 Packing Diagram



Pyrimethamine Salicylate Isopropanol Solvate

Table 5.7

Positional parameters (fractional co-ordinates)

$\times 10^4$ )

With estimated standard deviations in  
parantheses

Atom	X/a	Y/b	Z/c
N1	9069(9)	3148(15)	7874(6)
C2	8553(11)	2455(19)	8684(7)
N3	9463(9)	1423(15)	9091(5)
C4	11021(11)	1080(19)	8623(7)
C5	11642(11)	1750(18)	7812(7)
C6	10664(11)	2852(19)	7442(7)
C61	11029(12)	3736(20)	6567(8)
C62	10623(16)	2950(23)	5767(10)
N2	6986(9)	2937(16)	9096(6)
N4	11872(9)	-18(15)	9053(6)
C1P	13365(13)	1261(22)	7364(8)
C2P	14289(14)	2149(20)	7487(7)
C3P	15971(15)	1709(23)	7080(9)
C4P	16490(14)	563(24)	6596(9)
C5P	15692(18)	-385(25)	6414(10)
C6P	13929(17)	63(26)	6836(11)
CL	18546(4)	-29(7)	6086(3)
C1S	5584(16)	3804(19)	3066(8)
C2S	5075(16)	3719(22)	4023(9)
C3S	6350(19)	3066(26)	4534(11)

Table 5.7 (contd.)

Atom	X/a	Y/b	Z/c
C4S	7803 (17)	2623 (23)	4038 (10)
C5S	8293 (15)	2811 (23)	3160 (10)
C6S	7218 (15)	3412 (22)	2602 (10)
C1C	4383 (14)	4471 (21)	2516 (9)
O1	4885 (9)	4661 (14)	1643 (5)
O2	2977 (8)	4934 (13)	2957 (5)
O3A	3655 (19)	4035 (31)	4455 (11)
O3B	7731 (15)	3675 (24)	1797 (10)
O4	4985 (8)	2145 (13)	10812 (5)
C1I	2756 (20)	3389 (28)	10184 (12)
C2I	3465 (22)	1964 (31)	10694 (14)
C3I	2682 (27)	1226 (35)	11341 (17)
H1	9029 (132)	3648 (167)	8121 (77)
H2	6472 (118)	3893 (157)	8724 (73)
H3	7075 (85)	3507 (134)	9519 (52)
H4	11496 (76)	-401 (113)	9709 (47)
H5	12681 (100)	-355 (135)	8660 (58)
H6	12089 (88)	3612 (130)	6421 (52)
H7	10464 (198)	4980 (262)	6260 (113)
H8	10893 (128)	3487 (189)	5010 (76)
H9	11433 (128)	2444 (169)	5668 (69)
H10	10826 (385)	3801 (456)	5653 (255)
H2F	13830 (105)	3037 (149)	7901 (64)
H5F	15987 (116)	-1449 (157)	6650 (64)
H6F	14177 (79)	-119 (119)	7094 (46)

Table 5.7 (contd.)

Atom	X/a	Y/b	Z/c
H3S	5668 (58)	2967 (102)	4822 (36)
H5S	11921 (460)	3550 (606)	4342 (36)
H1I	3371 (89)	3253 (126)	9657 (52)
H2I	2231 (89)	4062 (140)	10656 (55)
H3I	1674 (180)	3029 (217)	10300 (106)
H4I	4693 (73)	3291 (111)	11444 (44)
H5I	3762 (83)	1022 (130)	10170 (50)
H6I	2194 (85)	2386 (125)	11585 (51)

Pyrimethamine Salicylate Isopropanol Solvate

Table 5.8

Isotropic temperature factors  
 (all atoms other than chlorine)  
 Anisotropic temperature factors  
 (chlorine atom only)

Atom	Uiso
N1	.0535(27)
C2	.0493(33)
N3	.0482(26)
C4	.0497(33)
C5	.0465(32)
C6	.0508(33)
C61	.0641(38)
C62	.1114(56)
N2	.0634(31)
N4	.0569(29)
C1P	.0579(37)
C2P	.0661(39)
C3P	.0769(45)
C4P	.0706(42)
C5P	.1077(57)
C6P	.0959(53)
C1S	.0704(41)
C2S	.0890(47)
C3S	.1249(63)

Table 5.8 (contd.)

Atom	Uiso
C4S	.1015 (52)
C5S	.0959 (51)
C6S	.0811 (44)
C1C	.0731 (41)
O1	.0823 (29)
O2	.0721 (27)
O3A	.0639 (79)
O3B	.0835 (66)
O4	.0729 (27)
C1I	.1463 (73)
C2I	.1424 (74)
C3I	.2008 (105)
H1	.1804 (538)
H2	.1135 (436)
H3	.0573 (286)
H4	.0510 (254)
H5	.0906 (350)
H6	.0622 (286)
H7	.2543 (850)
H8	.1041 (483)
H9	.0449 (348)
H10	.2693 (1573)
H2P	.1036 (379)
H5P	.0996 (423)
H6P	.0417 (257)
H3S	.0151 (188)

Table 5.8 (contd.)

Atom	Uiso
H5S	.8239 (1567)
H1I	.0638 (276)
H2I	.0599 (299)
H3I	.2251 (722)
H4I	.0427 (240)
H5I	.0628 (300)
H6I	.0628 (290)

Atom	U11	U22	U33	U23	U13	U12
CL	.0414 (17)	.1719 (93)	.1748 (39)	.0206 (46)	.0239 (20)	.0004 (30)

Pyrimethamine Salicylate Isopropanol Solvate

Table 5.9

Bond Distances in Angstrom with estimated standard deviation in parentheses

Bond	Interatomic Distance	Bond	Interatomic Distance
N1-C2	1.353 (15)	N1-C6	1.389 (12)
N1-H1	0.621 (155)	C2-N3	1.315 (16)
C2-N2	1.368 (12)	N3-C4	1.373 (12)
C4-C5	1.369 (17)	C4-N4	1.341 (17)
C5-C6	1.356 (18)	C5-C1F	1.499 (14)
C6-C61	1.494 (18)	C61-C62	1.643 (25)
C61-H6	0.908 (80)	C61-H7	1.252 (215)
C62-H8	1.187 (121)	C62-H9	0.751 (101)
C62-H10	0.870 (446)	N2-H2	1.078 (124)
N2-H3	0.908 (114)	N4-H4	1.016 (72)
N4-H5	0.818 (77)	C1F-C2F	1.397 (27)
C1F-C6F	1.362 (28)	C2F-C3F	1.452 (16)
C2F-H2F	1.029 (124)	C3F-C4F	1.285 (28)
C4F-C5F	1.388 (33)	C5F-C6F	1.521 (20)
C5F-H5F	1.070 (138)	C6F-H6F	0.491 (76)
C1S-C2S	1.387 (17)	C1S-C6S	1.431 (16)
C1S-C1C	1.506 (19)	C2S-C3S	1.516 (23)
C2S-O3A	1.254 (20)	C3S-C4S	1.315 (20)
C3S-H3S	0.680 (58)	C4S-C5S	1.283 (20)
C5S-C6S	1.418 ((21)	C6S-O3B	1.200 (20)
C1C-O1	1.278 (14)	C1C-O2	1.258 (13)

Table 5.9 (contd.)

Bond	Interatomic Distance	Bond	Interatomic Distance
O4-C2I	1.495(26)	C1I-C2I	1.553(33)
C1I-H1I	0.835(70)	C1I-H2I	0.946(102)
C1I-H3I	1.102(193)	C2I-C3I	1.307(36)
C2I-H5I	1.183(112)	C3I-H6I	1.136(115)
CL-C4P	1.782(12)		

Pyrimethamine Salicylate Isopropanol Solvate

Table 5.10

Interatomic angles( $^{\circ}$ ) with estimated standard deviations in parentheses

Atoms	Bond Angle ( $^{\circ}$ )	Atoms	Bond Angle ( $^{\circ}$ )
C2-N1-C6	120.4(1.0)	C2-N1-H1	84.9(11.6)
C6-N1-H1	99.0(10.7)	N1-C2-N3	124.2(0.8)
N1-C2-N2	115.4(1.1)	N3-C2-N2	120.3(1.0)
C2-N3-C4	114.4(1.0)	N3-C4-C5	124.9(1.1)
N3-C4-N4	111.5(1.0)	C5-C4-N4	123.6(0.9)
C4-C5-C6	118.3(0.9)	C4-C5-C1P	119.7(1.1)
C6-C5-C1P	122.0(1.1)	N1-C6-C5	117.4(1.1)
N1-C6-C61	113.3(1.0)	C5-C6-C61	129.0(0.9)
C6-C61-C62	106.2(1.4)	C6-C61-H6	105.4(5.8)
C6-C61-H7	136.5(6.8)	C62-C61-H6	107.0(6.5)
C62-C61-H7	91.9(10.3)	H6-C61-H7	106.4(11.4)
C61-C62-H8	115.5(8.8)	C61-C62-H9	91.0(10.8)
C61-C62-H10	59.8(26.8)	H8-C62-H9	90.5(10.0)
H8-C62-H10	57.0(27.3)	H9-C62-H10	102.2(24.1)
C2-N2-H2	109.8(5.2)	C2-N2-H3	97.8(4.6)
H2-N2-H3	90.3(9.9)	C4-N4-H4	125.0(4.1)
C4-N4-H5	105.1(6.9)	H4-N4-H5	129.6(8.3)
C5-C1P-C2P	115.8(1.5)	C5-C1P-C6P	120.2(1.6)
C2P-C1P-C6P	124.0(1.2)	C1P-C2P-C3P	117.9(1.5)
C1P-C2P-H2P	122.0(6.3)	C3P-C2P-H2P	119.8(6.3)
C2P-C3P-C4P	117.3(1.8)	C3P-C4P-C5P	129.9(1.3)
C4P-C5P-C6P	113.3(1.7)	C4P-C5P-H5P	119.1(7.1)

Table 5.10 (contd.)

Atoms	Bond Angle (°)	Atoms	Bond Angle (°)
C6P-C5P-H5P	101.8(5.4)	C1P-C6P-C5P	117.4(1.9)
C1P-C6P-H6P	80.5(11.9)	C5P-C6P-H6P	73.6(7.3)
C2S-C1S-C6S	121.8(1.2)	C2S-C1S-C1C	118.3(1.0)
C6S-C1S-C1C	119.6(1.1)	C1S-C2S-C3S	115.5(1.1)
C1S-C2S-O3A	123.8(1.5)	C3S-C2S-O3A	120.4(1.4)
C2S-C3S-C4S	117.8(1.4)	C2S-C3S-H3S	73.9(5.2)
C4S-C3S-H3S	154.2(8.1)	C3S-C4S-C5S	126.6(1.6)
C4S-C5S-C6S	120.8(1.2)	C1S-C6S-C5S	116.9(1.2)
C1S-C6S-O3B	124.2(1.4)	C5S-C6S-O3B	118.6(1.3)
C1S-C1C-O1	117.6(1.0)	C1S-C1C--O2	117.7(1.0)
O1-C1C-O2	124.3(1.2)	C2I-C1I-H1I	99.7(7.0)
C2I-C1I-H2I	105.1(6.2)	C2I-C1I-H3I	88.4(9.3)
H1I-C1I-H2I	146.2(11.4)	H1I-C1I-H3I	115.7(11.7)
H2I-C1I-H3I	87.8(11.1)	O4-C2I-C1I	105.0(2.0)
O4-C2I-C3I	117.7(2.0)	O4-C2I-H5I	107.9(4.0)
C1I-C2I-C3I	126.6(1.8)	C1I-C2I-H5I	105.9(4.6)
C3I-C2I-H5I	90.7(5.2)	C2I-C3I-H6I	77.1(4.6)
CL-C4P-C3P	119.1(1.5)	CL-C4P-C5P	111.0(1.3)

Pyrimethamine Salicylate Isopropanol Solvate

Table 5.11

Torsion Angles

Atoms	Angle(°)
C6-N1-C2-N3	-4.0
C6-N1-C2-N2	173.5
H1-N1-C2-N3	-101.4
H1-N1-C2-N2	76.1
C2-N1-C6-C5	6.6
C2-N1-C6-C61	-178.7
H1-N1-C6-C5	95.9
H1-N1-C6-C61	-89.4
N1-C2-N3-C4	-0.2
N2-C2-N3-C4	-177.5
N1-C2-N2-H2	-6.8
N1-C2-N2-H3	-99.9
N3-C2-N2-H2	170.7
N3-C2-N2-H3	77.6
C2-N3-C4-C5	1.7
C2-N3-C4-N4	-177.4
N3-C4-C5-C6	1.1
N3-C4-C5-C1F	-179.3
N4-C4-C5-C6	-179.9
N4-C4-C5-C1F	-0.3
N3-C4-N4-H4	-13.4
N3-C4-N4-H5	161.2

Table 5.11 (contd.)

Atoms	Angle (°)
C5-C4-N4-H4	167.5
C5-C4-N4-H5	-17.9
C4-C5-C6-N1	-5.1
C4-C5-C6-C61	-178.8
C1P-C5-C6-N1	175.3
C1P-C5-C6-C61	1.6
C4-C5-C1P-C2P	-102.3
C4-C5-C1P-C6P	81.0
C6-C5-C1P-C2P	77.3
C6-C5-C1P-C6P	-99.4
N1-C6-C61-C62	-79.3
N1-C6-C61-H6	167.3
N1-C6-C61-H7	31.6
C5-C6-C61-C62	94.6
C5-C6-C61-H6	-18.8
C5-C6-C61-H7	-154.5
C6-C61-C62-H8	-177.7
C6-C61-C62-H9	-86.7
C6-C61-C62-H10	169.8
H6-C61-C62-H8	-65.4
H6-C61-C62-H9	25.6
H6-C61-C62-H10	-77.9
H7-C61-C62-H8	42.3
H7-C61-C62-H9	133.4
H7-C61-C62-H10	29.9

Table 5.11 (contd.)

Atoms	Angle(°)
C5-C1P-C2P-C3P	179.0
C5-C1P-C2P-H2P	4.6
C6P-C1P-C2P-C3P	-4.5
C6P-C1P-C2P-H2P	-178.8
C5-C1P-C6P-C5P	-179.1
C5-C1P-C6P-H6P	-113.3
C2P-C1P-C6P-C5P	4.5
C2P-C1P-C6P-H6P	70.3
C1P-C2P-C3P-C4P	3.1
H2P-C2P-C3P-C4P	177.6
C2P-C3P-C4P-C5P	-2.4
C3P-C4P-C5P-C6P	2.3
C3P-C4P-C5P-H5P	-117.3
C4P-C5P-C6P-C1P	-3.1
C4P-C5P-C6P-H6P	-72.8
H5P-C5P-C6P-C1P	126.0
H5P-C5P-C6P-H6P	56.3
C6S-C1S-C2S-C3S	-5.0
C6S-C1S-C2S-O3A	-179.1
C1C-C1S-C2S-C3S	-178.7
C1C-C1S-C2S-O3A	7.2
C2S-C1S-C6S-C5S	5.3
C2S-C1S-C6S-O3B	-167.9
C1C-C1S-C6S-C5S	179.0
C1C-C1S-C6S-O3B	5.7

Table 5.11 (contd.)

Atoms	Angle (°)
C2S-C1S-C1C-01	173.9
C2S-C1S-C1C-02	0.8
C6S-C1S-C1C-01	0.0
C6S-C1S-C1C-02	-173.1
C1S-C2S-C3S-C4S	-0.9
C1S-C2S-C3S-H4S	-156.1
O3A-C2S-C3S-C4S	173.4
O3A-C2S-C3S-H3S	18.2
C2S-C3S-C4S-C5S	7.3
H3S-C3S-C4S-C5S	119.2
C3S-C4S-C5S-C6S	-7.2
C4S-C5S-C6S-C1S	0.6
C4S-C5S-C6S-O3B	174.2
H1I-C1I-C2I-04	72.7
H1I-C1I-C2I-C3I	-144.5
H1I-C1I-C2I-H5I	-41.3
H2I-C1I-C2I-04	-84.3
H2I-C1I-C2I-C3I	58.6
H2I-C1I-C2I-H5I	161.7
H3I-C1I-C2I-04	-171.5
H3I-C1I-C2I-C3I	-28.7
H3I-C1I-C2I-H5I	74.5
O4-C2I-C3I-H6I	90.3
C1I-C2I-C3I-H6I	-48.6
H5I-C2I-C3I-H6I	-159.1

Pyrimethamine Salicylate Isopropanol Solvate

Table 5.12

Calculation of  $\theta$  Angle between planes

Plane 1:                    L = 0.1492  
                                 M = 0.7413  
                                 N = 0.6544  
                                 D = 14.2119

Deviations:                -0.0280  
                                 0.0035  
                                 0.0161  
                                 -0.0107  
                                 -0.0140  
                                 0.0331

Plane 2:                    L = 0.1448  
                                 M = -0.5340  
                                 N = 0.8330  
                                 D = 11.3610

Deviations:                0.0199  
                                 -0.0147  
                                 0.0073  
                                 -0.0046  
                                 0.0077  
                                 -0.0156

If  $\theta$  = Angle between planes  $P_1$  and  $P_2$

Then  $\cos \theta = L_1 L_2 + M_1 M_2 + N_1 N_2$

Provided that  $L_1^2 + M_1^2 + N_1^2 = 1$

and  $L_2^2 + M_2^2 + N_2^2 = 1$

5.3 PYRIMETHAMINE SALICYLATE

5.3.1 Abstract

2,4-diamino-5-(4-chlorophenyl)-6-ethyl pyrimidine  
salicylate

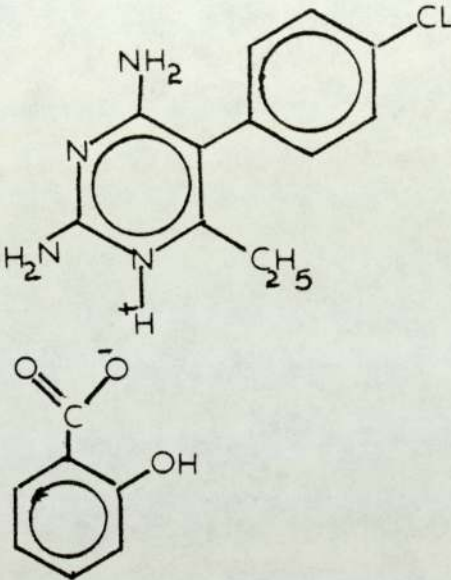
Pyrimethamine salicylate ( $C_{12}H_{13}ClN_4 \cdot C_7H_6O_3$ ) crystallises in the triclinic space group  $P\bar{1}$  with unit cell dimensions of  $a = 11.723(4) \text{ \AA}$  ;  $b = 13.186(7) \text{ \AA}$  ;  $c = 13.899(7) \text{ \AA}$  ;  $\alpha = 79.35(5)^\circ$  ;  $\beta = 66.29(4)^\circ$  ;  $\gamma = 86.34(4)^\circ$ .

The unit cell has a volume of  $1933.1(9) \text{ \AA}^3$  and there are four molecules per unit cell. The relative molar mass is  $386.83(9) \text{ g mol}^{-1}$  giving a calculated density  $D_x$  of  $1.329 \text{ g cm}^{-3}$ .

Using  $M_o\text{-K}\alpha$  radiation of wavelength  $0.71069 \text{ \AA}$  the linear absorption coefficient  $\mu$  is  $1.82 \text{ cm}^{-1}$ ,  $F(000)$  of 808.00 and the final value of R was 0.069 using 5373 unique reflections.

Figure 17

STRUCTURE OF PYRIMETHAMINE SALICYLATE



### 5.3.2 Experimental

#### Crystal Preparation

The crystals were prepared as for pyrimethamine salicylate isopropanol solvate but the second recrystallisation from propan-2-ol/water in equal proportions was not carried out.

#### Data Collection

The data were collected from a spear shaped crystal of size 0.15mm x 0.05mm x 0.40mm mounted along its long axis on an Enraf-Nonius CAD4 diffractometer using an  $\omega$ -2 $\theta$  scan with graphite monochromated  $M_{O-K_{\alpha}}$  radiation ( $\lambda = 0.71069 \text{ \AA}$ ). The scan range in terms of  $\theta$  was  $(1.00 + 0.35 \tan \theta^{\circ})$  at a scan rate of  $3 \frac{1}{3} \text{ }^{\circ} \text{min}^{-1}$  to  $0.53 \text{ }^{\circ} \text{min}^{-1}$  depending upon the individual intensities. Intensity monitor reflections were measured every two hours and subsequently fitted to a linear function of intensity against time that was used to rescale the data.

The monitor reflections were -5,0,-4 ; -2,7,1 ; and 4,9,4 being h,k and l respectively and the intensities of these reflections declined by 5.3% ; 8.2% and 8.1% respectively during the data collection. Orientation controls were used every 100 reflections on these monitor reflections.

Initially the unit cell dimensions were determined by least squares analysis from the setting angles of 25

reflections which were :-

-4 6 1 ; -1 5 1 ; -5 5 -1 ; -4 2 -4 ; -7 4 -2 ;  
-4 3 -2 ; -3 6 2 ; -2 7 1 ; -6 0 -4 ; -5 6 -2 ;  
-3 5 1 ; -4 9 4 ; -5 -3 -4 ; -3 6 -3 ; -7-1 -4 ;  
-2 5 3 ; -6-1 -3 ; -5 -1 -3 ; -4 0 -1 ; -5 0 -4 ;  
-4 -1 -2 ; -2 5 1 ; -4 1 0 ; -4 1 -4 ; -3 4 -1

The data were collected using  $\theta$  limits of  $2^\circ$  and  $23^\circ$  for  $^+ h, ^+ k, ^+ l$  with  $h_{\max} = 12$  ;  $k_{\max} = 14$  and  $l_{\max} = 15$  and 5682 reflections collected of which 5373 were unique and 2557 unobserved with an F value of greater than  $3\sigma(F)$  as the criterion for recognizing unobserved reflections. The value of  $R_{\text{int}}$  from merging equivalent reflections was 0.0237. The maximum value of  $(\sin \theta) / \lambda$  reached in intensity measurements was 0.5498.

### 5.3.3 Structure Analysis

The structure was solved by direct methods using both MULTAN (2) and SHELX (3) and F magnitudes were used in the least squares refinement. The hydrogen atoms were identified from the difference Fourier and were refined. The parameters which were refined were scale, co-ordinates and anisotropic temperature factors for non-hydrogen atoms.

The final value of R from the last refinement was 0.0690 and  $wR = 0.0963$ . The parameter w was calculated by :-

$$1.000/(\text{Sigma}^{**2}(F) + \text{weight}*F*F)$$

where the weight was initially set at 0.004272.

The ratio of maximum least squares shift to error in the final refinement cycle  $(\Delta/\sigma)_{\text{max}}$  was 0.123 for atom C61'. The maximum positive and maximum negative electron density in the final difference Fourier synthesis was  $(\Delta\rho)_{\text{max}}$  0.4307 and  $(\Delta\rho)_{\text{min}}$  -0.3697 respectively.

The results of the final refinement cycle are to be found in Tables 5.13 and 5.14 and also results of the co-ordinate data being processed by GEOM and the computer graphics program PLUTO (51) to calculate torsion angles and least squares given in Tables 5.13 to 5.17 (inclusive). PLUTO was also used to produce the crystal structure diagrams Figs. 18 - 20.

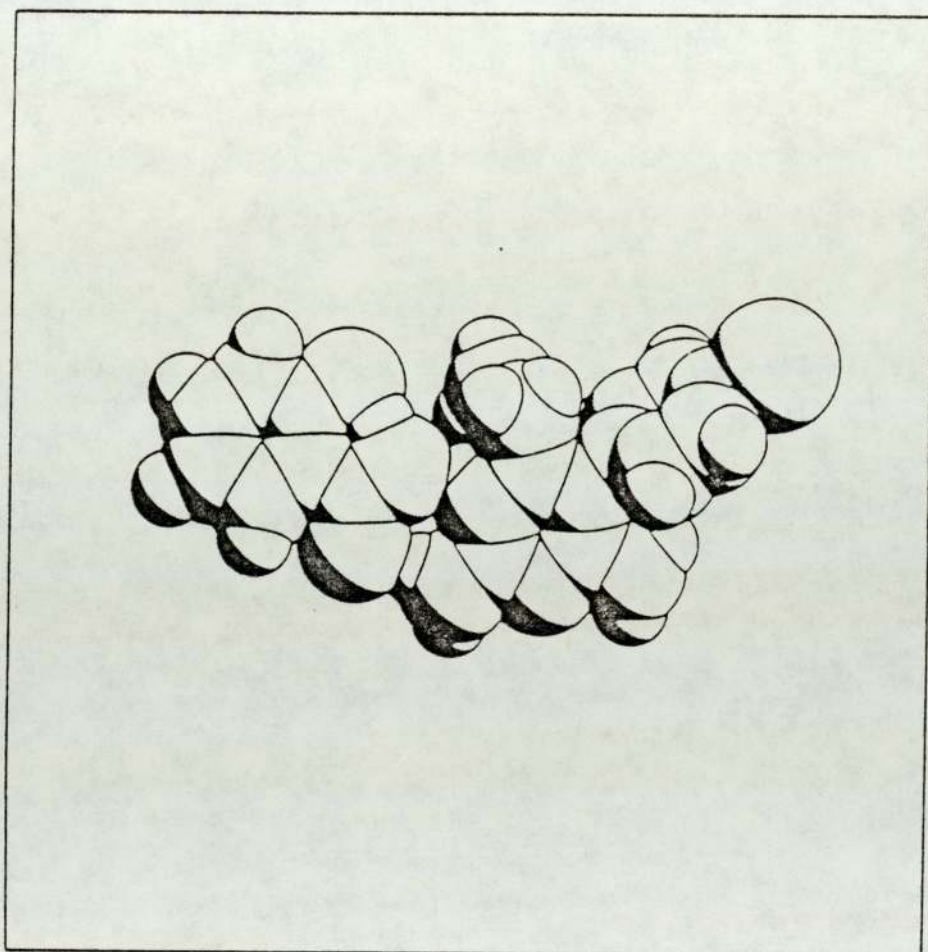
The angles calculated by GEOM between the two rings in the structures of pyrimethamine salicylate were found to be

$70^\circ$  and  $76^\circ$ .



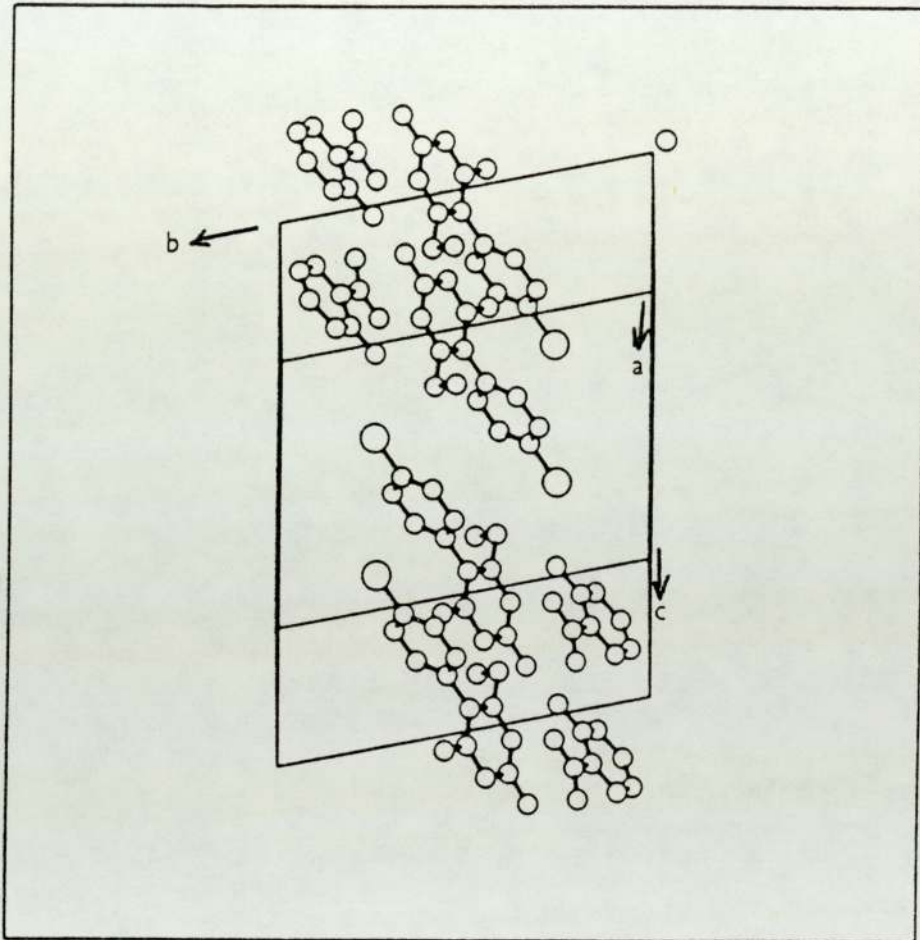
PYRIMETHAMINE SALICYLATE

Fig. 19 Space Filling Diagram



PYRIMETHAMINE SALICYLATE

Fig. 20 Packing Diagram



Pyrimethamine Salicylate

Table 5.13

Positional parameters (fractional co-ordinates  
 $\times 10^4$ )

With estimated standard deviations in parentheses

Atom	X/a	Y/b	Z/c
N1	8047(4)	6265(3)	243(3)
C2	7470(5)	6176(4)	-369(4)
N3	6467(4)	5559(3)	-35(3)
C4	6078(5)	5034(4)	983(4)
C5	6675(5)	5111(4)	1679(4)
C6	7689(5)	5734(4)	1269(4)
N2	7876(5)	6712(3)	8647(3)
N4	5071(4)	4430(4)	1301(3)
C61	8498(6)	5884(4)	1835(4)
C62	9705(6)	5323(5)	1470(5)
C1P	6217(5)	4491(4)	2760(4)
C2P	6885(6)	3673(4)	3020(5)
C3P	6442(9)	3066(5)	4031(6)
C4P	5319(8)	3303(6)	4770(5)
C5P	4641(6)	4117(6)	4556(5)
C6P	5092(6)	4707(5)	3536(4)
CL	4784(3)	2553(2)	6041(2)
C1R	11805(6)	8459(4)	-1991(5)
C2R	12623(7)	8207(5)	-1446(5)
C3R	13778(8)	8608(7)	-1861(7)

Table 5.13 (contd.)

Atom	X/a	Y/b	Z/c
C4R	14164 (8)	9322 (7)	-2805 (8)
C5R	13444 (8)	9585 (6)	-3316 (7)
C6R	12243 (7)	9158 (4)	-2966 (5)
C1A	10586 (6)	7964 (4)	-1602 (4)
O1R	9993 (4)	8068 (3)	-2190 (3)
O2R	10168 (4)	7417 (3)	-672 (3)
O3R	12229 (5)	7525 (4)	-511 (4)
N1'	1581 (4)	7292 (3)	3861 (3)
C2'	1087 (5)	7775 (4)	4703 (4)
N3'	873 (4)	8781 (3)	4607 (3)
C4'	1134 (5)	9307 (4)	3617 (4)
C5'	1717 (6)	8843 (4)	2694 (4)
C6'	1909 (6)	7816 (4)	2847 (4)
N2'	787 (5)	7207 (3)	5675 (3)
N4'	812 (5)	10296 (3)	3538 (3)
C61'	2399 (10)	7156 (6)	1995 (5)
C62'	3707 (14)	7085 (10)	1596 (9)
C1P'	2038 (8)	9498 (5)	1615 (5)
C2P'	1333 (10)	9522 (7)	1053 (6)
C3P'	1680 (16)	10192 (9)	54 (7)
C4P'	2734 (20)	10802 (9)	-304 (8)
C5P'	3448 (16)	10803 (9)	268 (9)
C6P'	3115 (10)	10135 (7)	1242 (7)
CL'	3093 (5)	11608 (2)	-1530 (2)
C1S	1716 (5)	3560 (4)	4992 (4)

Table 5.13 (contd.)

Atom	X/a	Y/b	Z/c
C2S	2290(5)	3166(4)	4053(4)
C3S	2504(6)	2136(4)	4065(4)
C4S	2156(7)	1453(4)	5037(5)
C5S	1595(7)	1825(4)	5976(5)
C6S	1378(6)	2879(4)	5948(4)
C1B	1549(5)	4691(4)	4985(4)
O1S	1081(4)	5032(3)	5815(3)
O2S	1936(4)	5258(3)	4054(3)
O3S	2682(4)	3804(3)	3082(3)
H1	8895	6450	96
H2	7758	6562	-1990
H3	8587	7170	-1623
H4	4661	4415	799
H5	4807	4040	2079
H6	8261	5761	2512
H7	8854	6651	1850
H8	9315	4593	1611
H9	10435	5256	1637
H10	10101	5511	594
H2F	7713	3517	2285
H2R	11036	7553	-395
H3R	14078	8605	-1175
H4R	15020	9572	-2947
H5R	14000	10232	-4243
H6R	11716	9520	-3452

Table 5.13 (contd.)

Atom	X/a	Y/b	Z/c
H1'	1809	6647	3897
H2'	803	6493	5760
H3'	1013	7636	6208
H4'	776	10796	2820
H5'	158	10663	4224
H6'	1982	6492	1850
H7'	2403	7524	1440
H8'	3827	6712	2173
H6P'	3401	10166	1783
H2S	2564	4592	3207
H3S	2957	1763	3357
H4S	2656	704	4957
H5S	1491	1316	6785
H6S	867	3210	6766
H5P	3888	4398	5087
H6P	4543	5348	3456
H2R	11036	7553	-395

Pyrimethamine Salicylate

Table 5.14

Anisotropic temperature factors

(non-hydrogen atoms)

Isotropic temperature factors

(hydrogen atoms)

With standard deviations in parentheses

Atom	U11	U22	U33	U23	U13	U12
N1	.0555 (30)	.0603 (27)	.0419 (25)	-.0001 (21)	-.0227 (23)	-.0073 (22)
C2	.0594 (39)	.0571 (34)	.0391 (30)	.0000 (26)	-.0211 (29)	.0005 (30)
N3	.0663 (33)	.0645 (28)	.0303 (23)	.0024 (20)	-.0149 (22)	-.0106 (26)
C4	.0623 (40)	.0574 (33)	.0333 (29)	-.0054 (25)	-.0093 (28)	-.0005 (31)
C5	.0519 (35)	.0508 (30)	.0356 (27)	-.0014 (23)	-.0209 (26)	-.0079 (27)
C6	.0659 (40)	.0509 (31)	.0356 (28)	-.0050 (24)	-.0208 (28)	.0064 (30)
N2	.0855 (37)	.0745 (31)	.0309 (24)	.0161 (22)	-.0195 (24)	-.0192 (28)
N4	.0685 (34)	.0790 (32)	.0395 (25)	.0102 (23)	-.0230 (24)	-.0273 (29)
C61	.0811 (46)	.0710 (38)	.0506 (33)	.0006 (28)	-.0388 (33)	-.0144 (34)
C62	.0618 (44)	.1043 (50)	.0762 (43)	.0054 (38)	-.0353 (37)	-.0014 (40)
C1F	.0547 (36)	.0580 (34)	.0342 (28)	.0053 (24)	-.0184 (28)	-.0084 (29)
C2F	.0941 (49)	.0531 (35)	.0596 (38)	.0055 (29)	-.0249 (36)	.0008 (34)
C3F	.1282 (70)	.0729 (45)	.0759 (49)	.0303 (39)	-.0409 (52)	-.0207 (46)
C4F	.0913 (56)	.0961 (52)	.0497 (38)	.0334 (37)	-.0311 (41)	-.0402 (45)
C5F	.0742 (48)	.1269 (60)	.0385 (34)	.0115 (37)	-.0174 (34)	-.0223 (45)
C6F	.0641 (43)	.1007 (47)	.0400 (32)	-.0027 (32)	-.0152 (32)	-.0027 (36)
CL	.1752 (23)	.1793 (23)	.0697 (12)	.0697 (14)	-.0539 (14)	-.0907 (19)
C1R	.0676 (43)	.0469 (32)	.0627 (37)	.0013 (28)	-.0167 (34)	-.0063 (31)
C2R	.0810 (52)	.0760 (44)	.0770 (46)	.0041 (36)	-.0322 (42)	-.0182 (39)

Table 5.14 (contd.)

Atom	U11	U22	U33	U23	U13	U12
C3R	.0256 (64)	.1334 (72)	.1170 (70)	-.0036 (58)	-.0359 (54)	-.0247 (55)
C4R	.0771 (60)	.1132 (65)	.1346 (79)	.0124 (58)	-.0341 (58)	-.0247 (51)
C5R	.0760 (56)	.0858 (52)	.1227 (68)	.0291 (47)	-.0264 (53)	-.0161 (45)
C6R	.0953 (55)	.0474 (34)	.0794 (45)	.0144 (32)	-.0176 (41)	-.0120 (36)
C1A	.0758 (45)	.0502 (33)	.0501 (35)	.0045 (27)	-.0286 (33)	-.0127 (31)
O1R	.0811 (30)	.0566 (23)	.0582 (24)	.0142 (19)	-.0223 (23)	-.0153 (21)
O2R	.0901 (32)	.0933 (30)	.0472 (23)	.0256 (22)	-.0277 (22)	-.0341 (25)
O3R	.1197 (42)	.1372 (43)	.0723 (30)	.0240 (30)	-.0575 (30)	-.0288 (35)
N1'	.0919 (38)	.0382 (24)	.0376 (25)	.0005 (20)	-.0165 (25)	.0126 (24)
C2'	.0582 (37)	.0533 (35)	.0345 (28)	.0014 (26)	-.0166 (26)	-.0008 (28)
N3'	.0742 (33)	.0405 (25)	.0384 (24)	.0021 (19)	-.0210 (23)	.0032 (22)
C4'	.0709 (39)	.0417 (31)	.0376 (30)	-.0010 (25)	-.0146 (28)	-.0011 (27)
C5'	.0928 (47)	.0438 (32)	.0275 (28)	.0046 (23)	-.0008 (28)	.0017 (30)
C6'	.1006 (50)	.0504 (36)	.0304 (29)	.0011 (25)	-.0050 (30)	.0126 (32)
N2'	.0915 (38)	.0456 (25)	.0415 (25)	.0042 (21)	-.0281 (25)	.0032 (24)
N4'	.0971 (39)	.0389 (26)	.0475 (27)	-.0019 (21)	-.0191 (27)	.0108 (25)
C61'	.1623 (84)	.0873 (50)	.0346 (34)	.0066 (33)	-.0005 (44)	.0459 (54)
C62'	.2005 (128)	.1738 (104)	.1215 (87)	-.0143 (74)	-.0449 (87)	.0608 (97)
C1P'	.1349 (67)	.0468 (35)	.0382 (35)	.0040 (28)	.0035 (40)	.0250 (40)
C2P'	.2060 (102)	.1155 (64)	.0524 (45)	.0039 (42)	-.0548 (57)	.0407 (64)
C3P'	.3371 (196)	.1356 (91)	.0467 (53)	.0111 (59)	-.0435 (81)	.0856 (100)
C4P'	.3461 (217)	.0717 (61)	.0391 (57)	.0265 (50)	.0304 (86)	.0733 (91)
C5P'	.3061 (194)	.0988 (74)	.0658 (70)	.0331 (64)	.0453 (89)	-.0056 (93)
C6P'	.1602 (86)	.0892 (56)	.0928 (62)	.0172 (49)	.0101 (59)	-.0306 (59)
CL'	.5918 (86)	.1180 (20)	.0502 (13)	.0398 (13)	.0344 (25)	.1269 (34)

Table 5.14 (contd.)

Atom	U11	U22	U33	U23	U13	U12
C1S	.0684 (38)	.0403 (29)	.0416 (31)	.0047 (24)	-.0203 (28)	-.0090 (26)
C2S	.0657 (39)	.0503 (33)	.0397 (30)	.0063 (25)	-.0213 (28)	-.0133 (28)
C3S	.0916 (48)	.0449 (34)	.0531 (35)	.0014 (28)	-.0170 (33)	-.0016 (31)
C4S	.1124 (57)	.0516 (36)	.0675 (43)	-.0013 (32)	-.0365 (40)	-.0016 (36)
C5S	.1136 (56)	.0471 (35)	.0613 (40)	.0168 (30)	-.0372 (39)	-.0231 (35)
C6S	.0780 (43)	.0535 (35)	.0407 (31)	.0084 (26)	-.0161 (29)	-.0147 (31)
C1B	.0718 (41)	.0524 (34)	.0387 (33)	-.0018 (27)	-.0167 (30)	.0022 (29)
O1S	.1160 (37)	.0510 (23)	.0482 (24)	-.0054 (19)	-.0183 (24)	.0077 (23)
O2S	.1058 (34)	.0461 (21)	.0496 (23)	.0108 (18)	-.0182 (23)	-.0002 (21)
O3S	.0937 (30)	.0554 (22)	.0345 (19)	.0065 (17)	-.0179 (19)	-.0100 (20)
Uiso						
H1	.0975 (63)					
H2	.0975 (63)					
H3	.0975 (63)					
H4	.0975 (63)					
H5	.0975 (63)					
H6	.0973 (74)					
H7	.0973 (74)					
H8	.0973 (74)					
H9	.0973 (74)					
H10	.0973 (74)					
H2F	.2180 (208)					
H3F	.2180 (208)					

Table 5.14 (contd.)

Atom	Uiso
H5P	.2180 (208)
H6P	.2180 (208)
H2R	.2108 (184)
H3R	.2108 (184)
H4R	.2108 (184)
H5R	.2108 (184)
H6R	.2108 (184)
H1'	.0975 (63)
H2'	.0975 (63)
H3'	.0975 (63)
H4'	.0975 (63)
H5'	.0975 (63)
H6'	.0973 (74)
H7'	.0973 (74)
H8'	.0973 (74)
H6P'	.4978 (747)
H2S	.1075 (99)
H3S	.1075 (99)
H4S	.1075 (99)
H5S	.1075 (99)
H6S	.1075 (99)

PYRIMETHAMINE SALICYLATE

Table 5.15 Bond distances in Angstroms with estimated standard deviation in parentheses

BOND LENGTHS

N1	C2	1.306	(9)	C2	N2	1.325	(6)
C4	C5	1.423	(9)	C6	C61	1.496	(10)
N2	H3	.963	(5)	C61	H6	.953	(6)
C62	H8	1.042	(7)	C1P	C6P	1.380	(7)
C2P	H2P	1.133	(6)	C4P	CL1	1.741	(7)
C5P	H5P	.998	(6)	C1R	C1A	1.458	(9)
C2R	O3R	1.359	(8)	C4R	H4R	1.007	(10)
C6R	H6R	1.115	(8)	N1'	C2'	1.338	(7)
N1'	H1'	.873	(4)	C4'	C5'	1.421	(7)
C5'	C6'	1.350	(8)	N2'	H3'	1.126	(5)
N4'	H5'	1.125	(4)	C62'	H8'	.917	(14)
C1P'	C6P'	1.419	(13)	C4P'	CL1'	1.738	(10)
C6P'	H6P'	.946	(12)	C2S	C3S	1.363	(8)
C3S	C4S	1.398	(8)	C5S	C6S	1.392	(8)
C6S	H6S	1.202	(5)	CL	C4P	1.742	(7)

C2	N3	1.343	(8)	N3	C4	1.358	(6)
C5	C1P	1.472	(6)	N2	H2	1.005	(5)
C61	C62	1.494	(9)	C61	H7	1.125	(7)
C1P	C2P	1.372	(9)	C2P	C3P	1.390	(9)
C4P	C5P	1.354	(11)	C5P	C6P	1.392	(8)
C1R	C6R	1.410	(8)	C2R	C3R	1.340	(12)
C4R	C5R	1.300	(16)	C5R	C6R	1.408	(12)
O2R	H2R	1.256	(5)	N1'	C6'	1.360	(6)
N3'	C4'	1.343	(6)	C4'	N4'	1.331	(7)
N2'	H2'	.927	(4)	N4'	H4'	1.103	(5)
C61'	H7'	.830	(7)	C1P'	C2P'	1.341	(16)
C4P'	C5P'	1.366	(29)	C5P'	C6P'	1.392	(14)
C1S	C1B	1.490	(7)	C2S	O3S	1.368	(6)
C4S	H4S	1.116	(6)	C5S	H5S	1.162	(6)
O3S	H2S	1.076	(4)				

N1	H1	.968	(5)	N1	C6	1.373	(6)
C5	C6	1.349	(8)	C4	N4	1.339	(8)
N4	H5	1.037	(4)	N4	H4	.996	(6)
C62	H10	1.099	(6)	C62	H9	.968	(8)
C3P	H3P	.935	(10)	C3P	C4P	1.366	(10)
C1R	C2R	1.434	(12)	C6P	H6P	1.046	(7)
C3R	H3R	1.140	(12)	C3R	C4R	1.390	(13)
C1A	O2R	1.273	(6)	C1A	O1R	1.255	(9)
C2'	N2'	1.337	(6)	C2'	N3'	1.326	(7)
C6'	C61'	1.503	(9)	C5'	C1P'	1.498	(8)
C61'	H6'	1.115	(10)	C61'	C62'	1.408	(18)
C3P'	C4P'	1.381	(26)	C2P'	C3P'	1.419	(12)
C1S	C6S	1.381	(7)	C1S	C2S	1.388	(7)
C4S	C5S	1.371	(9)	C3S	H3S	1.103	(6)
C1B	O2S	1.286	(6)	C1B	O1S	1.219	(7)

PYRIMETHAMINE SALICYLATE

Table 5.16 Interatomic angles ( $^{\circ}$ ) with estimated standard deviations in parentheses

BOND ANGLES			
C2	N1	C6	123.1 (5)
N3	C2	N2	118.4 (6)
C4	C5	C6	116.1 (4)
C5	C6	C61	125.2 (5)
C4	N4	H5	112.8 (5)
C62	C61	H6	102.4 (6)
C61	C62	H10	105.8 (6)
C5	C1P	C6P	120.8 (5)
C2P	C3P	C4P	118.4 (7)
C5P	C4P	CL1	119.6 (5)
C1P	C6P	H6P	125.1 (5)
C1R	C2R	C3R	121.0 (7)
C4R	C3R	H3R	125.5 (10)
C1R	C6R	C5R	117.3 (8)
O1R	C1A	O2R	122.0 (6)
N1'	C2'	N3'	122.7 (4)
N3'	C4'	N4'	116.5 (4)
N1'	C6'	C5'	118.9 (5)
H2'	N2'	H3'	122.0 (5)
C6'	C61'	H6'	132.1 (7)
C61'	C62'	H8'	102.0 (9)
C2P'	C3P'	C4P'	118.5 (15)
C1P'	C6P'	C5P'	119.2 (12)
C6S	C1S	C1B	120.3 (5)
C2S	C3S	H3S	125.8 (5)
C4S	C5S	C6S	119.5 (5)
C5S	C6S	H6S	120.0 (4)
N1	C2	N3	122.1 (4)
N3	C4	N4	115.1 (6)
N1	C6	C5	118.9 (6)
H2	N2	H3	106.8 (3)
C6	C61	H6	123.9 (6)
C61	C62	H8	96.2 (5)
H9	C62	H10	103.1 (5)
C1P	C2P	H2P	110.5 (5)
C3P	C4P	C5P	122.2 (6)
C6P	C5P	H5P	114.9 (7)
C2R	C1R	C1A	121.9 (5)
C2R	C3R	C4R	119.4 (10)
C5R	C4R	H4R	131.3 (9)
C1R	C1A	O1R	119.8 (5)
C2'	N1'	H1'	124.4 (5)
C2'	N3'	C4'	117.0 (4)
C4'	C5'	C1P'	119.0 (5)
C2'	N2'	H2'	120.0 (5)
H4'	N4'	H5'	104.7 (4)
C62'	C61'	H7'	93.7 (8)
C2P'	C1P'	C6P'	121.8 (7)
C5P'	C4P'	CL1'	121.2 (13)
C2S	C1S	C6S	118.1 (5)
C3S	C2S	O3S	117.7 (5)
C3S	C4S	H4S	112.6 (5)
C1S	C6S	C5S	121.4 (5)
O1S	C1B	O2S	123.8 (8)
C6	N1	H1	100.2 (5)
N3	C4	C5	123.6 (5)
C6	C5	C1P	123.6 (6)
C2	N2	H3	121.2 (6)
H4	N4	H5	128.2 (5)
C62	C61	H7	99.2 (6)
H8	C62	H9	109.1 (6)
C2P	C1P	C6P	118.1 (5)
C2P	C3P	H3P	110.6 (7)
C4P	C5P	C6P	118.5 (6)
C5P	C6P	H6P	113.4 (5)
C1R	C2R	O3R	119.1 (6)
C3R	C4R	C5R	121.5 (9)
C1R	C6R	H6R	128.5 (7)
C1A	O2R	H2R	99.4 (4)
N1'	C2'	N2'	117.9 (5)
C5'	C4'	N4'	121.1 (4)
N1'	C6'	C61'	114.9 (5)
C4'	N4'	H4'	126.1 (5)
C6'	C61'	H7'	106.2 (7)
C5'	C1P'	C2P'	122.8 (7)
C3P'	C4P'	C5P'	123.0 (10)
C1P'	C6P'	H6P'	112.5 (7)
C1S	C2S	C3S	121.3 (5)
C4S	C3S	H3S	114.1 (5)
C4S	C5S	H5S	121.0 (5)
C1S	C1B	O1S	121.0 (4)

Table 5.16 (contd.)

N1	C2	N2	119.5 (5)
C5	C4	N4	121.3 (4)
N1	C6	C61	115.9 (5)
C4	N4	H4	119.0 (4)
C6	C61	H7	125.1 (5)
C61	C62	H9	136.2 (8)
C5	C1P	C2P	121.0 (4)
C3P	C2P	H2P	127.4 (6)
C3P	C4P	CL1	118.1 (6)
C1P	C6P	C5P	121.3 (6)
C6R	C1R	C1A	120.0 (7)
C2R	C3R	H3R	107.7 (7)
C4R	C5R	C6R	122.7 (7)
C1R	C1A	O2R	118.2 (7)
C6'	N1'	H1'	113.8 (4)
N3'	C4'	C5'	122.4 (5)
C6'	C5'	C1P'	123.6 (5)
C2'	N2'	H3'	110.9 (4)
C6'	C61'	C62'	111.7 (10)
H6'	C61'	H7'	91.8 (9)
C1P'	C2P'	C3P'	119.2 (11)
C4P'	C5P'	C6P'	118.3 (14)
C2S	C1S	C1B	121.5 (4)
C2S	C3S	C4S	120.1 (5)
C5S	C4S	H4S	124.5 (7)
C1S	C6S	H6S	118.6 (5)
C2S	O3S	H2S	108.7 (4)
CL	C4P	C3P	118.1 (6)
CL	C4P	C5P	119.6 (5)

PYRIMETHAMINE SALICYLATE

Table 5.17 Torsion Angles ( $^{\circ}$ )

TORSION ANGLES				
C6	N1	C2	N3	.6
C2	N1	C6	C5	-1.8
N1	C2	N3	C4	.4
N3	C2	N2	H2	-24.2
N3	C4	C5	C6	-1.1
N3	C4	N4	H4	-1.7
C4	C5	C6	N1	2.0
C4	C5	C1P	C2P	108.6
N1	C6	C61	C62	-75.1
C5	C6	C61	H6	-21.9
C6	C61	C62	H10	49.0
H7	C61	C62	H8	169.6
C5	C1P	C2P	H2P	-6.9
C5	C1P	C6P	H6P	-7.1
C1P	C2P	C3P	H3P	-156.8
C2P	C3P	C4P	CL1	-178.8
C3P	C4P	C5P	H5P	-169.7
C4P	C5P	C6P	H6P	-176.0
C6R	C1R	C2R	O3R	-179.1
C2R	C1R	C6R	H6R	-171.7
C2R	C1R	C1A	O2R	10.9
C1R	C2R	C3R	H3R	155.3
C2R	C3R	C4R	H4R	175.2
H4R	C4R	C5R	C6R	-178.1
O1R	C1A	O2R	H2R	-179.1
H1'	N1'	C2'	N2'	-8.2
H1'	N1'	C6'	C61'	9.8
N1'	C2'	N2'	H3'	141.3
C2'	N3'	C4'	N4'	174.1
N4'	C4'	C5'	C1P'	3.6
C5'	C4'	N4'	H5'	164.9
C1P'	C5'	C6'	C61'	-3.4
C6'	C5'	C1P'	C6P'	-105.3
C5'	C6'	C61'	C62'	90.8
H6'	C61'	C62'	H8'	-89.9
C5'	C1P'	C6P'	C5P'	-177.1
C1P'	C2P'	C3P'	C4P'	-.3
CL1'	C4P'	C5P'	C6P'	-179.5
C6S	C1S	C2S	O3S	-178.0
C2S	C1S	C6S	H6S	-179.2
C2S	C1S	C1B	O2S	2.2
C1S	C2S	C3S	H3S	-179.7
C3S	C2S	O3S	H2S	-172.2
H3S	C3S	C4S	H4S	18.9
H4S	C4S	C5S	H5S	-8.5
H5S	C5S	C6S	H6S	-14.2

Table 5.17 (contd.)

C6	N1	C2	N2	-179.7
C2	N1	C6	C61	176.7
N2	C2	N3	C4	-179.3
N3	C2	N2	H3	179.3
N3	C4	C5	C1P	-178.1
N3	C4	N4	H5	179.6
C4	C5	C6	C61	-176.5
C4	C5	C1P	C6P	-70.4
N1	C6	C61	H6	159.7
C5	C6	C61	H7	-135.3
H6	C61	C62	H8	80.5
H7	C61	C62	H9	43.4
C6P	C1P	C2P	C3P	.9
C2P	C1P	C6P	C5P	-.0
H2P	C2P	C3P	C4P	-170.0
H3P	C3P	C4P	C5P	151.3
CL1	C4P	C5P	C6P	179.7
H5P	C5P	C6P	C1P	171.2
C1A	C1R	C2R	C3R	174.6
C1A	C1R	C6R	C5R	-178.1
C6R	C1R	C1A	O1R	8.3
O3R	C2R	C3R	C4R	-178.7
H3R	C3R	C4R	C5R	-148.7
C4R	C5R	C6R	C1R	3.4
C6'	N1'	C2'	N3'	.8
C2'	N1'	C6'	C5'	-.7
N1'	C2'	N3'	C4'	2.2
N3'	C2'	N2'	H2'	169.3
N3'	C4'	C5'	C6'	5.6
N3'	C4'	N4'	H4'	-166.6
C4'	C5'	C6'	N1'	-2.4
C4'	C5'	C1P'	C2P'	-100.0
N1'	C6'	C61'	C62'	-92.6
C5'	C6'	C61'	H6'	-117.9
H7'	C61'	C62'	H8'	176.7
C5'	C1P'	C6P'	H6P'	-11.8
C2P'	C3P'	C4P'	C5P'	-1.1
C4P'	C5P'	C6P'	C1P'	-1.5
C1B	C1S	C2S	C3S	176.2
C1B	C1S	C6S	C5S	-176.0
C6S	C1S	C1B	O1S	-2.2
O3S	C2S	C3S	C4S	178.1
C2S	C3S	C4S	C5S	.2
C3S	C4S	C5S	C6S	.1
C4S	C5S	C6S	C1S	.0

Table 5.17 (contd.)

H1	N1	C2	N3	154.4
H1	N1	C6	C5	-162.7
N1	C2	N2	H2	156.1
C2	N3	C4	C5	-.2
N4	C4	C5	C6	179.3
C5	C4	N4	H4	177.9
C1P	C5	C6	N1	178.9
C6	C5	C1P	C2P	-68.2
N1	C6	C61	H7	46.2
C6	C61	C62	H8	-55.5
H6	C61	C62	H9	-45.6
H7	C61	C62	H10	-86.0
C6P	C1P	C2P	H2P	172.2
C2P	C1P	C6P	H6P	173.9
H2P	C2P	C3P	H3P	33.5
H3P	C3P	C4P	CL1	-26.4
CL1	C4P	C5P	H5P	8.0
H5P	C5P	C6P	H6P	-3.4
C1A	C1R	C2R	O3R	-3.2
C1A	C1R	C6R	H6R	12.3
C6R	C1R	C1A	O2R	-173.3
O3R	C2R	C3R	H3R	-26.9
H3R	C3R	C4R	H4R	28.9
C4R	C5R	C6R	H6R	174.6
C6'	N1'	C2'	N2'	179.9
C2'	N1'	C6'	C61'	-177.5
N2'	C2'	N3'	C4'	-176.8
N3'	C2'	N2'	H3'	-39.5
N3'	C4'	C5'	C1P'	-176.8
N3'	C4'	N4'	H5'	-14.7
C4'	C5'	C6'	C61'	174.1
C4'	C5'	C1P'	C6P'	77.2
N1'	C6'	C61'	H6'	58.6
C5'	C6'	C61'	H7'	-10.0
C5'	C1P'	C2P'	C3P'	177.8
C2P'	C1P'	C6P'	C5P'	.2
C2P'	C3P'	C4P'	CL1'	-179.6
C4P'	C5P'	C6P'	H6P'	-164.5
C1S	C1S	C2S	O3S	-2.5
C1S	C1S	C6S	H6S	5.3
C6S	C1S	C1S	O2S	177.5
O3S	C2S	C3S	H3S	-.9
C2S	C3S	C4S	H4S	-160.3
C3S	C4S	C5S	H5S	-166.6
C4S	C5S	C6S	H6S	178.7

Table 5.17 (contd.)

H1	N1	C2	N2	-25.9
H1	N1	C6	C61	15.9
N1	C2	N2	H3	-.4
C2	N3	C4	N4	179.5
N4	C4	C5	C1P	2.3
C5	C4	N4	H5	-.7
C1P	C5	C6	C61	.5
C6	C5	C1P	C6P	112.8
C5	C6	C61	C62	103.4
C6	C61	C62	H9	178.4
H6	C61	C62	H10	-175.0
C5	C1P	C2P	C3P	-178.1
C5	C1P	C6P	C5P	179.0
C1P	C2P	C3P	C4P	-.4
C2P	C3P	C4P	C5P	-1.2
C3P	C4P	C5P	C6P	2.0
C4P	C5P	C6P	C1P	-1.4
C6R	C1R	C2R	C3R	-1.3
C2R	C1R	C6R	C5R	-2.1
C2R	C1R	C1A	01R	-167.6
C1R	C2R	C3R	C4R	3.5
C2R	C3R	C4R	C5R	-2.3
C3R	C4R	C5R	C6R	-1.2
C1R	C1A	02R	H2R	2.5
H1'	N1'	C2'	N3'	172.7
H1'	N1'	C6'	C5'	-173.3
N1'	C2'	N2'	H2'	-9.8
C2'	N3'	C4'	C5'	-5.5
N4'	C4'	C5'	C6'	-174.0
C5'	C4'	N4'	H4'	13.0
C1P'	C5'	C6'	N1'	-179.8
C6'	C5'	C1P'	C2P'	77.4
N1'	C6'	C61'	H7'	166.5
C6'	C61'	C62'	H8'	67.6
C6P'	C1P'	C2P'	C3P'	.7
C2P'	C1P'	C6P'	H6P'	165.4
C3P'	C4P'	C5P'	C6P'	2.0
C6S	C1S	C2S	C3S	.8
C2S	C1S	C6S	C5S	-.5
C2S	C1S	C1S	01S	-177.5
C1S	C2S	C3S	C4S	-.7
C1S	C2S	03S	H2S	6.6
H3S	C3S	C4S	C5S	179.4
H4S	C4S	C5S	C6S	158.2
H5S	C5S	C6S	C1S	167.1

Chapter Six

Structure of Substituted Antifolate

6.1 AZIDOPYRIMETHAMINE ETHANESULPHONATE

Abstract

2,4-diamino-5-(3-azido-4-chlorophenyl)-6-ethyl  
pyrimidine ethanesulphonate

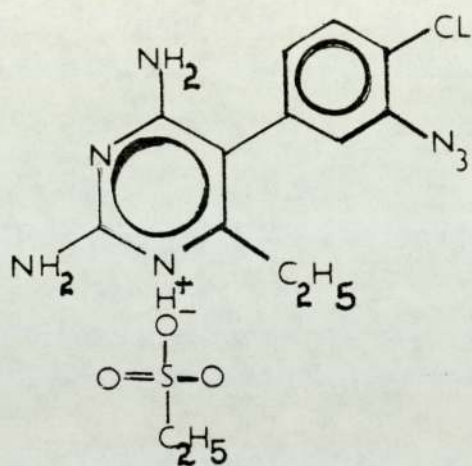
Azidopyrimethamine ethanesulphonate ( $C_{12}H_{12}ClN_7 \cdot EtSO_3H$ ) crystallises in the monoclinic space group  $P 2_1/c$  with unit cell dimensions of  $a = 9.199(5) \text{ \AA}$ ;  $b = 26.176(4) \text{ \AA}$ ;  $c = 18.944(8) \text{ \AA}$ ;  $\alpha = 90.0(3)^\circ$ ;  $\beta = 125.44(3)^\circ$ ;  $\gamma = 90.0(3)^\circ$ .

The unit cell has a volume of  $3716.4(6) \text{ \AA}^3$  and there are eight molecules per unit cell. The relative molar mass is  $399.85(6) \text{ g mol}^{-1}$  giving a calculated density  $D_x$  of  $1.215(2) \text{ g cm}^{-3}$ . The measured density  $D_m$  was  $1.252 \text{ g cm}^{-3}$ .

Using  $M_o-K\alpha$  radiation of wavelength  $0.71069 \text{ \AA}$ , the linear absorption coefficient is  $\mu = 2.98 \text{ cm}^{-1}$ ,  $F(000)$  of 1664.0 and the final value of R was 0.0918 using 5825 unique reflections.

Figure 21

STRUCTURE OF AZIDOPYRIMETHAMINE ETHANESULPHONATE



## 6.2 Experimental

### Crystal Preparation

The crystals were prepared by Dr. R.Griffin by the following method. Pyrimethamine (100g) was added in portions over one hour to a stirred mixture of nitric acid (300ml) and sulphuric acid (300ml) at a temperature maintained below 5°C. The mixture was stirred for a further twelve hours at room temperature, poured onto ice and basified with concentrated aqueous ammonia. The yellow solid was collected and washed with water.

A suspension of the nitro analogue, so prepared above, (20g) in ethanol (250ml) was stirred at 60°C-65°C and Raney nickel (c.a. 20g) was added. Hydrazine hydrate (75ml) was added dropwise over two hours as a solution in ethanol (75ml) at a rate such that the temperature did not exceed 70°C. When effervescence had subsided the solution was filtered hot through a Kieselguhr pad and on evaporation of the solvent a cream solid remained which was triturated with water and collected. Crystallisation from 50% ethanol afforded pale yellow needles of the amine monhydrate.

A solution of the amine (8g) in 5M-hydrochloric acid (150ml) was diazotised at 0°C by the addition of sodium nitrite (2.1g) as a solution in water (10ml) over thirty minutes. After stirring for a further thirty minutes, sodium azide (7.2g) was added in portions over one hour the

agitation being maintained. The mixture was stirred for a further one hour, diluted with water (200ml) and basified with concentrated aqueous ammonia, whereupon the product precipitated and was collected. A sample crystallised from aqueous ethanol as photosensitive microprisms of the azide monohydrate.

To a stirred suspension of the azide base (6.0g) in water (60ml) ethanesulphonic acid (2.5g) was added over five minutes and the mixture was boiled until all solids dissolved. Following filtration the pale yellow solution was allowed to cool and the product collected. Slow recrystallisation from water furnished pale yellow prisms of the azidopyrimethamine ethanesulphonate.

The density was measured using the flotation method using cyclohexane and carbon tetrachloride of densities  $0.778 \text{ gcm}^{-3}$  and  $1.6 \text{ gcm}^{-3}$  respectively.

#### Data Collection

The data were collected from a spear point shaped crystal of size  $0.11 \text{ mm} \times 0.075 \text{ mm} \times 0.41 \text{ mm}$  mounted along its long axis on an Enraf-Nonius CAD4 diffractometer using an  $\omega$ - $2\theta$  scan with graphite monochromated  $\text{M}_\alpha\text{-K}_\alpha$  radiation ( $\lambda = 0.71069 \text{ \AA}$ ). The scan range in terms of  $\theta$  was  $(1.00 + 0.35 \tan \theta^\circ)$  at a scan rate of  $2.5^\circ \text{ min}^{-1}$  to  $0.74^\circ \text{ min}^{-1}$  depending upon the individual intensities. Intensity monitor reflections were measured every two hours and subsequently fitted to a linear

function of intensity against time that was used to rescale the data.

The monitor reflections used were 2,11,0 and 0,9,3 being h,k and l respectively and the intensity of these reflections declined by 4.8% and 3.8% respectively during the data collection. Orientation controls were used every 100 reflections on these monitor reflections.

Initially the unit cell dimensions were determined by least squares analysis from the setting angles of 25 reflections which were :-

1 11 2 ; 0 12 -6 ; 1 8 2 ; 0 11 -2 ; 0 7 -5;  
2 10 1 ; 2 11 0 ; 1 12 -2 ; -1 13 -2 ; 0 12 3;  
0 9 3 ; -1 10 -1 ; -1 7 -1 ; -1 8 -1 ; 0 6 3;  
0 8 -2 ; 1 7 0 ; 1 7 1 ; 0 6 -4 ; 1 8 -2;  
1 6 -4 ; 1 7 -4 ; 3 15 1 ; -1 16 1 ; -1 12 2

The data were collected using  $\theta$  limits of  $2^\circ$  and  $25^\circ$  for h,k,<sup>±</sup> l with  $h_{\max} = 10$  ;  $k_{\max} = 31$  and  $l_{\max} = 22$  and 7234 reflections collected of which 5825 were unique and 4102 unobserved with an F value of greater than  $4\sigma(F)$  as the criterion for recognizing unobserved reflections. The value of  $R_{\text{int}}$  from merging equivalent reflections was 0.0623. The maximum value of  $(\sin \theta) / \lambda$  reached in intensity measurements was 0.5723.

### 6.3 Structure Analysis

The structure was solved by direct methods, SHELX (3), and F magnitudes were used in the least squares refinement. The hydrogen atoms were identified in the difference Fourier and were refined by using an option in the SHELX program called AFIX. The parameters which were refined were scale, co-ordinates, anisotropic temperature factors for non-hydrogen atoms and isotropic temperature factors for hydrogen atoms.

The final value of R from the last refinement was 0.0918 and wR = 0.0853. The parameter, w was calculated by :-

$$1.000/(\text{Sigma}^{**2}(\text{F}) + \text{weight}*\text{F}*\text{F})$$

where the weight was initially set to 0.001.

The ratio of maximum least squares shift to error in the final refinement cycle,  $(\Delta/\sigma)_{\text{max}}$  was 1.667 for hydrogen atoms (H7') on the C5 atom and 0.624 for non-hydrogen atoms (N3P). The position of the hydrogen atom was in fact identified in a slightly different position in the final refinement explaining the high ratio.

The maximum positive and maximum negative electron density in the final difference Fourier synthesis were  $(\Delta\rho)_{\text{max}}$  0.4034 and  $(\Delta\rho)_{\text{min}}$  -0.4226 respectively.

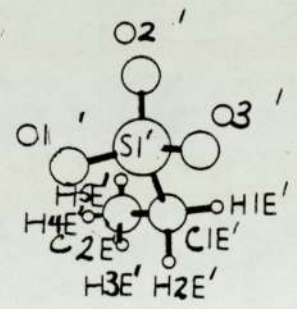
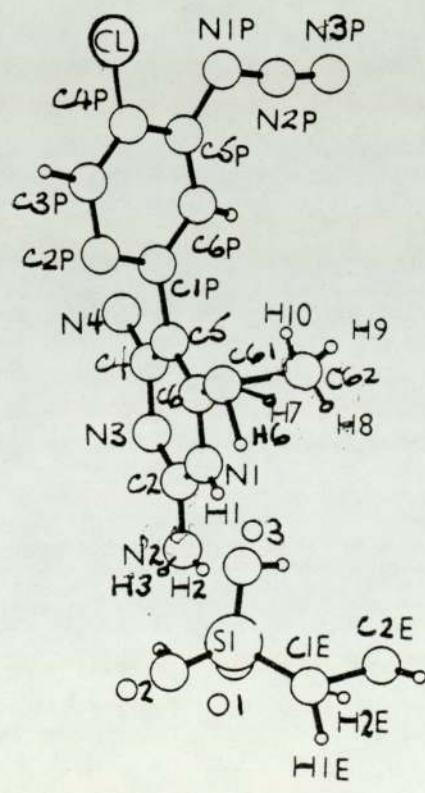
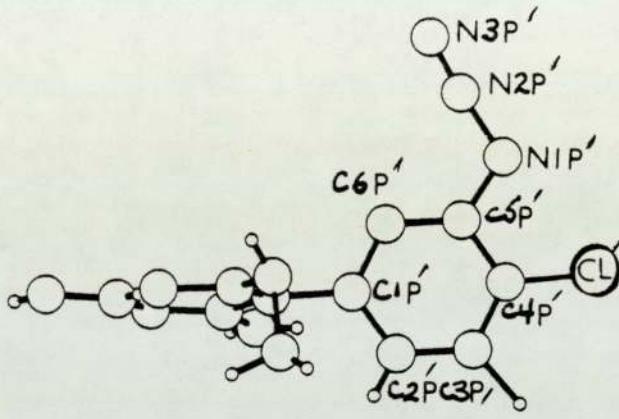
The results of the final refinement cycle are to be found in Tables 6.1 and 6.2 and also results of the co-ordinate data being processed by GEOM and the computer graphics program PLUTO (51) used to calculate torsion angles and least squares

planes given in Tables 6.3 to 6.6 (inclusive). PLUTO was also used to produce the crystal structure diagrams Figs. 22 - 24.

The angles calculated by GEOM between the two rings in the two azidopyrimethamine ethanesulphonate molecules were found to be  $70^{\circ} 8'$  and  $84^{\circ} 51'$ .

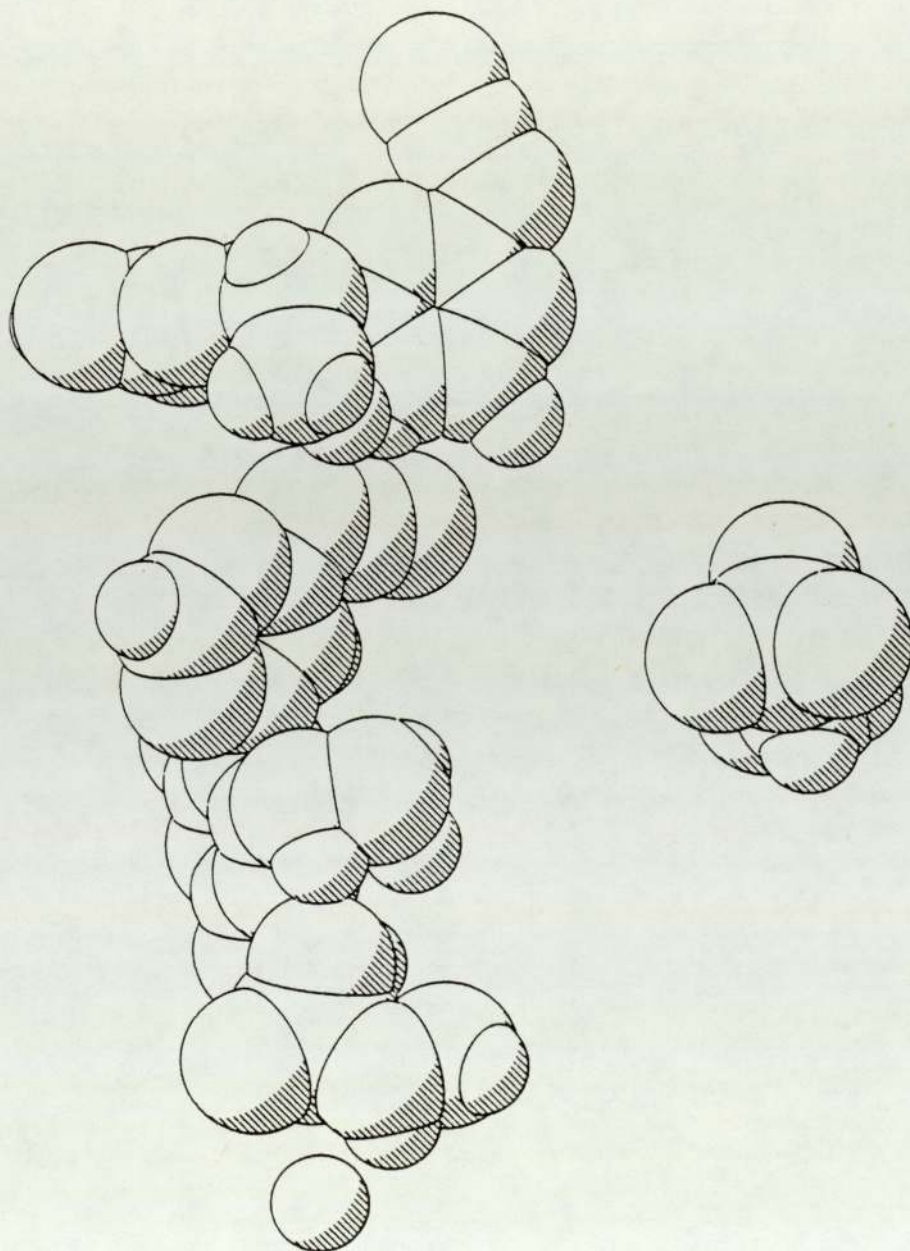
AZIDOPYRIMETHAMINE ETHANESULPHONATE

Fig. 22 Molecular Diagram



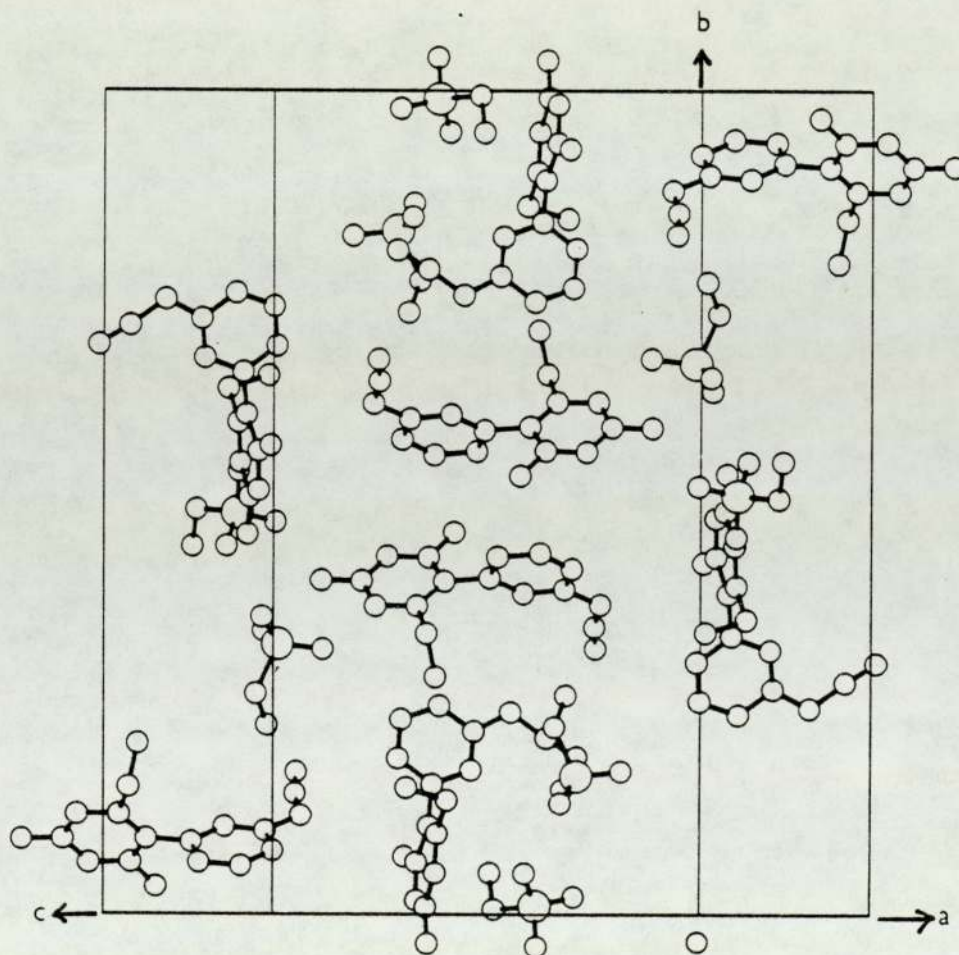
AZIDOPYRIMETHAMINE ETHANESULPHONATE

Fig. 23 Space Filling Diagram



AZIDOPYRIMETHAMINE ETHANESULPHONATE

Fig. 24 Packing Diagram



## Azidopyrimethamine ethanesulphonate

Table 6.1

Positional parameters (fractional co-ordinates  
x 10<sup>4</sup>)

With estimated standard deviations in  
parantheses

Atom	X/a	Y/b	Z/c
N1	3570(16)	3767(5)	6464(7)
C2	2239(22)	4065(7)	6297(11)
N3	1299(15)	4379(5)	5604(9)
C4	1745(21)	4340(6)	5051(11)
C5	3228(20)	4071(6)	5172(10)
C6	4098(18)	3784(6)	5907(11)
N2	1812(20)	4080(7)	6870(10)
N4	830(17)	4645(5)	4343(9)
C61	5774(22)	3436(6)	6203(11)
H6	6592(22)	3415(6)	6002(11)
H7	6523(22)	3613(6)	5993(11)
C62	5252(26)	2928(8)	5851(15)
H8	6443(26)	2710(8)	6071(15)
H9	4407(26)	2936(8)	5151(15)
H10	4543(26)	2751(8)	6083(15)
C1P	3809(24)	4124(6)	4620(11)
C2P	2866(23)	3918(6)	3791(12)
C3P	3481(25)	3975(6)	3297(10)
C4P	5124(24)	4231(6)	3653(13)
C5P	6070(32)	4431(7)	4463(12)

Table 6.1 (contd.)

Atom	X/a	Y/b	Z/c
C6F	5507 (25)	4354 (7)	5001 (12)
CL	5872 (7)	4299 (2)	2979 (4)
N1F	2684 (24)	3805 (6)	2430 (10)
N2F	1347 (29)	3522 (7)	2157 (12)
N3F	131 (25)	3241 (9)	1810 (13)
S1	276 (6)	101 (2)	2848 (3)
O1	1118 (13)	-397 (5)	3074 (7)
O2	-675 (14)	221 (5)	1932 (6)
O3	1487 (12)	517 (4)	3380 (6)
C1E	-1268 (18)	4945 (6)	8094 (10)
H1E	-1870 (18)	5314 (6)	7835 (10)
H2E	-458 (18)	4959 (6)	8793 (10)
C2E	-2538 (21)	4499 (7)	7773 (10)
H3E	-3504 (21)	4569 (7)	7912 (10)
H4E	-1869 (21)	4141 (7)	8059 (10)
H5E	-3208 (21)	4483 (7)	7080 (10)
H1	4067 (114)	3459 (38)	7019 (60)
H2	1394 (184)	4540 (66)	6877 (96)
H3	1967 (116)	3773 (36)	7078 (58)
H4	1213 (128)	4876 (45)	3852 (73)
H5	238 (140)	4898 (46)	4480 (69)
H5F	7019 (161)	4555 (56)	4869 (88)
H2F	1866 (167)	3832 (59)	3833 (89)
N1'	5241 (18)	4487 (5)	948 (8)
C2'	4119 (21)	4910 (7)	752 (9)

Table 6.1 (contd.)

Atom	X/a	Y/b	Z/c
N3'	2405 (16)	4833 (4)	461 (7)
C4'	1739 (22)	4351 (6)	246 (8)
C5'	2795 (21)	3922 (6)	356 (9)
C6'	4591 (24)	4007 (6)	706 (10)
N2'	4797 (17)	5375 (5)	926 (9)
N4'	92 (17)	4279 (6)	-22 (9)
C61'	5922 (20)	3611 (6)	909 (10)
H6'	5270 (20)	3292 (6)	474 (10)
H7'	6908 (20)	3770 (6)	834 (10)
C62'	6824 (22)	3441 (7)	1838 (11)
H8'	7768 (22)	3145 (7)	1969 (11)
H9'	5873 (22)	3294 (7)	1947 (11)
H10'	7525 (22)	3761 (7)	2264 (11)
C1F'	2003 (19)	3415 (6)	37 (13)
C2F'	1414 (20)	3250 (6)	-808 (10)
C3F'	639 (25)	2751 (8)	-1041 (14)
C4F'	503 (21)	2466 (7)	-495 (16)
C5F'	1131 (22)	2608 (7)	342 (13)
C6F'	1994 (23)	3093 (7)	646 (16)
CL'	-434 (7)	1843 (2)	-812 (4)
N1F'	70 (22)	2584 (8)	-1928 (15)
N2F'	78 (22)	2963 (8)	-2655 (16)
N3F'	172 (87)	2845 (23)	-3721 (45)
S1'	5760 (6)	1695 (2)	3707 (3)
O1'	7132 (15)	1364 (4)	4370 (7)

Table 6.1 (contd.)

Atom	X/a	Y/b	Z/c
O2'	5836(16)	1762(5)	2973(7)
O3'	3978(13)	1529(4)	3465(7)
C1E'	6171(22)	2292(6)	4199(11)
H1E'	7488(22)	2409(6)	4403(11)
H2E'	6151(22)	2247(6)	4760(11)
C2E'	4959(27)	2694(8)	3658(14)
H3E'	5473(27)	3049(8)	4010(14)
H4E'	3660(27)	2620(8)	3516(14)
H5E'	4849(27)	2720(8)	3060(14)
H1'	4934(154)	4664(52)	557(68)
H3'	5794(145)	4409(48)	8975(74)
H4'	-932(147)	4707(49)	-108(70)
H5'	-697(132)	4217(46)	64(68)
H6P'	1308(136)	3290(50)	475(76)
H5P'	902(106)	2744(36)	5733(51)

## Azidopyrimethamine ethanesulphonate

Table 6.2

Anisotropic temperature factors  
(non-hydrogen atoms)

Isotropic temperature factors  
(hydrogen atoms)

With standard deviations in  
parentheses

Atom	U11	U22	U33	U23	U13	U12
N1	.0380(80)	.0635(96)	.0372(80)	.0171(73)	.0227(72)	.0236(72)
C2	.0441(108)	.0521(114)	.0488(110)	.0129(95)	.0298(96)	-.0088(92)
N3	.0301(77)	.0647(97)	.0579(89)	-.0073(82)	.0250(74)	.0099(70)
C4	.0373(103)	.0397(105)	.0592(112)	-.0006(95)	.0278(95)	-.0085(84)
C5	.0327(97)	.0511(107)	.0279(92)	.0167(84)	.0077(82)	.0158(84)
C6	.0285(92)	.0484(107)	.0555(103)	-.0213(93)	.0254(89)	-.0132(82)
N2	.0782(108)	.0783(118)	.0740(107)	.0402(99)	.0444(90)	.0119(96)
N4	.0492(89)	.0529(95)	.0617(93)	.0146(80)	.0320(78)	.0302(75)
C61	.0760(124)	.0546(119)	.0765(124)	-.0138(98)	.0374(104)	.0111(105)
C62	.0551(140)	.1491(193)	.2071(199)	-.0314(176)	.0371(146)	.0020(140)
C1F	.0679(122)	.0403(106)	.058(116)	-.0222(94)	.037(102)	-.0021(96)
C2F	.0661(115)	.0350(102)	.076(120)	.0064(92)	.0536(106)	.0350(88)
C3F	.0756(124)	.0747(130)	.0385(105)	.0020(92)	.0424(104)	.0210(104)
C4F	.0536(113)	.0569(121)	.1308(149)	.0122(112)	.0767(115)	.0175(95)
C5F	.1163(176)	.0520(133)	.0379(123)	-.0182(105)	-.0119(125)	-.215(119)
C6F	.0866(144)	.0510(121)	.0866(130)	.0395(105)	.0575(118)	.0094(103)
CL	.1042(46)	.1681(63)	.1209(44)	-.0040(42)	.0864(40)	.0085(40)

Table 6.2 (contd.)

Atom	U11	U22	U33	U23	U13	U12
N1P	.1307(145)	.0671(114)	.0511(108)	-.0113(92)	.0220(106)	-.0136(105)
N2P	.1303(162)	.0863(141)	.0977(142)	-.0318(116)	.0599(134)	.0048(118)
N3P	.1134(144)	.1965(188)	.1276(148)	-.0544(140)	.0670(122)	-.0655(135)
S1	.0371(26)	.0743(34)	.0579(31)	-.0055(30)	.0272(25)	-.0001(28)
O1	.0391(70)	.0929(95)	.1072(91)	.0124(79)	.0311(67)	.0380(68)
O2	.0676(80)	.1349(105)	.0427(72)	-.0120(71)	.0396(65)	-.0143(74)
O3	.0374(68)	.0717(77)	.0746(75)	-.0322(68)	.0191(62)	-.0239(60)
C1E	.255(83)	.0673(116)	.0705(110)	-.0034(94)	.0293(83)	-.0152(85)
C2E	.0541(121)	.1485(169)	.0637(122)	-.0021(121)	.0281(103)	-.0204(122)
N1'	.0582(95)	.0373(96)	.0497(92)	.0274(73)	.0261(80)	.0247(79)
C2'	.0362(97)	.0708(127)	.0161(81)	-.0013(89)	.0156(77)	.0096(101)
N3'	.0417(82)	.0193(74)	.0621(85)	-.0031(68)	.0317(71)	.0042(67)
C4'	.0617(114)	.0321(99)	.0228(83)	-.0038(76)	.0243(84)	.0217(94)
C5'	.0444(98)	.0280(100)	.0450(94)	-.0105(77)	.0289(83)	-.0136(83)
C6'	.0718(122)	.0301(104)	.0538(103)	.0033(86)	.0403(95)	-.0026(99)
N2'	.0385(86)	.0345(95)	.0893(105)	-.0112(82)	.0263(78)	.0001(73)
N4'	.0106(73)	.0835(112)	.0716(90)	.0169(80)	.0215(70)	.0122(79)
C61'	.0425(99)	.0343(97)	.0722(116)	-.0048(96)	.0129(91)	.0227(87)
C62'	.0623(119)	.1039(151)	.1240(151)	.0304(130)	.0470(115)	.0545(115)
C1P'	.0288(92)	.0324(110)	.1112(140)	.0239(109)	.0440(98)	.0124(81)
C2P'	.0596(106)	.0479(115)	.0546(102)	-.0194(94)	.0263(90)	.0171(93)
C3P'	.0782(131)	.0518(133)	.1072(156)	-.0436(125)	.0536(119)	-.0197(109)
C4P'	.0349(100)	.0554(129)	.0988(145)	-.0353(120)	.0264(104)	-.0177(91)
C5P'	.0588(111)	.0470(120)	.0825(128)	.0087(105)	.0517(104)	.0217(95)
C6P'	.0206(100)	.0304(121)	.1717(183)	.0094(129)	.0273(113)	.0168(93)

Table 6.2 (contd.)

Atom	U11	U22	U33	U23	U13	U12
CL'	.0806(40)	.0620(36)	.1466(50)	-.0176(36)	.0452(38)	-.0142(30)
N1P'	.0819(124)	.1351(154)	.1575(152)	-.1244(134)	.0474(118)	-.0473(111)
N2P'	.0541(115)	.1391(160)	.2065(184)	-.0926(145)	.0275(128)	-.0243(112)
N3P'	.6310(292)	.5044(285)	.8918(302)	-.1320(293)	.0083(295)	-.3562(268)
S1'	.0561(30)	.0406(29)	.0619(31)	-.0029(27)	.0291(26)	.0025(27)
O1'	.0727(86)	.0562(79)	.1042(93)	.0073(75)	.0163(76)	.0138(70)
O2'	.1184(104)	.1082(105)	.0690(78)	-.0356(77)	.0526(78)	-.0505(81)
O3'	.0364(69)	.0927(92)	.1113(91)	-.0162(77)	.0373(68)	-.0189(65)
C1E'	.0669(125)	.0483(118)	.0949(131)	.0023(103)	.0395(107)	-.0016(98)
C2E'	.0998(164)	.0973(165)	.1758(186)	.0151(153)	.0338(149)	.0122(142)

## Uiso

H1	.0208(225)
H2	.1629(292)
H3	.0001(224)
H4	.0555(244)
H5	.0504(258)
H5P	.0803(280)
H2P	.1118(284)
H6	.1025(277)
H8	.1340(286)
H9	.1044(275)
H10	.0758(273)

Table 6.2 (contd.)

Atom	Uiso
H7	.1975 (299)
H1E	.0488 (251)
H2E	.1392 (286)
H3E	.1032 (279)
H4E	.1557 (292)
H5E	.0585 (254)
H1'	.0244 (260)
H3'	.0439 (265)
H4'	.0686 (251)
H5'	.0226 (246)
H6F'	.0238 (259)
H5F'	.0001 (200)
H6'	.0836 (267)
H8'	.0591 (255)
H9'	.0946 (277)
H10'	.1749 (295)
H7'	.0879 (275)
H1E'	.1126 (280)
H2E'	.0437 (255)
H3E'	.0620 (258)
H4E'	.1620 (292)
H5E'	.1322 (290)

## Azidopyrimethamine ethanesulphonate

Table 6.3

Bond distances in Angstroms with estimated standard deviation in parentheses

Bond	Interatomic Distance	Bond	Interatomic Distance
N1-C2	1.326(25)	N1-C6	1.394(30)
N1-H1	1.186(103)	C2-N3	1.352(21)
C2-N2	1.352(34)	N3-C4	1.332(32)
C4-C5	1.430(27)	C4-N4	1.354(21)
C5-C6	1.360(22)	C5-C1F	1.430(35)
C6-C61	1.587(25)	N2-H2	1.266(177)
N2-H3	0.869(97)	N4-H5	0.983(144)
C61-C62	1.439(27)	C61-H6	1.080(24)
C61-H7	1.079(34)	C62-H8	1.081(32)
C62-H9	1.080(32)	C62-H10	1.079(43)
C1F-C2F	1.389(26)	C1F-C6F	1.419(28)
C2F-C3F	1.338(38)	C2F-H2F	1.012(187)
C3F-C4F	1.416(28)	C5F-N1F	1.427(25)
C4F-C5F	1.355(28)	C5F-C6F	1.400(43)
C5F-H5F	0.824(111)	N1F-N2F	1.261(30)
N2F-N3F	1.171(29)	S1-O1	1.448(13)
S1-O2	1.454(12)	S1-O3	1.463(10)
C1E-C2E	1.507(24)	C1E-H1E	1.079(21)
C1E-H2E	1.079(21)	C2E-H3E	1.078(34)
C2E-H4E	1.078(25)	C2E-H5E	1.080(25)
CL - c4P	1.777(31)	S1 - C1E	1.736

Table 6.3(contd.)

Bond	Interatomic Distance	Bond	Interatomic Distance
N1'-C2'	1.408(24)	N1'-C6'	1.352(21)
N1'-H1'	0.775(129)	C2'-N3'	1.350(23)
C2'-N2'	1.319(23)	C2'-H1'	1.197(162)
N3'-C4'	1.357(19)	C4'-C5'	1.419(24)
C4'-N4'	1.302(25)	C5'-C6'	1.395(27)
C5'-C1P'	1.465(21)	C6'-C61'	1.475(25)
N4'-H5'	0.846(151)	C61'-C62'	1.513(25)
C61'-H6'	1.078(20)	C61'-H7'	1.079(30)
C62'-H8'	1.079(28)	C62'-H9'	1.079(34)
C62'-H10'	1.079(24)	C1P'-C2P'	1.427(29)
C1P'-C6P'	1.432(37)	C2P'-C3P'	1.429(25)
C3P'-C4P'	1.338(40)	C3P'-N1P'	1.506(37)
C4P'-C5P'	1.387(36)	C5P'-C6P'	1.429(26)
C6P'-H6P'	0.729(121)	N1P'-N2P'	1.700(40)
S1'-O1'	1.443(11)	S1'-O2'	1.442(18)
S1'-O3'	1.488(14)	S1'-C1E'	1.745(17)
C1E'-C2E'	1.440(24)	C1E'-H1E'	1.080(28)
C1E'-H2E'	1.080(35)	C2E'-H3E'	1.079(29)
C2E'-H4E'	1.079(37)	C2E'-H5E'	1.079(41)
CL' - c4P'	1.777(18)	N2P' - N3P'	2.094

## Azidopyrimethamine ethanesulphonate

Table 6.4

Interatomic angles ( $^{\circ}$ ) with estimated standard deviations in parantheses

Atoms	Bond Angle	Atoms	Bond Angle
C2-N1-C6	118.6(1.4)	C2-N1-H1	116.1(6.4)
C6-N1-H1	124.6(6.4)	N1-C2-N3	124.8(2.2)
N1-C2-N2	118.9(1.5)	N3-C2-N2	116.2(1.8)
C2-N3-C4	113.7(1.6)	N3-C4-C5	127.7(1.4)
N3-C4-N4	115.8(1.7)	C5-C4-N4	115.8(2.1)
C4-C5-C6	112.1(2.0)	C4-C5-C1P	124.1(1.5)
C6-C5-C1P	123.7(1.7)	N1-C6-C5	122.4(1.6)
N1-C6-C61	114.0(1.4)	C5-C6-C61	123.6(2.0)
C2-N2-H2	105.5(9.8)	C2-N2-H3	106.8(8.9)
H2-N2-H3	147.7(13.2)	C4-N4-H5	104.9(7.1)
C6-C61-C62	111.8(1.4)	C6-C61-H6	107.8(2.2)
C6-C61-H7	108.7(1.6)	C62-C61-H6	109.2(1.8)
C62-C61-H7	109.8(2.4)	H6-C61-H7	109.5(1.9)
C61-C62-H8	108.5(1.9)	C61-C62-H9	111.1(2.2)
C61-C62-H10	109.0(2.8)	H8-C62-H9	109.3(3.4)
H8-C62-H10	109.4(2.7)	H9-C62-H10	109.5(2.4)
C5-C1P-C2P	123.1(1.8)	C5-C1P-C6P	115.9(1.6)
C2P-C1P-C6P	120.7(2.4)	C1P-C2P-C3P	121.1(1.8)
C1P-C2P-H2P	89.1(8.4)	C3P-C2P-H2P	148.6(7.8)
C2P-C3P-C4P	118.4(1.7)	C2P-C3P-N1P	128.6(1.8)
C4P-C3P-N1P	112.9(2.3)	C3P-C4P-C5P	121.9(2.7)
C4P-C5P-C6P	120.2(2.2)	C4P-C5P-H5P	147.7(14.3)

Table 6.4 (contd.)

Atoms	Bond Angle	Atoms	Bond Angle
C6P-C5P-H5P	90.9(13.9)	C1P-C6P-C5P	117.0(1.8)
C3P-N1P-N2P	112.5(2.4)	N1P-N2P-N3P	170.3(3.2)
O1-S1-O2	113.3(0.8)	O1-S1-O3	113.8(0.6)
O2-S1-O3	110.6(0.7)	C2E-C1E-H1E	115.9(1.3)
C2E-C1E-H2E	110.1(1.8)	H1E-C1E-H2E	109.5(1.9)
C1E-C2E-H3E	109.0(1.9)	C1E-C2E-H4E	112.8(1.5)
C1E-C2E-H5E	106.4(2.1)	H3E-C2E-H4E	109.6(2.5)
H3E-C2E-H5E	109.4(1.8)	H4E-C2E-H5E	109.5(2.3)
C2'-N1'-C6'	121.9(1.5)	C2'-N1'-H1'	58.2(11.9)
C6'-N1'-H1'	112.8(8.9)	N1'-C2'-N3'	119.6(1.6)
N1'-C2'-N2'	119.4(1.6)	N1'-C2'-H1'	33.4(6.2)
N3'-C2'-N2'	120.7(1.7)	N3'-C2'-H1'	125.8(5.6)
N2'-C2'-H1'	106.5(6.9)	C2'-N3'-C4'	118.6(1.5)
N3'-C4'-C5'	122.7(1.6)	N3'-C4'-N4'	118.2(1.6)
C5'-C4'-N4'	119.0(1.5)	C4'-C5'-C6'	117.7(1.4)
C4'-C5'-C1P'	121.5(1.5)	C6'-C5'-C1P'	120.6(1.6)
N1'-C6'-C5'	118.6(1.7)	N1'-C6'-C61'	115.3(1.6)
C5'-C6'-C61'	125.9(1.4)	C4'-N4'-H5'	152.4(6.5)
C6'-C61'-C62'	108.8(1.8)	C6'-C61'-H6'	109.6(1.4)
C6'-C61'-H7'	109.2(1.6)	C62'-C61'-H6'	110.4(1.7)
C62'-C61'-H7'	109.3(1.4)	H6'-C61'-H7'	109.6(2.4)
C61'-C62'-H8'	107.7(2.2)	C61'-C62'-H9'	111.6(1.5)
C61'-C62'-H10'	109.2(1.9)	H8'-C62'-H9'	109.5(1.8)
H8'-C62'-H10'	109.4(1.8)	H9'-C62'-H10'	109.4(2.7)
C5'-C1P'-C2P'	120.8(1.9)	C5'-C1P'-C6P'	115.7(1.8)
C2P'-C1P'-C6P'	123.3(1.6)	C1P'-C2P'-C3P'	114.8(2.0)

Table 6.4 (contd.)

Atoms	Bond Angle	Atoms	Bond Angle
C2P'-C3P'-C4P'	121.6(2.2)	C2P'-C3P'-N1P'	113.5(2.2)
C4P'-C3P'-N1P'	124.9(1.8)	C3P'-C4P'-C5P'	124.8(1.8)
C4P'-C5P'-C6P'	117.7(2.3)	C1P'-C6P'-C5P'	117.3(2.2)
C1P'-C6P'-H6P'	68.5(13.1)	C5P'-C6P'-H6P'	108.3(9.1)
C3P'-N1P'-N2P'	124.9(1.7)	O1'-S1'-O2'	113.9(0.9)
O1'-S1'-O3'	110.1(0.8)	O1'-S1'-C1E'	105.3(0.7)
O2'-S1'-O3'	113.5(0.7)	O2'-S1'-C1E'	106.8(1.0)
O3'-S1'-C1E'	106.5(1.0)	S1'-C1E'-C2E'	115.8(1.2)
S1'-C1E'-H1E'	107.2(1.9)	S1'-C1E'-H2E'	107.8(1.5)
C2E'-C1E'-H1E'	107.0(1.9)	C2E'-C1E'-H2E'	109.4(2.3)
H1E'-C1E'-H2E'	109.5(1.9)	C1E'-C2E'-H3E'	107.9(1.7)
C1E'-C2E'-H4E'	109.5(2.4)	C1E'-C2E'-H5E'	110.8(2.6)
H3E'-C2E'-H4E'	109.5(3.1)	H3E'-C2E'-H5E'	109.6(2.9)
H4E'-C2E'-H5E'	109.5(2.3)	N1'-H1'-C2'	88.5(14.5)
CL - C4P - C3P	117.1 (1.6)	CL' -C4P' - C3P'	119.5 (1.9)
CL - C4P - C5P	120.9 (1.9)	CL' - C4P' - C5P'	115.5 (1.9)

## Azidopyrimethamine ethanesulphonate

Table 6.5

Torsion Angles ( $^{\circ}$ )

Atoms	Angle ( $^{\circ}$ )
C6-N1-C2-N3	2.1
C6-N1-C2-N2	-174.9
H1-N1-C2-N3	-168.7
H1-N1-C2-N2	14.3
C2-N1-C6-C5	-4.1
C2-N1-C6-C61	176.6
H1-N1-C6-C5	165.8
H1-N1-C6-C61	-13.5
N1-C2-N3-C4	4.4
N2-C2-N3-C4	-178.5
N1-C2-N2-H2	142.8
N1-C2-N2-H3	-36.0
N3-C2-N2-H2	-34.5
N3-C2-N2-H3	146.7
C2-N3-C4-C5	-10.0
C2-N3-C4-N4	179.6
N3-C4-C5-C6	8.1
N3-C4-C5-C1P	-167.8
N4-C4-C5-C6	178.5
N4-C4-C5-C1P	2.6
N3-C4-N4-H5	14.7
C5-C4-N4-H5	-156.9

Table 6.5 (contd.)

Atoms	Angle(°)
C4-C5-C6-N1	-0.4
C4-C5-C6-C61	178.9
C1F-C5-C6-N1	175.5
C1F-C5-C6-C61	-5.2
C4-C5-C1F-C2F	-73.5
C4-C5-C1F-C6F	113.2
C6-C5-C1F-C2F	111.1
C6-C5-C1F-C6F	-62.2
N1-C6-C61-C62	90.0
N1-C6-C61-H6	-30.0
N1-C6-C61-H7	-148.6
C5-C6-C61-C62	-89.3
C5-C6-C61-H6	150.7
C5-C6-C61-H7	32.1
C6-C61-C62-H8	179.7
C6-C61-C62-H9	59.6
C6-C61-C62-H10	-61.2
H6-C61-C62-H8	-61.0
H6-C61-C62-H9	178.8
H6-C61-C62-H10	58.1
H7-C61-C62-H8	59.0
H7-C61-C62-H9	-61.1
H7-C61-C62-H10	178.1
C5-C1F-C2F-C3F	-179.7
C5-C1F-C2F-H2F	9.2

Table 6.5 (contd.)

Atoms	Angle (°)
C6P-C1P-C2P-C3P	-6.7
C6P-C1P-C2P-H2P	-177.9
C5-C1P-C6P-C5P	-177.2
C2P-C1P-C6P-C5P	9.3
C1P-C2P-C3P-C4P	2.9
C1P-C2P-C3P-N1P	-177.8
H2P-C2P-C3P-C4P	165.5
H2P-C2P-C3P-N1P	-15.2
C2P-C3P-C4P-C5P	-2.0
N1P-C3P-C4P-C5P	178.6
C2P-C3P-N1P-N2P	-7.8
C4P-C3P-N1P-N2P	171.5
C3P-C4P-C5P-C6P	5.0
C3P-C4P-C5P-H5P	167.7
C4P-C5P-C6P-C1P	-8.4
H5P-C5P-C6P-C1P	-179.3
C3P-N1P-N2P-N3P	-165.5
H1E-C1E-C2E-H3E	-57.2
H1E-C1E-C2E-H4E	-179.2
H1E-C1E-C2E-H5E	60.7
H2E-C1E-C2E-H3E	67.7
H2E-C1E-C2E-H4E	-54.2
H2E-C1E-C2E-H5E	-174.3
C6'-N1'-C2'-N3'	12.6
C6'-N1'-C2'-N2'	-173.3

Table 6.5 (contd.)

Atoms	Angle (°)
C6'-N1'-C2'-H1'	-98.6
H1'-N1'-C2'-N3'	111.2
H1'-N1'-C2'-N2'	-74.6
H1'-N1'-C2'-H1'	0.0
C2'-N1'-C6'-C5'	-8.7
C2'-N1'-C6'-C61'	176.1
H1'-N1'-C6'-C5'	-74.3
H1'-N1'-C6'-C61'	110.5
C2'-N1'-H1'-C2'	0.0
C6'-N1'-H1'-C2'	114.5
N1'-C2'-N3'-C4'	-9.4
N2'-C2'-N3'-C4'	176.5
H1'-C2'-N3'-C4'	29.8
N1'-C2'-H1'-N1'	0.0
N3'-C2'-H1'-N1'	-90.6
N2'-C2'-H1'-N1'	118.9
C2'-N3'-C4'-C5'	3.3
C2'-N3'-C4'-N4'	179.0
N3'-C4'-C5'-C6'	0.4
N3'-C4'-C5'-C1P'	-173.6
N4'-C4'-C5'-C6'	-175.2
N4'-C4'-C5'-C1P'	10.7
N3'-C4'-N4'-H5'	-88.7
C5'-C4'-N4'-H5'	87.2
C4'-C5'-C6'-N1'	2.2

Table 6.5 (contd.)

Atoms	Angle (°)
C4'-C5'-C6'-C61'	176.9
C1F'-C5'-C6'-N1'	176.4
C1F'-C5'-C6'-C61'	-9.0
C4'-C5'-C1F'-C2F'	92.0
C4'-C5'-C1F'-C6F'	-92.5
C6'-C5'-C1F'-C2F'	-81.9
C6'-C5'-C1F'-C6F'	93.6
N1'-C6'-C61'-C62'	83.6
N1'-C6'-C61'-H6'	-155.7
N1'-C6'-C61'-H7'	-35.6
C5'-C6'-C61'-C62'	-91.2
C5'-C6'-C61'-H6'	29.5
C5'-C6'-C61'-H7'	149.6
C6'-C61'-C62'-H8'	178.6
C6'-C61'-C62'-H9'	58.4
C6'-C61'-C62'-H10'	-62.7
H6'-C61'-C62'-H8'	58.3
H6'-C61'-C62'-H9'	-61.8
H6'-C61'-C62'-H10'	177.1
H7'-C61'-C62'-H8'	-62.3
H7'-C61'-C62'-H9'	177.6
H7'-C61'-C62'-H10'	56.5
C5'-C1F'-C2F'-C3F'	-178.9
C6F'-C1F'-C2F'-C3F'	6.0

Table 6.5 (contd.)

Atoms	Angle (°)
C5'-C1P'-C6P'-C5P'	176.1
C5'-C1P'-C6P'-H6P'	76.0
C2P'-C1P'-C6P'-C5P'	-8.5
C2P'-C1P'-C6P'-H6P'	-108.7
C1P'-C2P'-C3P'-C4P'	-0.5
C1P'-C2P'-C3P'-N1P'	-178.7
C2P'-C3P'-C4P'-C5P'	-2.3
N1P'-C3P'-C4P'-C5P'	175.7
C2P'-C3P'-N1P'-N2P'	-7.3
C4P'-C3P'-N1P'-N2P'	174.5
C3P'-C4P'-C5P'-C6P'	-0.3
C4P'-C5P'-C6P'-C1P'	5.4
C4P'-C5P'-C6P'-H6P'	80.2
O1'-S1'-C1E'-C2E'	179.9
O1'-S1'-C1E'-H1E'	60.6
O1'-S1'-C1E'-H2E'	-57.2
O2'-S1'-C1E'-C2E'	58.5
O2'-S1'-C1E'-H1E'	-60.8
O2'-S1'-C1E'-H2E'	-178.6
O3'-S1'-C1E'-C2E'	-63.1
O3'-S1'-C1E'-H1E'	177.6
O3'-S1'-C1E'-H2E'	59.7
S1'-C1E'-C2E'-H3E'	-172.0
S1'-C1E'-C2E'-H4E'	68.9
S1'-C1E'-C2E'-H5E'	-52.0

Table 6.5 (contd.)

Atoms	Angle (°)
H1E'-C1E'-C2E'-H3E'	-52.5
H1E'-C1E'-C2E'-H4E'	-171.7
H1E'-C1E'-C2E'-H5E'	67.4
H2E'-C1E'-C2E'-H3E'	66.0
H2E'-C1E'-C2E'-H4E'	-53.1
H2E'-C1E'-C2E'-H5E'	-174.0

Azidopyrimethamine ethanesulphonate

Table 6.6

Calculation of  $\theta$  Angle between planes

Plane 1:                    L = 0.6294  
                                 M = 0.7574  
                                 N = 0.1737  
                                 D = 10.9782

Deviations:                -0.0297  
                                 0.0015  
                                 0.0397  
                                 -0.0505  
                                 0.0182  
                                 0.0209

Plane 2:                    L = -0.4863  
                                 M = 0.8704  
                                 N = -0.0768  
                                 D = 7.4552

Deviations:                0.0370  
                                 -0.0132  
                                 -0.0040  
                                 -0.0040  
                                 0.0279  
                                 -0.0437

Table 6.6 (contd.)

Plane 3:                    L = 0.2634  
                                  M = -0.1059  
                                  N = 0.9589  
                                  D = -1.2922

Deviations:                0.0038  
                                  0.0348  
                                  -0.0130  
                                  -0.0259  
                                  0.0222  
                                  -0.0220

Plane 4:                    L = 0.8941  
                                  M = -0.4025  
                                  N = -0.1965  
                                  D = -1.9953

Deviations:                -0.0326  
                                  -0.0206  
                                  -0.0289  
                                  -0.0035  
                                  0.0410  
                                  0.0446

Let  $\theta_1$  be the angle between planes 1 and 2,  
 and  $\theta_2$  be the angle between planes 3 and 4.  
 Then  $\cos \theta_1 = L_1 L_2 + M_1 M_2 + N_1 N_2$

and  $\cos \theta_2 = L_3 L_4 + M_3 M_4 + N_3 N_4$

Table 6.6(contd.)

Provided that:-

$$L_1^2 + M_1^2 + N_1^2 = 1$$

$$L_2^2 + M_2^2 + N_2^2 = 1$$

$$L_3^2 + M_3^2 + N_3^2 = 1$$

$$L_4^2 + M_4^2 + N_4^2 = 1$$

## Chapter Seven

### Conformational Analysis

#### 7.1 The Theoretical Calculations of possible drug conformations and electron distribution

Theoretical calculations should be capable of providing two information types in addition to experimental studies :-

1. the range of non-equilibrium conformations which must include the unique conformation essential for the binding of the drug,
- and 2. the electron distribution in that conformation.

### 7.1.1 The Schroedinger Equation

This was proposed by Erwin Schroedinger in 1926, as the wave-mechanical theory of the hydrogen atom. Prior to this Bohr's theory of 1913 was used to explain the observed spectra of elements by a quantitative treatment based on Planck's hypothesis. Planck's theory supposed that a solid contained a very large number of oscillators (atoms or molecules) having a fundamental frequency of  $\nu$ . The energy of such an oscillator being given by :-

$$E = nh\nu$$

where n is a positive integer

h is the Planck constant.

Bohr's theory was unable to account for the emission spectra of complex atoms as well as for the behaviour of atoms in a magnetic field, unlike the Schroedinger equation.

In its barest form, the Schroedinger equation is given by :-  $H\psi = E\psi$

where H is an operator i.e. operates on a mathematical function

$\psi$  is an atomic wave function which represents the wave properties of the particle

E is the energy of the system.

The equation can only be solved exactly for the case of a simple hydrogen atom system provided that the wave function obeys a set of reasonable restrictions on its behaviour,

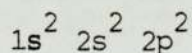
- i.e.
1.  $\psi$  must be single-valued at any particular point
  2.  $\psi$  must be finite at any point
  3.  $\psi$  must be a smooth or continuous function of its co-ordinates.

In molecular quantum mechanics, as the problems concern three dimensional molecular systems then the wave function also varies in these co-ordinates.

## 7.2 Atomic Orbitals and Orbital Approximation

The wave functions which satisfy the Schroedinger equation for the hydrogen atom are sometimes called orbitals. Thus a hydrogenic atomic orbital is merely a three dimensional function from which one can calculate the energy or other properties of the single electron system.

In the study of polyelectron atomic structures researchers adopt the "orbital approximation" i.e. each electron is treated separately, each with its own one electron wave function or orbital. This mathematical approximation is nothing more than the fundamental basis of the universal procedure of describing atoms by means of orbital configurations for example, the atomic electron configuration of carbon is :-



and treats each electron separately. In carbon then :

2 electrons have functions associated with them  
which are of the 1s shape;

2 electrons have functions associated with them  
which are of the 2s shape;

2 electrons have functions associated with them  
which are of the 2p shape.

An orbital is therefore merely a synonym for a one electron wave function, each a three dimensional mathematical function which describes the behaviour of a single electron.

Generally, then for a polyelectronic atom system the total

wave function for an atom,  $\psi$  is a product of one electron atomic wave functions ( $\chi_i$ ) one for each electron, i.e.

$$\psi = \chi_1, \chi_2, \dots, \chi_n$$

### 7.3 Molecular Orbitals

The wave function for a molecule is then not in principle any different from that of an atom. If  $\bar{\Psi}$  represents the molecular wave function, the orbital approximation can be used as in the atomic case :

$$\bar{\Psi} = \phi_1\phi_2\cdots\phi_n$$

where  $\phi$  is a three dimensional function which determines the properties of an individual electron in the molecule.

Molecular orbitals can then be calculated, most frequently using atomic orbitals of the "Slater-type". The Slater type of atomic orbitals are the set of atomic orbitals found by fitting analytical exponential functions to numerical atomic wave functions, Gaussian shape functions, of three or four in number being then fitted to the exponential.

However, all molecular wave functions are approximate but some will be more approximate than others, and the preparation of small Gaussian basis sets for such molecular calculations is currently being researched (52).

"Ab initio" methods of calculation the orbital wave functions use the technique introduced by Hartree and Fock. This is known as the self-consistent field (SCF) method and reduces the many electron Schroedinger equation. This method choses an apporximate set of atomic orbitals and from these the average potential acting on each electron is calculated. These potentials are then used to calculate new orbitals from which

better approximations to the average potentials are obtained. The process is repeated until a set of orbitals reproduces the potentials which gave these orbitals (53).

When running an ab initio calculation the starting point is a particular molecular geometry, the nature and co-ordinates of each atom being defined. However there are two sources of error in the starting equation :-

1. The whole theory based on the Schroedinger equation is not realistically correct i.e. the fast moving inner electrons may move with speeds which are not negligible by comparison with the velocity of light. As a result relativistic effects may contribute so the mass involved may not be constant. This error however can usually be ignored as it will be a constant as calculations do not involve the core electrons. The Gaussian 70 package actually includes the 1s electrons, however they are unlikely to be significantly affected by changes in molecular geometry;

2. Correlation Energy

Any defect in the wave functions results in the calculated energy being less in magnitude than the true energy and results from electron-pair effects.

Molecular orbitals can then lead to an understanding of the electron organisation within the molecule and attributable energy values, the eigenvalues, to the molecular orbital. This energy value is then an approximation to the ionisation potential of the electron in the closed shell area (Koopmans Theorem).

#### 7.4 The Gaussian 70 Package (54)

To use the package the only input needed is the specification of the geometry of the molecule, using bond lengths, bond angles and torsion angles as the main geometrical information.

The information which the package returns to the user is as follows :-

1. The total energy of the molecule.

The absolute value of this is not directly useful; however, the comparison of two absolute energies, for example at different bond lengths is directly useful.

2. The energies of the molecular orbitals, which are expected roughly to correspond to the observable ionisation energies of the molecule.

3. The forms of the molecular orbitals as linear combinations of atomic orbitals, which are generally useful in understanding the electron organisation within the molecule.

4. The Mulliken populations, which give some insight into the charge distribution within the molecule.

5. The electric dipole moment within the molecule, which can be used in the calculation of electrostatic interaction energies between two molecules.

The upper limits of the size of the molecule which may be dealt with are :-

maximum no. of atoms	35 (plus up to 15 dummy atoms)
----------------------	--------------------------------

maximum no. of atomic orbitals 70 (inner shells must be included)  
maximum value of atomic number 18 (argon)

The accuracy of the package has been shown to give a wave function which corresponds to greater than 98 per cent of the total energy of the molecule.

The basic Gaussian package has been updated so that the forces on the nuclei in a molecule can be calculated and geometry optimisations carried out using the forces to minimise the total energy of the molecule. This amendment is based on force calculations on the nuclei made according to the method of Pulay (55). The resulting forces acting on the atoms are calculated in cartesian co-ordinates and allow the molecule, or parts of the molecule, to relax to its equilibrium geometry, i.e. where the forces vanish (56). The force calculations on the nuclei (being negative derivatives of the total energy with respect to the nuclear co-ordinates) are applied for Hartree Fock wave functions.

## Chapter Eight

### Conformational Analysis and Quantitative Structure Analysis Relationships of Folates and Folate Analogues

---

#### 8.1 Conformation Analysis

The compounds studied by M.J. Spark, D.A. Winkler & P.R. Andrews (57) include folic acid, dihydrofolate, tetrahydrofolate, methotrexate and aminopterin. The analysis shows that a large number of conformations are energetically accessible to these molecules and some are common to all. This work involved the parametrization method of Giglio (58) on a CYBER 73 computer at the Royal Melbourne Institute of Technology using the program COMOL (59). The program performs classical conformational calculations by pairwise summation of the van der Waals interactions between non-bonded atoms together with electrostatic and torsional potentials.

Of particular interest are the conformations adopted by methotrexate when bound to dihydrofolate reductases from various sources. These conformations are found to be of surprisingly high energy relative to the global minimum and the proposition that the pteridine ring of dihydrofolate may bind upside down with respect to that of methotrexate was tested via conformational energy calculations. The superposition of the low energy conformations of dihydrofolate on the bound conformations of methotrexate demonstrates that

a reasonable match may be achieved with the pteridine ring upside down. Electrostatic potential calculations show that these conformations fit into the binding cavity of DHFR in a way that permits non-bonded interactions (57).

## 8.2 QSAR of DHFR Inhibitors

These relationships have been used to determine the basic dissociation constants of representative 5- and 6-substituted derivatives of 2,4-diaminopyrimidines in order to analyze electronic and steric effects upon the basicities of these molecules and possible relationships to enzyme binding (60). The conclusions of Roth & Strelitz are that the effect of substituents in either the 5- or 6- position is primarily inductive in character and that with the exception of alkyl or 5-amino groups, the consequence of all 5- or 6- substitution is to lower the  $pK_a$  values of the pyrimidines. Also that compounds which have useful inhibitory action against DHFR (61) have  $pK_a$  values above 6; the most active compounds have  $pK_a$  values of 7 or over.

Further research by Fukunaga (62) compares the QSAR for the quiazolines causing 50% inhibition of pigeon liver DHFR, with those for triazine and pyrimidine inhibitors. The three QSAR's suggest new possibilities for the design of inhibitors of mammalian DHFR.

## Chapter Nine

### Molecular Orbital Calculations

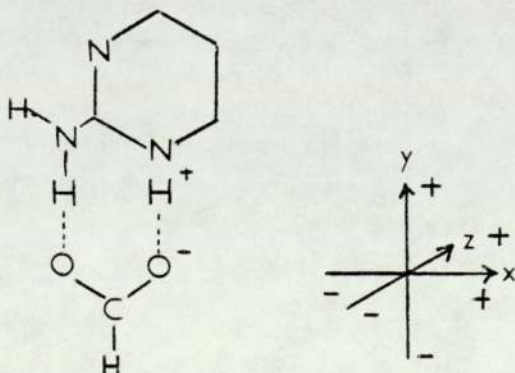
The Gaussian 70 package (54) was used to determine the total energy of the following structures :-

1. Pyrimidine Ring

Co-ordinates taken from the last cycle of refinement of pyrimethamine acetate hydrate (5.1)

2. Pyrimidine Ring with a Formate Ion

Co-ordinates for the pyrimidine ring as in 1. above. The position of the formate ion was determined from the position of the acetate molecule in pyrimethamine acetate hydrate's last refinement cycle. The position of the formate ion was then recalculated to shift the formate as a rigid structure in three dimensions by approximately  $0.1\text{\AA}$  along the hydrogen bonds between the formate and the protonated N1 atom and the  $\text{NH}_2$  group on the C2 atom, as shown below :-



3. Protonated and Unprotonated 2,4 diaminopyrimidines

4. Protonated and Unprotonated 2-amino-4-oxo-

pyrimidines

5. Protonated and Unprotonated 1, 3, 5, Triazines

6. Pyrimidine Ring

Co-ordinates taken from the last cycle of refinement of pyrimethamine salicylate isopropanol solvate (5.2)

7. Pyrimidine Ring

Co-ordinates taken from the last cycle of refinement of azidopyrimethamine ethanesulphonate (6).

### Results

The total energy figures are the absolute magnitudes and are quoted in Atomic Units ( 1 A.U. =  $2625 \text{ kJmol}^{-1}$ ). The results are shown in Table 9.

Table 9

## RESULTS OF MOLECULAR ORBITAL CALCULATIONS

Structure	Total Energy (A.U.)
Pyrimidine Ring	
(pyrimethamine acetate hydrate)	-368.402
Pyrimidine Ring and Formate Ion	
(pyrimethamine acetate hydrate)	-554.114
Pyrimidine Ring and Formate Ion	
(pyrimethamine acetate hydrate)	
with hydrogen bond lengths altered by $0.1\text{\AA}$	
in :-	
X-direction positive	-554.114
negative	-554.113
Y-direction positive	-554.130
negative	-554.097
Z-direction positive	-554.059
negative	-554.125
2,4 diaminopyrimidine (63)	
protonated form	-368.511
unprotonated form	-368.511
2-amino-4-oxo-pyrimidine (64)	
protonated form	-388.005
unprotonated form	-387.546
Triazine	
protonated form	-385.438

Table 9 (contd.)

Structure	Total Energy (A.U.)
Triazine	
unprotonated form	-384.920
Pyrimidine Ring	
(pyrimethamine salicylate isopropanol solvate)	-367.810
Pyrimidine Ring	
(azidopyrimethamine ethanesulphonate)	-368.282

## Discussion of Results

The values of the total energy of each of the structures in themselves are not very meaningful. However when compared against each other the values can give more information. For example, the pyrimidine ring values of the determined crystal structures of pyrimethamine acetate hydrate, pyrimethamine salicylate isopropanol solvate and azidopyrimethamine ethanesulphonate give total energies which vary by only 0.592 A.U.. Also, the values of the pyrimidine ring and formate ion, even with variation in the hydrogen bonds, only gives a range of 0.071 A.U.. The more accurate geometry of the pyrimidine ring from pyrimethamine acetate hydrate giving more stability than the pyrimidine rings of pyrimethamine salicylate isopropanol solvate and azidopyrimethamine ethanesulphonate.

Obviously these results are far from conclusive and further research could be done so as to ascertain whether the co-ordinates of atoms from the pyrimethamine series of crystal structures are or are near energy minimal positions. The hydrogen bonding of the carboxylate group, which exists in the binding of the pyrimethamine derivative to dihydrofolate reductase, could be investigated either by greater shift of the formate ion or by using a different carboxylate molecule.

## Chapter Ten

### Discussion and Conclusion of the Determined Crystal Structures

---

In Table 10.1 is shown the pyrimidine ring geometry of the determined antifolate carboxylate and substituted structures with pyrimethamine hydrochloride given as a comparison. Pyrimethamine salicylate isopropanol solvate and azidopyrimethamine ethanesulphonate had determined bond distances with high standard deviations and so their bond distances and angles are reported to a lower degree of accuracy than the others. For pyrimethamine isopropanol solvate the data collected as compared to that of the others was less in number and less accurate as reflected by the decline in the monitor reflection intensities. This loss of diffracting power was possibly due to the loss of isopropanol from the irradiated crystal. For azidopyrimethamine ethanesulphonate the structure showed for the primed azide unit either large thermal motion or some undetected disorder, for which the standard method of full-matrix least-squares refinement did not yield an acceptable geometry. This spoilt the agreement between the structural model and the data.

A high degree of consistency can be seen in the pyrimidine ring geometry if the averages of the two molecules for pyrimethamine salicylate and azidopyrimethamine ethanesulphonate are considered. The latter structure would have been expected

TABLE 10.1

## PYRIMIDINE RING GEOMETRY

Compound	1	2	3	4	5	6	7
Distances (Å)							
N1-C2	1.369	1.356	1.306	1.339	1.35	1.33	1.40
C2-N3	1.334	1.339	1.344	1.327	1.33	1.35	1.35
N3-C4	1.344	1.346	1.359	1.344	1.37	1.33	1.35
C4-C5	1.431	1.427	1.423	1.422	1.36	1.43	1.41
C5-C6	1.346	1.359	1.350	1.351	1.38	1.36	1.39
C6-N1	1.365	1.375	1.373	1.361	1.38	1.39	1.35
C5-C1P	1.486	1.489	1.473	1.499	1.48	1.43	1.46
Interior Angles (°)							
C2-N1-C6	121.9	120.7	123.1	121.4	120	119	121
N3-C2-N1	120.9	121.9	122.1	122.7	124	124	119
C4-N3-C2	118.3	117.6	116.2	117.0	114	113	118
C5-C4-N3	122.2	122.9	123.6	122.4	127	127	122
C6-C5-C4	117.7	116.7	116.1	117.4	116	112	117
N1-C6-C5	119.0	119.6	118.9	118.9	119	122	118
Exterior Angles (°)							
N2-C2-N1	116.9	116.9	119.5	117.9	115	118	119
N2-C2-N3	122.3	121.1	118.4	119.4	121	116	120
N4-C4-N3	115.0	115.6	115.1	116.5	111	115	118
N4-C4-C5	122.8	121.5	121.3	121.1	122	115	119
C1P-C5-C4	120.7	121.0	120.2	119.0	122	124	121
C1P-C5-C6	121.6	122.2	123.6	123.6	122	123	120

Compound (1)	Pyrimethamine Hydrochloride (65)
(2)	Pyrimethamine Acetate Hydrate
(3)	Pyrimethamine Salicylate - A
(4)	Pyrimethamine Salicylate - B
(5)	Pyrimethamine Salicylate Isopropanol Solvate
(6)	Azidopyrimethamine Ethanesulphonate - A
(7)	Azidopyrimethamine Ethanesulphonate - B

to vary from the others due to the azido group on the chlorophenyl ring.

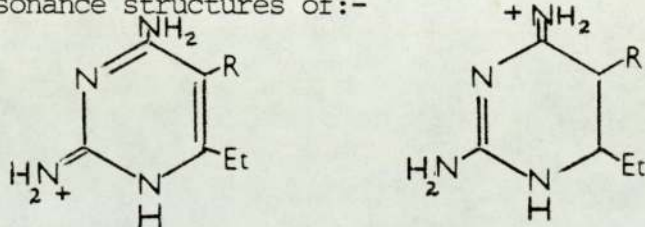
In all structures is found a consistent pattern of intermolecular interactions with the protonated ring N1 atom and the 2-amino group of the pyrimethamine cation acting as proton donors to the counter ion (carboxylate or ethanesulphonate). Adjacent pyrimethamines are linked into dimers via paired N-H ... N hydrogen bonds using the remaining proton donor and acceptor site, the N4 amino group and the ring N3 atom respectively.

Several types of evidence suggest the site of protonation. To support the conclusion that the N1 atom is protonated in all structures the difference Fourier maps were reviewed to ensure all hydrogen atoms had been identified; however, this proved difficult due to the "bad" data in pyrimethamine salicylate isopropanol solvate and azidopyrimethamine ethanesulphonate. The interior angles of C2-N1-C6 are shown in Table 10.1 for the structures and all lie within the range  $119^{\circ}$  to  $123.1^{\circ}$ . This interior angle has been shown to be  $\approx 117^{\circ}$  for unprotonated N1 atoms and  $\approx 121^{\circ}$  for protonated (66) due to the effects of valence shell electron pair repulsion. The C2-N1-C6 angle in pyrimethamine hydrobromide (49) was reported as  $121^{\circ}$  with a protonated N1 atom.

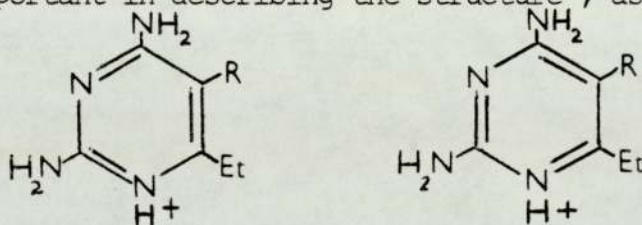
Also from Table 10.1 it can be seen that the bond distances N1-C2 fall in the range  $1.306\text{\AA}$  to  $1.400\text{\AA}$  and C6-N1 in the range

1.35Å to 1.39Å. These can be compared to those of pyrimethamine hydrobromide (49) of 1.35Å and 1.38Å respectively.

In Table 10.2 are reported other geometry features of the determined structures which show that the distances from the ring carbon atoms, C2 and C4 to the amino groups, N2 and N4 respectively are generally short enough to suggest that the resonance structures of:-



are important in describing the structure, as well as:-



The first two resonance structures would be less favoured in the unprotonated molecule.

Further, all bond lengths in the carboxyl group of the structures are relatively similar :-

	Oxygen atom closest to N1		Other oxygen
	Å		Å
Pyrimethamine acetate hydrate	C1A-O2 1.234		C1A-O1 1.259
Pyrimethamine salicylate			
isopropanol solvate	C1C-O2 1.258		C1C-O1 1.278
Pyrimethamine salicylate	C1A-O2R 1.273		C1A-O1R 1.255
	C1B-O2S 1.286		C1B-O1S 1.219

TABLE 10.2

## OTHER GEOMETRY FEATURES OF THE PYRIMIDINE RING

Compound	1	2	3	4	5	6
N1...O (Å)	2.670	2.708	2.668	2.72	2.74	2.74
N2...O (Å)	2.773	2.860	2.847	2.75	2.98	2.88
N3...N (Å)	3.054	2.980	2.964	3.06	3.25	3.03
C2-N2 (Å)	1.322	1.325	1.337	1.38	1.35	1.32
C4-N4 (Å)	1.322	1.340	1.331	1.37	1.35	1.30
$\tau$ (°)	76	71	80	78	74	88
$\phi$ (°)	88	75	87	79	90	84
Compound (1)	Pyrimethamine Acetate Hydrate					
(2)	Pyrimethamine Salicylate - A					
(3)	Pyrimethamine Salicylate - B					
(4)	Pyrimethamine Salicylate Isopropanol Solvate					
(5)	Azidopyrimethamine Ethanesulphonate - A					
(6)	Azidopyrimethamine Ethanesulphonate - B					

$\tau$  = C4-C5-C1P-C2P

$\phi$  = N1-C6-C61-C62

It is known that the carboxyl C-O bonds in a carboxyl group are of different lengths whilst those of a carboxylate are of the same length. A C-O bond length is expected to be  $1.44\text{\AA}$  and that of a C=O bond is  $1.22\text{\AA}$  (67).

From the above observations it can be concluded that:-

1. all samples studied contain salts rather than complexes of neutral molecules, and
2. the N1 atom in all heterocycles is protonated.

The angle C5-C6-C61 falls within the range  $124^\circ$  to  $129^\circ$  for the determined structures whereas the angle C6-C5-C1P is in the range  $120^\circ$  to  $124^\circ$ . This can be explained by the fact that the ethyl side chain is freer to move than the benzene ring and so the C61 atom will position itself to avoid as much steric hindrance as possible with the C2P atom and its associated hydrogen atom.

The length of the C61-C62 bond in the ethyl side group in the determined structures varies from  $1.4\text{\AA}$  in the pyrimethamine salicylate B molecule to  $1.6\text{\AA}$  in the pyrimethamine salicylate isopropanol solvate molecule. This variation may demonstrate some distortion of the ethyl side chain position to avoid steric interference in the structures. Also there is the effect of thermal motion that causes the measured distances, which are a time-average, to appear somewhat shorter than the actual values. The particularly short C61'-C62' distance in pyrimethamine salicylate is associated with unusually large  $U_{11}$  values of 0.162(8) and 0.201(13)  $\text{\AA}^2$ .

From Table 10.2 it can be seen that the hydrogen bond distances from the pyrimidine ring to the carboxylate ion in compounds (1) to (4) are consistent. However those of the substituted antifolate to the ethanesulphonate ion are comparable for N1 ... O and N2 ... O but as would have been expected the three oxygens on the sulphur atom have slightly affected the packing arrangements. The hydrogen bonds N1 ... O and N2 ... O on average are shorter for the antifolate carboxylate structures than for the substituted antifolate emphasizing the strength of the interaction with the carboxylate ion. The N3 ... N bond distance for the interaction that links the bases into a dimer varies little between the six structures and has an average value of 3.06Å.

The pyrimidine ring, carbon to nitrogen bonds of C2-N2 and C4-N4 also show good consistency with both having an average value of 1.34Å which might indicate the optimal geometrical arrangement of these atoms.

The observed rotations about the bonds C5-C1P and C6-C61, being the torsion angles denoted  $\gamma$  and  $\phi$  are shown in Table 10.2. These results can be compared to the torsion angles of the independent molecules of pyrimethamine (65) which have angles  $\gamma$  of 74° and 81°;  $\phi$  of 79° and 80°.

If the torsion angle  $\gamma$  were 0° there would be collision between the ring and the ethyl side chain whereas if it were 90° the rings would be perpendicular and there would be loss of all conjugation between them.

If the torsion angle  $\phi$  were  $0^\circ$  there could be some interference between the hydrogen atom on N1 and the methyl group on the end of the ethyl side chain. If it were  $\pm 60^\circ$  a staggered configuration would result and if it were  $180^\circ$  the ethyl side chain would be zig-zag in the plane and would run into the benzene ring.

The observed rotations for  $\gamma$  fall in the range  $71^\circ$  to  $88^\circ$  and those for  $\phi$  in the range  $75^\circ$  to  $90^\circ$  which compare well with those of pyrimethamine and correspond to expected values.

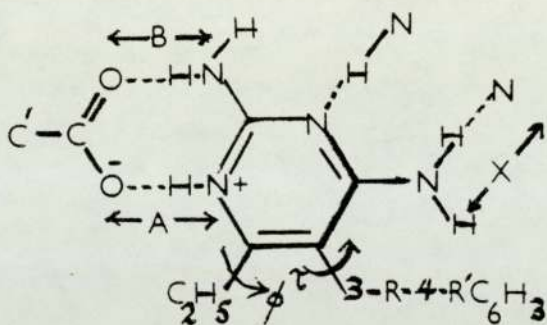
The chlorine atom in all the determined structures displays very anisotropic thermal motion because the atom in the structures is at the end of a "lever arm". The centre of mass of the pyrimethamine molecule falls approximately half way along the bond from C5 to C1P due to the high atomic mass of the chlorine atom. Motion of the chlorine atom along a line to this centre of mass is restricted, while motion of the chlorine atom perpendicular to this line is easy and may be augmented by rotation of the whole molecule.

In Figure 25 is shown the model of the bonding between an antifolate drug and the carboxylate side chain of dihydrofolate reductase and the bond distances are noted in Table 10.3. These bond distances also show consistency between the determined antifolate carboxylate structures.

The azide group is an interesting substituent for antifolate drugs because it is both lipophilic and degradable. It is these properties which may lead to a drug with a

Figure 25

MODEL OF THE IONIC AND HYDROGEN BONDING LINK BETWEEN THE ANTIFOLATE DRUG AND A SIDE CHAIN CARBOXYLATE ION OF DHFR, WHICH IS BELIEVED TO BE OF MAJOR IMPORTANCE FOR DRUG BINDING (69)



- (1) Pyrimethamine Hydrochloride (65)
  - (2) Pyrimethamine Acetate Hydrate
  - (3) Pyrimethamine Salicylate
  - (4) Pyrimethamine Salicylate Isopropanol Solvate
- (1) - (4)      R = H  
 and R' = CL

TABLE 10.3

DISTANCES ( Å ) BETWEEN ATOMS CONNECTED BY HYDROGEN BONDS  
IN THE DETERMINED ANTIFOLATE CARBOXYLATE STRUCTURES  
(with reference to Fig. 25)

Compound	1	2	3	4
A (Å)	2.670	2.708	2.668	2.72
B (Å)	2.773	2.860	2.847	2.75
X (Å)	3.054	2.980	2.964	3.06

Compound (1)	Pyrimethamine Acetate Hydrate
(2)	Pyrimethamine Salicylate - A
(3)	Pyrimethamine Salicylate - B
(4)	Pyrimethamine Salicylate Isopropanol Solvate

usefully short biological half life. Azidopyrimethamine ethanesulphonate inhibits rat liver dihydrofolate reductase more strongly than pyrimethamine and is presently in Phase I clinical trial as an antitumour agent (68).

The azidopyrimethamine ethanesulphonate crystals were highly sensitive to atmospheric conditions and the change in the crystals was observed by eye after approximately seven days. The difference in the density of the crystals as measured ( $1.252 \text{ gcm}^{-3}$ ) and as calculated ( $1.215 \text{ gcm}^{-3}$ ) would suggest that not all the solvent molecules had been located in the crystal structure. However rechecking the difference Fourier map confirmed that all such molecules had been determined. Thus there are two possible explanations for the difference :-

1. there had been some change in the packing of the crystals in consequence of atmospheric exposure as the density was measured some seven days after the crystals had been made, and
2. the rather crude method used for density determination had overestimated the density.

While ethanesulphonate salts of antifolate drugs crystallise well and have been extensively studied, the carboxylate salts to date have not. From the determined structures it can be seen that the interaction of the protonated ring and the carboxylate ion is uniformly strong. Although it does not impose coplanarity the consistency in

distance should serve as a useful anchor point for model building.

Explanations for the enhanced affinity of the 2,4 diamino derivatives of triazine, pteridine, quinazoline and pyrimidine have focused on the modified pattern of hydrogen bond donors and acceptors or on an increased basicity of the heterocycle. Therefore, an analysis of the hydrogen bonding and molecular packing of these compounds in their crystal lattice offers insight into the molecular details of hydrogen bond strength and directionality of drug binding to the enzyme active site.

The antifolate diamino groups can act as hydrogen bond donors, while N1 and N3 can act as hydrogen bond acceptors, or be protonated. These patterns are in contrast to those of the natural substrates in which only the 2-amino group can be a proton donor, where N3 has a proton, and where the enzymatic protonation site is N5, although N1 or N8 can be protonated.

In the determined crystal structures the N1 atom is protonated and the hydrogen atoms on N2 are tightly bound. These results are consistent with those hydrogen bonding preferences found in the protein crystal structures of DHFR-drug complexes (14 & 40).

#### REFERENCES

1. Stout,G.H. and Jensen,L.H.  
X-ray Structure Determination. publ. Macmillan,  
New York (1968)
2. Main,R.,Woolfson,M.M and Germain,G. (1978)  
Mulan: A Computer program for the automatic  
solution of Crystal Structures. University of  
York.
3. Sheldrick,G. (1976)  
Shelx: Program for Crystal Structure Determination,  
Cambridge University.
4. Wilson,A.J.C. - Nature 150 151 (1942)
5. Finney,J.L. - Water A comprehensive Treatise  
Vol.6 ed.F.Franks publ.Plenum New York (1979)
6. Blundell,T.L. - SERC Bulletin 2 6(August 1982)
7. Caillet,J. and Claverie,P.  
Acta Cryst A31,448 (1975)
8. Lehninger,A.L. - Biochemistry  
publ. Worth Publishers Inc. New York (1977)
9. Clement,R.P., Tofilon,P.J. and Piper,W.N.  
Nutrition and Cancer 3(2) 63-71 (1981)
10. Pfliegerer,W. Ed. - Chemistry and Biochemistry  
of Pteridines publ. De Gruyter Berlin (1976)
11. Jukes,T.H. and Broquist,H.P. - Metabolic  
Inhibitors Ed. Hochster,R.M. and Quastel,J.H.  
publ.Academic Press New York.(1963)

12. Schultz,G.E. and Schirmer,R.H.  
Principles of Protein Structure publ.Springer-  
Verlag New York Inc. (1979)
13. Bolin,J.T., Filman,E.J., Matthews,D.A.,  
Hamlin,R.C., and Kraut,J.  
J.Biol.Chem. 257 13650-13662 (1982)
14. Volz,K.W., Matthews,D.A., Alden,R.A., Freer,S.T.,  
Hansch,C., Kaufman,B.T., Kraut,J.  
J.Biol.Chem. 257 2528-2536 (1981)
15. Hitchings,G.H. and Smith,S.L. - Adv. in Enzyme  
Regulation 18 349-371 (1980)
16. Fersht,A. - Enzyme Structure and Mechanism  
publ.W.H.Freeman & Co. Reading & San Francisco  
(1977)
17. Baker,B. - Design of Active-site Directed  
Irreversible Enzyme Inhibitors  
publ.Wiley New York (1967)
18. Baker,B. - J.Med.Chem. 7 24 (1964)
19. Daniel,L.J., Norris,L.C., Scott,M.L., Heuser,G.F.  
J.Biol.Chem. 169 689-697 (1947)
20. Daniel,L.J., and Norris,L.C.  
J.Biol.Chem. 170 747 (1947)
21. Hitchings,G.H., Falco,E.A. and Sherwood,M.B.  
Science 102 251-252 (1945)
22. Hitchings,G.H., Elien,G.B., Vanderwerff,H., Falco,E.A.  
J.Biol.Chem. 174 765-766 (1948)

23. Falco, E.A., Goowin, L.G., Hitchings, G.H., Rollo, M. and Russell, P.B.  
Brit. J. Pharmacol. Chemoth. 6 185-200 (1951)
24. Falco, E.A., Hitchings, G.H., Russell, P.B. and Vanderwerff, H. - Nature 164 107-108 (1949)
25. Carrington, H.C., Crowther, A.F., Davey, D.G., Levi, A.A. and Rose, F.L. - Nature 168 1080 (1951)
26. Matthews, D.A., Bolin, J.T., Burridge, J.M., Filman, D.J. Volz, K.W. and Kraut, J.  
J. Biol. Chem. 260 392-399 (1985)
27. Zakrzewski, S.F. - J. Biol. Chem. 238 4002-4004 (1963)
28. Perault, A.M. and Pullman, B.  
Biochim. Biophys. Acta 52 266-280 (1961)
29. Hunt, W.E., Schwalbe, C.H., Bird, K. and Mallinson, D.  
J. Biochem. 187 533-536 (1980)
30. Hood, K. and Roberts, G.K.C.  
J. Biochem. 171 357 (1978)
31. Charlton, P.A. and Young, W.D.  
Chem. Commun. 922 (1979)
32. Matthews, D.A., Alden, R.A., Bolin, J.T. and Freer, S.T. - Science 197 452-455 (1977)
33. Gready, J.E. - Nature 282 674-675 (1979)
34. Cocco, L., Roth, B., Temple, C., Mongomery, J.A., London, R.E., Raymond, K. and Blakely, L.  
Arch. Biochem. Biophys. 226 567 (1983)
35. Bolin, J.T., Filman, D.J., Matthews, D.A.

- Hamlin,R.C. and Kraut,J.  
J.Biol.Chem. 257 13650-13662 (1982)
36. Villafranca,J.E. - Science 222 782 (1983)
37. Matthews,D.A., Villafranca,J.E. and Kraut,J.  
Crystallography in Biochemistry and Pharmacology  
C-59 =3 X-14
38. Villafranca,J.E., Howell,E.E., Abelson,J.N. and  
Kraut,J. - Structural Molecular Biology  
C - 24 O2 X-12
39. Crouse,G.F., McEwan,R.N. and Pearson,M.L.  
Molecular and Cellular Biology  
3(2) 257-266 (1983)
40. Matthews,D.A., Alden,R.A., Bolin,J.T., Filman,D.J.,  
Freer,S.T., Hamlin,R., Hol,W.G.J., Kisliuk,R.L.,  
Pastore,E.J., Plante,L.T. Xuong,N. and Kraut,J.  
J.Biol.Chem. 253 6946-6954 (1978)
41. Koetzle,T.F. and Williams,G.J.B.  
J.Amer.Chem.Soc. 98 2074-2078 (1976)
42. Cody,V. and Zakrewski,S.F.  
J.Med.Chem. 25 427-430 (1982)
43. Gready,J.E. - Adv.Pharm.Chem. 17 37 (1980)
44. Sirotnak,F.M. - New Approaches to the Design of  
Antineoplastic Agents.  
Proc.Annu.Med.Chem.Symp 22nd 1981 157-176  
Ed.Barroos publ. Kalman & Elsevier (1982)
45. Cooper,B.A. and Peyman,J. - Biochem.Biophys.Acta

- 692(1) 161-164 (1982)
46. New Scientist 24.2.1983 p.519
47. Thompson,P.E. and Werbel,L.M.  
Antimalarial Agents - Chemistry and Pharmacology  
publ. Academic Press London 1972
48. Schwalbe,C.H. and Hunt,W.E.  
Journal of the Chemical Society. Chemical  
Communications 188-190 (1978)
49. Phillips,T. and Bryan,R.F.  
Acta Cryst A25 S200 (1969)
50. Gringauz,A. - Drugs: How They Act and Why  
publ.C.V.Mosby Company Saint Louis (1978)
51. Motherwell,W.D.S. - PLUTO A Program for plotting  
Molecular and Crystal Structures  
University Cambridge England (1978)
52. Andzelm,J.,Radzio-Andzelm,E. and Klobukowski,M.  
Journal of Molecular Structure 94 197-199  
publ. Elsevier Science Amsterdam (1983)
53. Murrell,J.N., Kettle,S.F.A. and Tedder,J.M.  
Valence Theory publ. John Wiley & Sons Ltd. Bath  
2nd Edition (1978)
54. Helve,W.J., Latham,W.A., Ditchfield,R., Newton,M.D.  
and Pople,J.A. - Gaussian 70 Program 236  
Quantum Chemistry Package Exchange, Indiana  
University (1971)
55. Pulay,P. - Molecular Physics 17 197-204 (1969)

56. Schlegel, H.B. - Queens University, Kingston  
Ontario Ph.D. Thesis (1975)
57. Spark, M.J., Winkler, D.A. and Andrews, P.R.  
Int. J. Quant. Chem. Quantum Biol. Symp. 9 321-333 (1982)
58. Giglio, E. - Nature (London) 222 339 (1969)
59. Koch, M.H.J. - Acta Crystallog. Sect. B. 29  
379 (1973)
60. Roth, B. and Strelitz, J.Z.  
Journal of Medicinal Chemistry Vol. 34 No. 4  
821 (1969)
61. Burchall, J.J. and Hitchings, G.H.  
Mol. Pharmacol. 1 126 (1965)
62. Fukunaga, J.Y., Hansch, C. and Stellar, E.E.  
Journal of Medicinal Chemistry Vol. 19 No. 5  
605-611 (1976)
63. Wong, K. - Third Year Project B.Sc. (Pharmacy)  
University of Aston in Birmingham
64. Lowe, P.R. - Ph.D. Thesis  
University of Aston in Birmingham
65. Jenks, R.G. - Third Year Project B.Sc. (Chemistry)  
Wolverhampton Polytechnic
66. Chatar Singh - Acta Cryst (1965)
67. Tables of Interatomic Distances  
Ed. L. Sutton, The Chemical Society (1965)
68. Bryant, P.K., Wong, K.P., Colby, J., Schwalbe, C.H.,  
Stevens, M.F.G, Griffin, R.J. and Bliss, G.A.

8th International Symposium - Pteridines and  
Folic Acid Derivatives

Montreal June 1986

69. Bryant, P.K., Colby, J., Jenks, R.G., Lowe, P.R.  
and Schwalbe, C.H.  
Crystallography in Biochemistry and Pharmacology  
C-79 03 3-20 (1986)